JOURNAL OF ENGINEERING RESEARCH & SCIENCES

JENRS

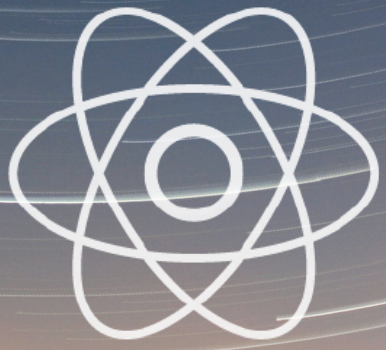

www.jenrs.com
ISSN: 2831-4085

Volume 1 Issue 2
February 2022

EDITORIAL BOARD

Editor-in-Chief

Editorial Board Members

Editorial

In this issue, we bring you five papers that delve into various facets of technology, ranging from power systems and IoT networks to telecommunications, gaming, and geophysical surveys. Each paper offers unique insights and contributions to their respective fields, reflecting the diverse and innovative nature of contemporary technological research.

Power quality monitoring is one of the most important aspects of designing compensators and other FACTS devices used in the power system." This paper introduces a novel sample manipulating technique for estimating power quality indices in harmonic polluted grids. By utilizing sample values of grid voltage and current signals along with a single standard sinusoidal signal, the proposed method reduces memory space requirements while providing accurate estimations. The techniques are validated through MATLAB simulations and real-time data extracted from digital storage oscilloscopes, offering promising advancements in power system monitoring [1].

IoT data collection networks have recently become one of the important research areas due to their fundamental role and wide application in many domains." Focusing on maximizing coverage in IoT networks, this paper presents a distributed approach combining Voronoi Diagrams and Genetic algorithms. Through experimental evaluations on real testbeds, the developed approach demonstrates superior performance in terms of coverage, RSSI, lifetime, and number of neighbouring objects compared to centralized algorithms, showcasing its potential for enhancing IoT network deployments [2].

As with previous generations of mobile cellular networks, rural regions are projected to face financial and technological challenges in deploying 5G services." This article explores the feasibility of utilizing TV White Spaces (TVWS) via High Altitude Platforms (HAPs) to bridge the broadband service gap in rural areas. Through performance evaluations using standard models, the study highlights the advantages and challenges of utilizing TVWS spectrum from HAP systems, offering valuable insights for future communication architectures [3].

Prakriti is a Sanskrit word which signifies Mother Nature." This paper introduces a multiplayer game, Prakriti, designed to educate players about water conservation. Developed using Unity 2D, the game provides an engaging platform for learning about water-saving techniques. Through iterative playtesting and feedback, the game demonstrates strong aesthetic quality and user interaction, effectively conveying information about water resources conservation in an immersive gaming environment [4].

A foundation study was carried out at a proposed Hostel site for the student of Federal University of Technology Akure, Nigeria." This study investigates the competence of overburden materials for foundation construction through geophysical surveys and geotechnical tests. The results reveal the presence of conductive clayey materials and shallow fractures, posing challenges for engineering structures. Recommendations are made for the design of deep foundations to ensure infrastructural development in the area [5].

In summary, the papers featured in this issue underscore the breadth and depth of technological advancements across various domains. From power systems and IoT networks to telecommunications, gaming, and geophysical surveys, these studies offer valuable insights, methodologies, and solutions to address contemporary challenges and drive innovation forward. We extend our gratitude to the authors for their insightful contributions and to our readers for their continued support of the Journal of Technological Advancements.

References:

[1] A. Rath, R. Saha, “Harmonic and Sequence Component Estimation by a Novel Method,” *Journal of Engineering Research and Sciences*, vol. 1, no. 2, pp. 1–9, 2022, doi:10.55708/js0102001.

[2] W. Abdallah, S. Mnasri, T. Val, “Distributed Approach for the Indoor Deployment of Wireless Connected Objects by the Hybridization of the Voronoi Diagram and the Genetic Algorithm,” *Journal of Engineering Research and Sciences*, vol. 1, no. 2, pp. 10–23, 2022, doi:10.55708/js0102002.

[3] H.M. Hussien, K. Katzis, L.P. Mfupe, E.T. Bekele, “Bridging the Urban-Rural Broadband Connectivity Gap using 5G Enabled HAPs Communication Exploiting TVWS Spectrum,” *Journal of Engineering Research and Sciences*, vol. 1, no. 2, pp. 24–32, 2022, doi:10.55708/js0102003.

[4] T. Bhattacharya, X. Peng, I. Joshi, T. Cao, J. Mao, X. Qin, “Prakriti: A Gamified Approach to Saving Water,” *Journal of Engineering Research and Sciences*, vol. 1, no. 2, pp. 33–40, 2022, doi:10.55708/js0102004.

[5] F.O. Eebo, A.B. Samuel, G.M. Olayanju, “Geophysical and Geotechnical Investigations for Subsoil Competence at a Proposed Hostel Site at Oba Nla, Akure Southwestern Nigeria,” *Journal of Engineering Research and Sciences*, vol. 1, no. 2, pp. 41–49, 2022, doi:10.55708/js0102005.

Editor-in-chief

Prof. Paul Andrew

JOURNAL OF ENGINEERING RESEARCH AND SCIENCES

Volume 1 Issue 2 **February 2022**

CONTENTS

Harmonic and Sequence Component Estimation by a Novel Method 01
Abinash Rath, Rumpa Saha

Distributed Approach for the Indoor Deployment of Wireless Connected Objects by the Hybridization of the Voronoi Diagram and the Genetic Algorithm 10
Wajih Abdallah, Sami Mnasri, Thierry Val

Bridging the Urban-Rural Broadband Connectivity Gap using 5G Enabled HAPs Communication Exploiting TVWS Spectrum 24
Habib M. Hussien, Konstantinos Katzis, Luzango P. Mfupe, Ephrem T. Bekele

Prakriti: A Gamified Approach to Saving Water 33
Tathagata Bhattacharya, Xiaopu Peng, Ishita Joshi, Ting Cao, Jianzhou Mao, Xiao Qin

Geophysical and Geotechnical Investigations for Subsoil Competence at a Proposed Hostel Site at Oba Nla, Akure Southwestern Nigeria 41
Festus Olusola Eebo, Abidakun Bayode Samuel, Gbenga Moses Olayanju

Received: 26 January 2022, Revised: 24 February 2022, Accepted: 26 February 2022, Online: 14 March 2022

DOI: https://dx.doi.org/10.55708/js0102001

Harmonic and Sequence Component Estimation by a Novel Method

Abinash Rath*[,1], Rumpa Saha[2]

[1]National Institute of Technology, Department of Electrical Engineering, Rourkela, 769008, India

[2]Aliah University, Department of Electrical Engineering, Kolkata, 700156, India

*Corresponding author: Abinash Rath, National Institute of Technology, Rourkela, Email: rabinash.nit@gmail.com

Corresponding author ORCID: https://orcid.org/0000-0001-7623-7627

ABSTRACT: Power quality monitoring is one of the most important aspects of designing of compensators and other FACTS devices used in the power system. This paper aims at finding the power quality indices from the voltage and current samples of a harmonic polluted grid, by using a newly proposed sample manipulating technique. Here, all the harmonic components of voltage, current, active and reactive powers are estimated along with the total harmonic distortion (THD) of the grid voltage and current waveforms. All the estimations are done using the sample values of the grid voltage and current signals along with only one standard sinusoidal signal of the fundamental frequency where conventional methods require standard signals of all the harmonic frequencies. Hence, the requisite memory space for the proposed scheme is reduced. In addition to that, the rms values of the sequence components in an unbalanced grid is estimated using the sample shifting technique. The proposed techniques are been verified with MATLAB simulation results and a comparative analysis is presented. The proposed method is also verified upon the real-time data extracted from a digital storage oscilloscope (DSO).

KEYWORDS: Power Quality, Fourier Transform, SMT, SST, THD, Sequence Components

1. Introduction

This Injection of other frequency components (harmonics) is getting proliferated with the increase in various non-linear loads, power electronic drives, [1] unbalanced load distribution, and introduction of renewable energy sources [2] in the existing power system which distorts the quality of power. Large power converters which can be modelled as a non-linear load also form a large source of harmonics. Hence researchers have been trying to improve system performance by improving the converter control algorithms as described in [3], [4]. Estimation of the harmonic components in a power system have great contribution in the filter designing aspect.

With poor power quality customer's sensitive devices are affected leading to data loss, corruption or damage of data, physical damage of sensitive devices [5]. There can be effects in terms of mal-operation in microprocessor-based technology which includes programmable logic controllers (PLC), Variable Speed Drives (VSD) etc. In other process control equipments, [6] flickering of computer screens, or complete loss of the power supply can also occur. Hence, the determination of the harmonic components or identifying the power quality problem becomes the step towards solving the power quality problem. Many researchers have been therefore interested in finding the characteristics of the load by observing the patterns of its current waveforms [7], [8].

The literature shows many methods of estimating the harmonic components from the voltage and current samples of a non-ideal grid [9]. The Fourier series method is widely used for simplicity [9]. The Fourier series method requires samples of sine and cosine waves of each harmonic frequency. This requires large memory space which is not always available in the RAM of a low-cost microcontroller. Introduction of the sample shifting technique has reduced much of the memory space requirement in which the standard signal waveform is shifted through different phase angles to achieve the power estimations for different orders of the harmonics [10]. This method becomes complex as the shifting of the waveform has to be done by different angles. The Sample Shifting Technique (SST) in [10] is modified such that the all the parameter estimation can be done only by shifting

the waveform by an angle 90^0 avoiding the multiple shifting of the standard signal waveform [11].

This paper proposes a noble Sample Manipulating Technique (SMT) which determines all the harmonic components of voltage, current, active power, reactive power, and the power quality indices of the grid from its voltage and current samples using only a single standard signal. This reduces the memory requirement. This method avoids the measurement of the phase angle for calculating both active and reactive power thus, the error associated with it is eliminated. The accuracy and effectiveness of the proposed method are verified by MATLAB simulation results and a comparative analysis is presented by comparing the obtained results with the existing methods in the literature.

2. Materials and Methods

2.1. Rms value of voltage and current signal

Let the voltage and current in a harmonically polluted grid be as given in (1) and (2).

$$v(t)=\sum_{n=1}^{h} v_n \sin(n\omega t+\varphi_n) \tag{1}$$

$$i(t)=\sum_{n=1}^{h} i_n \sin(n\omega t+\alpha_n) \tag{2}$$

According to the IEEE standard, 1459-2010, [12] the voltage and current rms values are estimated from their respective sample values of voltage signals using (3). [13]

$$\left.\begin{aligned} V_{rms} &= \sqrt{\frac{1}{2\pi}\int_0^{2\pi} v^2 d(\omega t)} = \sqrt{\frac{1}{N}\sum_{j=1}^{N} v_j^2} \\ i_{rms} &= \sqrt{\frac{1}{2\pi}\int_0^{2\pi} i^2 d(\omega t)} = \sqrt{\frac{1}{N}\sum_{j=1}^{N} i_j^2} \end{aligned}\right\} \tag{3}$$

The individual harmonic components of active and reactive powers can be defined by (4-5) [14], [13].

$$P_n = V_{nrms}.I_{nrms}\cos\phi_n \tag{4}$$

$$Q_n = V_{nrms}.I_{nrms}\sin\phi_n \tag{5}$$

P_n and Q_n represent the active and reactive power consumed by 'n^{th}' harmonic. V_{nrms}, and I_{nrms} represent the rms values of 'n^{th}' harmonics of voltage and current respectively.'ϕ_n' is defined as

$$\phi_n = \varphi_n - \alpha_n \tag{6}$$

According to Fortescue's theorem, the three unbalanced phasors of a three-phase system can be resolved into three balanced systems of phasors. The balanced sets of components are positive sequence component (V_{a1}), negative sequence component (V_{a2}), and zero sequence component(V_{a0}).

$$\left.\begin{aligned} V_{a1} &= \frac{1}{3}(V_a + aV_b + a^2V_c) \\ V_{a2} &= \frac{1}{3}(V_a + a^2V_b + aV_c) \\ V_{a0} &= \frac{1}{3}(V_a + V_b + V_c) \end{aligned}\right\} \tag{7}$$

where 'a' is an operator which shift the operand waveform by 120^0.

$$a = 1\angle 120^0$$

3. Fourier Series Method

Any periodic non-sinusoidal signal can be represented by the Fourier series. The phase and magnitude of the individual harmonic components of the signal can be determined by using the Fourier series technique [15].

If $f(t)$ is a periodic function, we can represent it by the following way as shown in (8) and (9) [15].

$$f(t) = a_0 + \sum_{n=1}^{n} a_n \cos n\omega t + b_n \sin n\omega t \tag{8}$$

$$f(t) = a_0 + \sum_{n=1}^{n} c_n \cos(n\omega t - \varphi) \tag{9}$$

To calculate a_n, b_n in the digital domain, the following expression is used. Where samples of $\sin n\omega t$ and $\cos n\omega t$ are created. They are multiplied with the samples of $f(t)$ to produce the Fourier coefficients [16].

$$a_n = \frac{1}{N}\sum_{k=1}^{N} v_k \cos(n\omega t)_k \tag{10}$$

$$b_n = \frac{1}{N}\sum_{k=1}^{N} v_k \sin(n\omega t)_k \tag{11}$$

$$c_n = \sqrt{a_n^2 + b_n^2} \tag{12}$$

$$\varphi_n = \tan^{-1}\left(\frac{b_n}{a_n}\right) \tag{13}$$

where 'N' is the number of samples per cycle and $\cos(n\omega t)_k$ $\sin(n\omega t)_k$ represent the 'k^{th}' sample of $\cos n\omega t$ and $\sin(n\omega t)$ respectively. By using (4-5), the active and reactive power components are calculated.

4. Sample Manipulating Technique

The basic idea of the proposed technique is to estimate the active power (P) and reactive power (Q) along with total harmonic distortion (THD) with this digital measurement process. In the Fourier method, the phase angle between the voltage and current phasor along with standard signals of each harmonic frequency is required for the power calculations. But, the proposed Sample Manipulating Technique (SMT) calculates the active and reactive power of each harmonic component without the

phase angle information. It also uses only one standard signal of a single frequency that is the fundamental. Thus, the error in active and reactive power calculation due to the phase angles standard signal only.

4.1. Measurement of the voltage in ideal grid condition

Let us assume, *v(t)* is the voltage samples which is given as (14).

$$v(t) = v_m \sin(\omega t + \varphi) \tag{14}$$

when *v(t)* is multiplied with a standard signal and averaged over one cycle, the result is given in (15).

$$\frac{1}{2\pi}\int_0^{2\pi} v(t).S(t)d\omega t = \mathrm{V_{rms}}\cos\phi \tag{15}$$

where the standard signal is taken as (16)

$$S = \sqrt{2}\sin\omega t \tag{16}$$

Similarly, if $\sqrt{2}\ cos\ \omega t$ is multiplied with *v(t)* and integrated from zero to 2π, the following results.

$$\frac{1}{2\pi}\int_0^{2\pi} v(t).S(t-90^0)d\omega t = V_{rms} sin\ \varphi \tag{17}$$

In the discrete domain, (16) and (17) can be represented in the following way as (18) and (19) respectively.

$$V_{1cos}=V_{rms}.\ cos\ \varphi = \frac{1}{N}\sum_{n=1}^{N} v_n.S_n \tag{18}$$

$$V_{1sin}=V_{rms}.\ sin\ \varphi = \frac{1}{N}\sum_{n=1}^{N} v_n.S_{-90^0 n} \tag{19}$$

where 'v_n' the voltage samples and S_n is the samples taken of the standard signal, $S_{-90^0 n}$ is the S_n samples shifted by angle 90^0. $S_{-90^0 n}$ is produced using the sample shifting technique. [11] From (18) and (19) the rms value of the measuring voltage signal can be calculated.

$$\mathrm{V_{1rms}} = \sqrt{(\mathrm{V_{1cos}})^2 + (\mathrm{V_{1sin}})^2} \tag{20}$$

4.2. Measurement of voltage harmonic components in non-ideal condition

But the input voltage will not be pure sine wave always. Suppose the voltage equation is given as

$$v(t) = v_1 + v_2 + \ldots + v_n \tag{21}$$

where v_1, v_2, v_n are mathematically given by

$$v_1 = v_{m1}\sin(\omega t + \varphi_1)$$

$$v_2 = v_{m2}\sin(2\omega t + \varphi_2)$$

$$v_n = v_{mn}\sin(n\omega t + \varphi_n)$$

4.2.1. Calculation of the fundamental component of v(t)

If *v(t)* is multiplied with the standard signal, the has resulted expression is given in (22a).

$$V_{1\cos} = \frac{1}{2\pi}\int_0^{2\pi} v(t)S(t)d(\omega t) \tag{22a}$$

$$= \frac{1}{2\pi}\int_0^{2\pi} V_{m1}\sin(\omega t + \phi_1).\sqrt{2}\sin(\omega t)d(\omega t)$$

$$+ \frac{1}{2\pi}\int_0^{2\pi} V_{m3}\sin(3\omega t + \phi_3).\sqrt{2}\sin(\omega t)d(\omega t)$$

$$+ \frac{1}{2\pi}\int_0^{2\pi} V_{m7}\sin(7\omega t + \phi_7).\sqrt{2}\sin(\omega t)d(\omega t)$$

The *2nd* and *3rd* integrals in the above expression are evaluated to be zero. Hence, the final result is given in (22b).

$$\frac{V_{m1}}{\sqrt{2}}.\cos\phi_1 = V_{rms1}\cos\phi_1 \tag{22b}$$

Similarly, if $\sqrt{2}\ cos\ \omega t$ is multiplied with the voltage sample and integrated, the result comes as presented in (23a).

$$V_{1\sin} = \frac{1}{2\pi}\int_0^{2\pi} v(t).S(t-90^0).d(\omega t) \tag{23a}$$

$$= \frac{1}{2\pi}\int_0^{2\pi} V_{m1}\sin(\omega t + \phi_1).\sqrt{2}\cos(\omega t)d(\omega t)$$

$$+ \frac{1}{2\pi}\int_0^{2\pi} V_{m3}\sin(3\omega t + \phi_3).\sqrt{2}\cos(\omega t)d(\omega t)$$

$$+ \frac{1}{2\pi}\int_0^{2\pi} V_{m7}\sin(7\omega t + \phi_7).\sqrt{2}\cos(\omega t)d(\omega t)$$

$$= \frac{V_{m1}}{\sqrt{2}}.\sin\phi_1 = V_{1rms}\sin\phi_1 \tag{23b}$$

From (22b) and (23b), the rms value of the voltage signal can be calculated as shown in (24).

$$\mathrm{V_{1rms}} = \sqrt{(\mathrm{V_{1cos}})^2 + (\mathrm{V_{1sin}})^2} \tag{24}$$

In the discrete domain (22) and (23) can be evaluated as presented in (25-26).

$$V_{1cos}=V_{1rms}.\cos\varphi=\frac{1}{N}\sum_{n=1}^{N}v_n.S_n \quad (25)$$

$$V_{1sin}=V_{1rms}.\sin\varphi=\frac{1}{N}\sum_{n=1}^{N}v_n.S_{-90^0 n} \quad (26)$$

4.2.2. Evaluation of 'n^{th}' order harmonic

To evaluate the 'n^{th}' order harmonic, it's required to multiply a signal having its frequency raised n times as the frequency of the standard signal with the voltage and current sample and then integrate

$$V_{n\cos}=\frac{1}{2\pi}\int_0^{2\pi}v(\omega t).S(n\omega t).d(\omega t) \quad (27)$$

$$V_{n\sin}=\frac{1}{2\pi}\int_0^{2\pi}v(\omega t).S(n\omega t-90^0).d(\omega t) \quad (28)$$

But in this paper, only one standard signal is used which has a frequency equal to the fundamental frequency present in the voltage sample. So in a discrete domain, (27) and (28) are realized as (29) and (30).

$$V_{n\cos}=\frac{1}{N}\sum_{k=0}^{N}V_{k+1}.S_{nk+1} \quad (29)$$

$$V_{n\sin}=\frac{1}{N}\sum_{k=0}^{N}V_{k+1}.S_{-90^0 nk+1} \quad (30)$$

During the calculation of the summation series replace ($nk+1$) with ($nk+1-N$) when ($nk+1$) goes beyond 'N'. The rms value of the 'n^{th}' harmonic component of the voltage waveform can the calculated using (29) and (30) as presented in (31).

$$V_{nrms}=\sqrt{(V_{ncos})^2+(V_{nsin})^2} \quad (31)$$

Table 1: Illustration of SMT

For Fundamental	For 3rd Harmonic	For 5th Harmonic	For 7th Harmonic
v(1).S(1)	v(1).S(1)	v(1).S(1)	v(1).S(1)
v(2).S(2)	v(2).S(4)	v(2).S(6)	v(2).S(8)
v(3).S(3)	v(3).S(7)	v(3).S(11)	v(3).S(15)
v(4).S(4)	v(4).S(10)	v(4).S(16)	v(4).S(2)
v(5).S(5)	v(5).S(13)	v(5).S(1)	v(5).S(9)
v(6).S(6)	v(6).S(16)	v(6).S(6)	v(6).S(16)
v(7).S(7)	v(7).S(19)	v(7).S(11)	v(7).S(3)
v(8).S(8)	v(8).S(1)	v(1).S(16)	v(1).S(10)
….	….	….	….
v(16).S(16)	v(16).S(6)	v(16).S(16)	v(16).S(6)
v(17) .S(17)	v(17) .S(9)	v(17) .S(1)	v(17) S(13)
v(18) .S(18)	v(18) S(12)	v(18) .S(6)	v(18) S(20)
v(19) .S(19)	v(19) S(15)	v(19) .S(11)	v(19)S(7)
v(20) .S(20)	v(20) S(18)	v(20) .S(16)	v(20) S(14)

4.3. Measurement of current in ideal condition

Suppose $i(t)$ is the current signal which is mathematically represented by (32).

$$i(t)=i_m \sin(\omega t+\alpha) \quad (32)$$

$i_{rms}.\cos\alpha$ and $i_{rms}.\sin\alpha$ can be calculated as (13) and (14) in the discrete domain

$$I_{1cos}=I_{1rms}.\cos\alpha=\frac{1}{N}\sum_{n=1}^{N}i_n.S_n \quad (33)$$

$$I_{1sin}=I_{1rms}.\sin\alpha=\frac{1}{N}\sum_{n=1}^{N}i_n.S_{-90^0 n} \quad (34)$$

$$I_{1rms}=\sqrt{(I_{1cos})^2+(I_{1sin})^2} \quad (35)$$

4.4. Measurement of current harmonics in non-ideal condition

Suppose the current is not pure sinusoidal and given by the following

$$i(t)=i_1+i_2....+i_n$$

where $i_1, i_2,...,i_n$ are mathematically represented as the following

$$i_1=i_{m1}sin(\omega t+\alpha_1)$$

$$i_2=i_{m2}sin(\omega t+\alpha_2)$$

$$i_n=i_{mn}sin(\omega t+\alpha_n)$$

4.4.1. Calculation of the fundamental components of i(t)

The current sample is multiplied with the standard signal to produce the following result.

$$I_{1\cos}=\frac{1}{2\pi}\int_0^{2\pi}i(t).S(t).d(\omega t)$$

$$=\frac{I_{m1}}{\sqrt{2}}.\cos\alpha_1=I_{rms1}\cos\alpha_1$$

To evaluate I_{1sin}, $S(t\text{-}90^0)$ that is $\sqrt{2}\cos\omega t$ is multiplied with the current samples and then integrated.

$$I_{1\sin} = \frac{1}{2\pi}\int_0^{2\pi} i(t)S(t-90^0)d(\omega t)$$

$$= \frac{I_{m1}}{\sqrt{2}}\sin\alpha_1 = I_{1rms}\sin\alpha_1$$

4.4.2. *Evaluation of 'n^{th}' order harmonic*

The 'n^{th}' order harmonic of current can be calculated just by replacing the voltage samples with current samples in (29-30).

$$i_{n\cos} = \frac{1}{N}\sum_{k=0}^{N} i_{k+1}.S_{nk+1} \tag{36}$$

$$i_{n\sin} = \frac{1}{N}\sum_{k=0}^{N} i_{k+1}.S_{-90^0 nk+1} \tag{37}$$

4.5. *Measurement of Active and Reactive power*

As per (3) and (4), the individual harmonic components of real power (P), and reactive power (Q) for the n^{th} order harmonic are given by (38) and (39) respectively.

$$P_n = V_{nrms}.I_{nrms}cos(\varphi_n - \alpha_n)$$

$$= (V_{nrms}cos\varphi_n)(I_{nrms}cos\alpha_n) + (V_{nrms}sin\varphi_n)(I_{nrms}sin\alpha_n)$$

$$= V_{ncos}I_{ncos} + V_{nsin}I_{nsin} \tag{38}$$

$$Q_n = V_{nrms}I_{nrms}sin(\varphi_n - \alpha_n)$$

$$= (V_{nrms}sin\varphi_n)(I_{nrms}cos\alpha_n) - (V_{nrms}cos\varphi_n)(I_{nrms}sin\alpha_n)$$

$$= V_{nsin}I_{ncos} - V_{ncos}I_{nsin} \tag{39}$$

In (38) and (39) the pre-calculated values of V_{ncos} , I_{ncos},V_{nsin} , I_{nsin} are used from (30), (36), (31) and (37) respectively. For the fundamental 'n' is replaced by 1. That is V_{1cos} , I_{1cos},V_{1sin}, I_{1sin} are used from (25), (33), (26), and (34) respectively.

4.6. *Measurement of Total Harmonic Distortion (THD)*

The overall deviation of a distorted wave from its fundamental can be estimated with the help of the total harmonic distortion. The total harmonic distortion of the voltage and current waveforms are estimated as (40) and (41) respectively. [12] [11]

$$\mathrm{THD_V} = \frac{\sqrt{\sum V_{nrms}^2}}{\mathrm{V_{1rms}}} \tag{40}$$

$$\mathrm{THD_i} = \frac{\sqrt{\sum I_{nrms}^2}}{\mathrm{I_{1rms}}} \tag{41}$$

5. Sample Shifting Technique (SST) and Sequence component estimation

The sample shifting technique (SST) produces a cosine wave from sine wave just by shifting the sample values by an angle 90^0. The shifting of the wave is illustrated in Figure. 1.

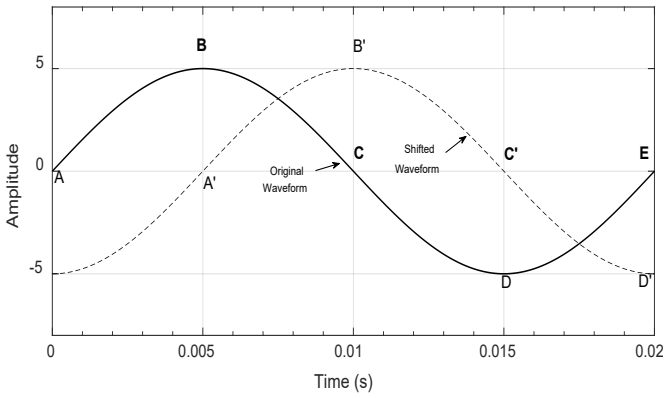

Figure 1: Illustration of the Sample Shifting Technique (SST)

Here A-B-C-D-E is the original wave. Suppose the whole cycle of the sine wave contains an 'N' number of samples.

To generate a waveform that is shifted by 90^0, the $N/4^{th}$ Sample value of the original wave is taken as the 1^{st} sample of the shifted wave and this process continues till the N^{th} sample of the original wave is put into the '$3N/4^{th}$' sample of the shifted wave. Then from the $3N/4^{th}$ sample to the N^{th} sample of the shifted wave carries the sample values of 1^{st} to $(N/4-1)^{th}$ sample of the shifted wave.

6. Results

6.1. *Implementation on a Theoretical System*

The numerical example given in the IEEE 1459-2010 [12] standards is taken for producing composite signals for voltage and current waves. The magnitude of voltage, the magnitude of current, active power, reactive power, and THD are estimated using both the techniques, and the comparative results are presented in Table 2-6. For all the methods, the sampling frequency is taken as 10 kHz.

$$v(t) = 100\sqrt{2}\sin(\omega t - 0^0) + 8\sqrt{2}\sin(3\omega t - 70^0)$$
$$+15\sqrt{2}\sin(5\omega t + 140^0) + 5\sqrt{2}\sin(7\omega t + 20^0)$$

$$i(t) = 100\sqrt{2}\sin(\omega t - 30^0) + 20\sqrt{2}\sin(3\omega t - 165^0)$$
$$+15\sqrt{2}\sin(5\omega t - 127^0) + 10\sqrt{2}\sin(7\omega t + 288^0)$$

Table 2: Comparative Magnitude of Individual Voltage Harmonic Components

Order of Harmonics	Rms Value of Voltage (in Volt)			% Difference	
	Theoretical	Fourier	SMT	Fourier	SMT
1	100	99.995	100.00	0.000	0
3	8	8.004	7.999	0.000	0.000
5	15	14.995	15.006	0.000	0.000
7	5	5.000	5.000	0.000	0

Table 3: Comparative Magnitude of Individual Current Harmonic Components

Order of Harmonics	Rms Value of Current (in Amp)			% Difference	
	Theoretical	Fourier	SMT	Fourier	SMT
1	100	99.998	100.00	0.000	0
3	20	19.994	20.002	0.000	0.000
5	15	15.008	15.006	0.000	0.000
7	10	10.0153	10.007	0.0015	0.000

Table 4: Comparative Magnitude of Individual Active Power Components

Order of Harmonics	Active Power (in Watt)			%Difference	
	Theoretical	SMT	Fourier	Fourier	SMT
1	8660	8660.3	8659.6	0.000	0.000
3	-13.94	-13.94	-14.0	-0.004	0
5	-11.78	-11.9	-11.9	-0.01	-0.01
7	–1.74	-1.8	-1.8	-0.0227	-0.022

Table 5: Comparative Magnitude of Individual Reactive Power Components

Order of Harmonics	Reactive Power (in Var)			% Difference	
	Theoretical	SMT	Fourier	Fourier	SMT
1	5000	5000	5000	0	0
3	159.4	159.4	159.4	0	0
5	-224.69	-224.8	-224.8	-0.004	-0.004
7	49.97	50.0	50.0	0.000	0.000

Table 6: Comparative Result of THD

Parameters	Theoretical	THD_v	THD_i	% Difference
THD_v	0.177	0.177	0.177	0
THD_I	0.269	0.269	0.269	0

In Table 2, the theoretical and estimated value values of the given harmonics from the conventional as well as the proposed method are presented. It can be observed that both methods are able to correctly estimate each of the harmonics present in the voltage signal. Similar observations can be derived for the current estimations which are presented in Table 3. Estimations of active power (P), reactive power (Q) presented in Table 4 and 5 are observed to give correct estimations with the proposed method and the conventional method. Voltage and line current THD values presented in Table 6 shows that the SMT is able to replicate the exact theoretical values of THD_v and THD_I.

6.2. Implementation into a Practical System

To implement the proposed methods on practical system data, the load voltage and load current sample values are collected from a DSO. The load used here is a household stand-fan. The waveform of the load voltage and current is presented in Figure. 2.

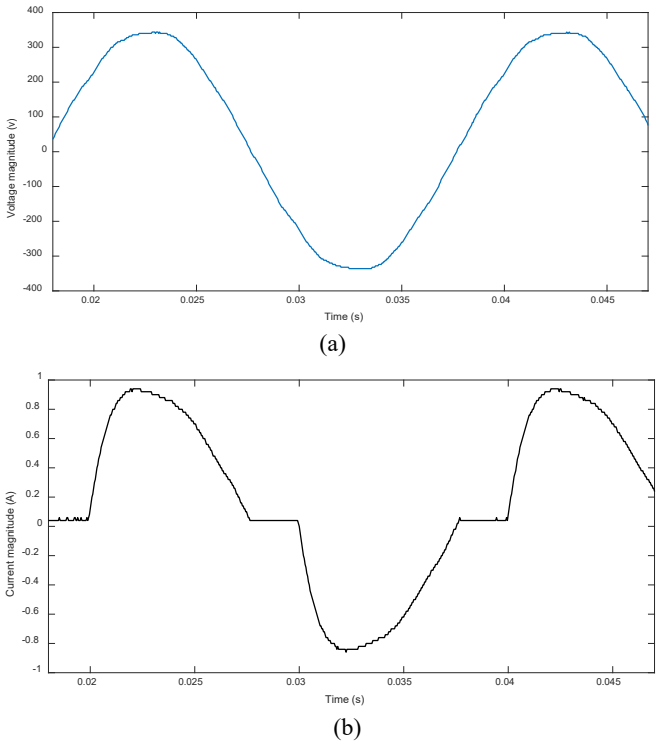

(a)

(b)

Figure 2: Voltage and current waveform of the stand-fan

The knowledge of the frequency of the sampled signal is very important to produce the standard signal. So at first the frequency of the sampled signal is determined by zero-crossing detection (ZCD) [17]. Then the standard signal is generated of this frequency. Now, this standard signal is used to calculate the magnitude of individual harmonic components of voltage, current, active power, and reactive power and compared with values obtained by the conventional method. The comparative results are given in Table 7 to Table 11 which present the individual harmonic components of the supply voltage, source current drawn by the load, the consumed active power, the consumed reactive power and the THD in the voltage and current waveforms in the respective order. The Fourier method is considered to be bench mark for the computation of the above mentioned parameters. The values of the above mentioned parameters obtained using the proposed method of SMT is also very close to the values obtained in the classical method. To quantify the accuracy of the proposed estimation process, percentage difference for each of the obtained with reference to the value obtained in classical method is presented in Table 7 to Table 11. It can be observed that the percentage difference in each case is found to be very low. This signifies the proposed estimation process is fairly accurate.

Table 7: Comparative Result of Magnitude of Individual Voltage Harmonic Components

Order of Harmonics	Rms Value of Voltage (in Volt)		Difference (in %)
	SMT	Fourier	
1	245.0711	244.7811	0.001
3	2.2120	1.9659	0.111
5	1.3827	1.5252	0.103
7	2.8074	2.6893	0.042

Table 8: Comparative Result of Magnitude of Individual Current Harmonic Components

Order of Harmonics	Rms Value of Current (in Amp)		Difference (in %)
	SMT	Fourier	
1	0.5606	0.5597	0.001
3	0.1101	0.1107	0.000
5	0.0737	0.0737	0
7	0.0352	0.0350	0.000

Table 9: Comparative Result of Magnitude of Individual Harmonic Components of Active Power

Order of Harmonics	Active Power (in Watt)		Difference (in %)
	SMT	Fourier	
1	134.8939	134.5448	0.002
3	-0.1886	-0.1567	0.169
5	-0.0281	-0.0261	0.028
7	0.0980	0.0937	0.043

Table 10: Comparative Result of Magnitude of Individual Harmonic Components of Reactive Power

Order of Harmonics	Reactive Power (in Var)		Difference (in %)
	SMT	Fourier	
1	26.0049	25.8936	0.004
3	-0.1540	-0.1510	0.019
5	0.0980	0.1094	-0.116
7	-0.0120	-0.0099	-.0175

Table 11: Comparative Result of THD

Parameters	SMT	Fourier	% Difference
THD_v (in %)	0.0161	0.0152	0.055
THD_i (in %)	0.2446	0.2457	-0.004

Figure 3 shows a comparative investigation of the memory requirement to store all the sample values of the standard signals used for different techniques for estimation of harmonics up to the 40th order. Here the memory requirement is compared with the Fourier method and the Sample Shifting Technique. The proposed technique requires only 80 kB memory to store the required standard signal where the Fourier method requires 6400 kB and SST requires 3200 kB which are 80 and 40 times more it.

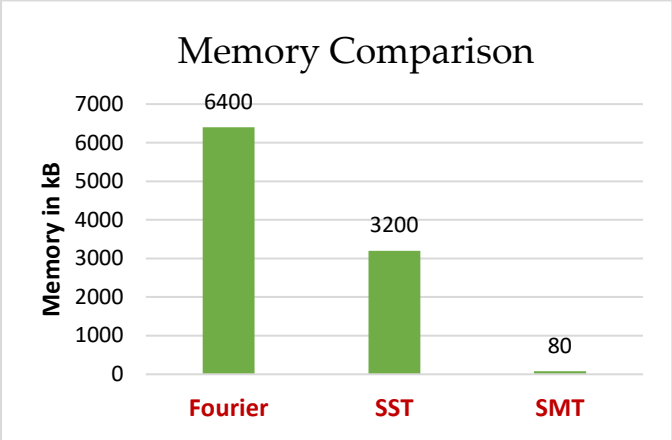

Figure 3: Graphical presentation of the required memory

The whole process of this implementation is represented in a flowchart which is presented in Figure 4.

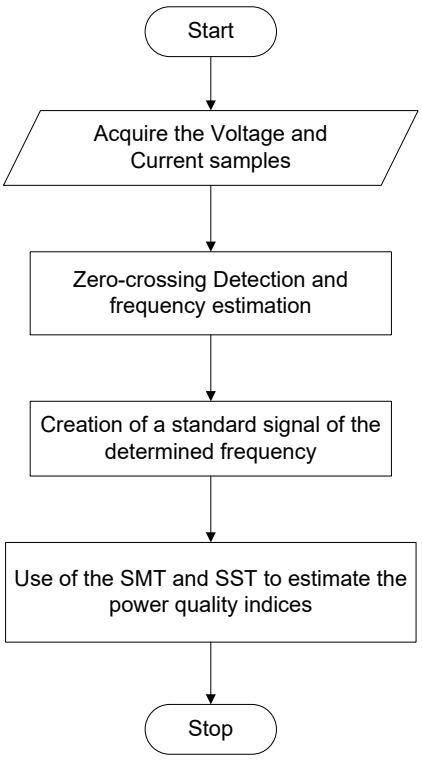

Figure 4: Flowchart showing the stepwise execution

6.3. Sequence Component Estimation by SST

A numerical example from [18] is taken up for implementation of the method which describes the unbalanced condition as the following.

$$V_a = 100\angle 0^0$$
$$V_b = 33\angle -100^0$$
$$V_c = 38\angle 176.5^0$$

The symmetrical components are determined using SST and the comparative result is shown in Table 12 with analytically determined value of the same parameters in the book.

Table 12: The Symmetrical Components for Unbalanced Condition

Sequence Components	Analytical	SST	% Difference
V_{a1}	52.6474	52.6539	-0.0001
V_{a2}	30.8549	30.8559	-0.0000
V_{a0}	21.3047	21.3047	0.0000

A three-phase, 60Hz, 735 kV power system transmitting power from a power plant consisting of six 350 MVA generators to an equivalent network through a 600 km transmission line is modelled in Simulink as shown in Figure 5. The transmission line is split into two 300 km lines connected between buses B1, B2, and B3. The generators are simulated with a simplified synchronous machine block. Voltages and currents are measured in B2 blocks. After the fault is introduced the voltage and current samples are imported from the bus bar for SLG, LL, LLG, fault conditions. The SST is used as the tool to find all the sequence components which are tabulated in Table 13. For the SLG, all the sequence components of the current have the same value up to two decimal places i.e. 27.39 A. For LL fault the magnitude of positive and negative sequence components of voltage and current are identical i.e. 0.35 pu and 17.13 A respectively confirming its theoretical correctness. For LLG fault, all their voltage sequence components have identical values of 0.19 pu. This again shows its theoretical truthfulness.

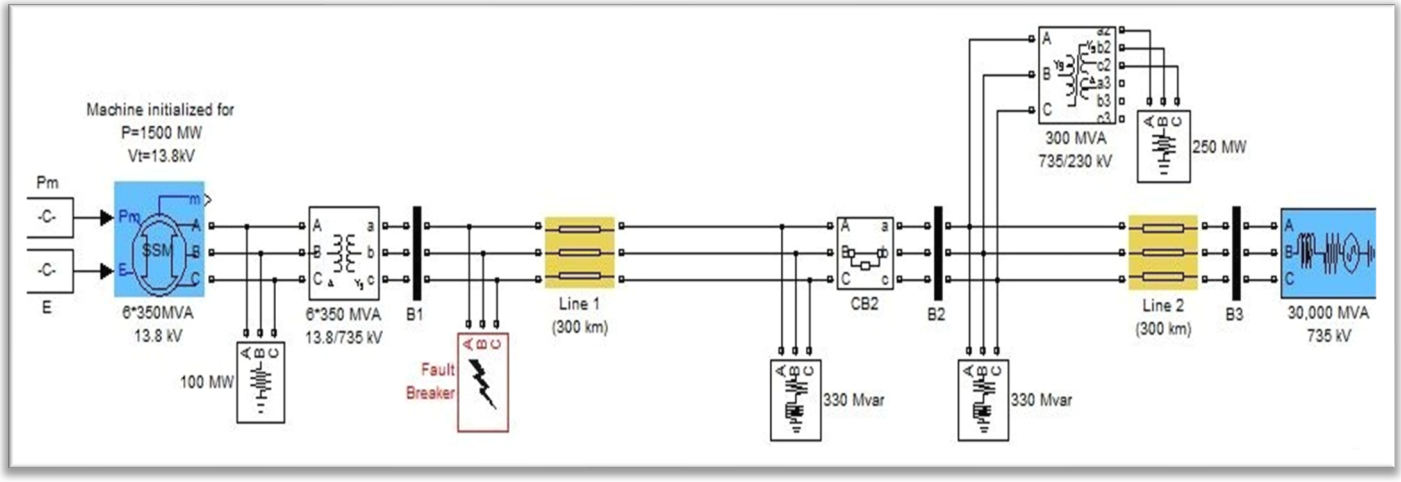

Figure 5: Diagram showing the Simulink model

Table 13: Estimated sequence components for different faults

Type of Fault	Sequence Components of the three-phase voltage			Sequence Components of the three-phase Current		
	(V_{a1})	(V_{a2})	(V_{a0})	(I_{a1})	(I_{a2})	(I_{a0})
SLG	0.4331	0.2730	0.1634	27.3954	27.3909	27.3902
LL	0.3543	0.3500	6.8547e-06	17.1318	-17.1383	6.04e-04
LLG	0.0260	0.0260	0.1920	36.5989	27.9187	36.6365

7. Conclusions

In this paper, a noble SMT is proposed for the estimation of power quality indices in a non-ideal grid. In addition to that, and the sequence component estimation by SST are proposed. The results obtained by the proposed SMT is compared with the classical Fourier series method. The comparative analysis shows that the proposed method produces reliable results. Furthermore, SMT does not need the measuring of the phase angle between the voltage and current signal. The comparative analysis of the memory space requirement proves that the use of SMT reduces the memory requirement considerably which gives the user the flexibility to use a low-cost microcontroller having less memory. On the other hand, it can be understood that the accuracy level for higher-order harmonics goes on decreasing as the standard signal has less number of samples per each cycle at the higher-order harmonics.

Conflict of Interest

The authors declare no conflict of interest.

Acknowledgment

The authors acknowledge National Institute of Technology, Rourkela for the necessary support.

References

[1] D. W. Petro, R. L. Wood, "Power quality issues regarding adjustable speed drives in petroleum terminals," pp. 227–234, 2002, doi:10.1109/pcicon.1994.347611.

[2] T. Ise, Y. Hayashi, K. Tsuji, "Definitions of power quality levels and the simplest approach for unbundled power quality services," *Proceedings of International Conference on Harmonics and Quality of Power, ICHQP*, vol. 2, pp. 385–390, 2000, doi:10.1109/ICHQP.2000.897711.

[3] A. Rath et al., "Power quality improvement using 18 sector algorithm based direct power control," *International Transactions on Electrical Energy Systems*, no. April 2020, pp. 1–17, 2021, doi:10.1002/2050-7038.12784.

[4] A. Rath, G. Srungavarapu, M. Pattnaik, " An advanced virtual flux integrated multifold table-based direct power control with delay compensation for active front-end rectifiers ," *International Transactions on Electrical Energy Systems*, no. October, pp. 1–22, 2021, doi:10.1002/2050-7038.13174.

[5] S. Bhattacharyya, J. M. A. Myrzik, W. L. Kling, "Consequences of poor power quality - An overview," *Proceedings of the Universities Power Engineering Conference*, no. 1, pp. 651–656, 2007, doi:10.1109/UPEC.2007.4469025.

[6] K. Schipman, F. Delincé, "The importance of good power quality," -, pp. 1–20, 2010.

[7] R. Saha, J. N. Bera, G. Sarkar, "An Improved Method for Load Taxonomy Using Sample Shifting Technique and Signature Analysis," *Electric Power Components and Systems*, vol. 47, no. 1–2, pp. 113–127, 2019, doi:10.1080/15325008.2019.1577928.

[8] A. S. Kulkarni, C. K. Harnett, K. C. Welch, "EMF signature for appliance classification," *IEEE Sensors Journal*, vol. 15, no. 6, pp. 3573–3581, 2015, doi:10.1109/JSEN.2014.2379113.

[9] Y. C. Chen, J. K. Lan, "Implementation of power measurement system with fourier series and zero-crossing algorithm," *Proceedings - 2014 International Symposium on Computer, Consumer and Control, IS3C 2014*, pp. 601–604, 2014, doi:10.1109/IS3C.2014.163.

[10] R. Saha et al., "Sample shifting technique (SST) for estimation of harmonic power in polluted environment," *Proceedings of IEEE International Conference on Circuit, Power and Computing Technologies, ICCPCT 2013*, pp. 535–539, 2013, doi:10.1109/ICCPCT.2013.6528921.

[11] R. Saha et al., "A simplified state-of-the-art sample shifting technique for microcontroller based single phase power measurement," *Measurement: Journal of the International Measurement Confederation*, vol. 58, pp. 459–467, 2014, doi:10.1016/j.measurement.2014.08.016.

[12] "IEEE Xplore Search Results." https://ieeexplore.ieee.org/search/searchresult.jsp?newsearch=true&queryText=1459-2010 . (accessed: 17-Dec-2020).

[13] A. Cataliotti, V. Cosentino, S. Nuccio, "The measurement of reactive energy in polluted distribution power systems: An analysis of the performance of commercial static meters," *IEEE Transactions on Power Delivery*, vol. 23, no. 3, pp. 1296–1301, 2008, doi:10.1109/TPWRD.2008.919239.

[14] M. Gray, W. G. Morsi, "New power quantities definition for low and high order harmonic distortion," *Electric Power Systems Research*, vol. 119, pp. 11–18, 2015, doi:10.1016/j.epsr.2014.09.004.

[15] ananta kankale, "Network theory by alaxander and sadiku." .

[16] T. Tarasiuk, "Method, algorithm and device for estimation of components above the harmonic frequency range up to 9 kHz," *Measurement: Journal of the International Measurement Confederation*, vol. 44, no. 1, pp. 219–229, 2011, doi:10.1016/j.measurement.2010.09.046.

[17] S. Väliviita, "Zerocrossing detection of distorted line voltages using 1b measurements," *IEEE Transactions on Industrial Electronics*, vol. 46, no. 5, pp. 917922, 1999, doi:10.1109/41.793339.

[18] C. L. Wadhwa *Electrical Power Systems*, 6th edition, New Age International, 2006

Received: 18 January 2022, Revised: 26 February 2022, Accepted: 27 February 2022, Online: 14 March 2022

DOI: https://dx.doi.org/10.55708/js0102002

Distributed Approach for the Indoor Deployment of Wireless Connected Objects by the Hybridization of the Voronoi Diagram and the Genetic Algorithm

Wajih Abdallah [*,1,2], **Sami Mnasri** [1,3], **Thierry Val** [1]

[1] UT2J, CNRS-IRIT (RMESS), University of Toulouse, Toulouse, France

[2] ISAM Gafsa, Dept. of Design, University of Gafsa, Tunisia

[3] University of Tabuk, Community College, Dept. of computer sciences, Tabuk, KSA

*Corresponding author: Wajih Abdallah, University of Toulouse, Toulouse, France, Email: Wajih.abdallah@irit.fr

ABSTRACT: IoT data collection networks have recently become one of the important research areas due to their fundamental role and wide application in many domains. The establishment of networks of objects is based essentially on the deployment of connected objects to process the collected data and transmit them to the various locations. Subsequently, a large number of nodes must be adequately deployed to achieve complete coverage. This manuscript introduces a distributed approach, which combines the Voronoi Diagram and the Genetic algorithm (VD-GA), to maximize the coverage of a region of interest. The Voronoi diagram is used to divide region into cells and generate initial solutions that present the positions of the deployed IoT objects. Then, a genetic algorithm is executed in parallel in several nodes to improve these positions. The developed VD-GA approach was evaluated on an experimental environment by prototyping on a real testbed utilizing M5StickC nodes equipped with ESP32 processor. The experiments show that the distributed approach provided better degree of coverage, RSSI, lifetime and number of neighboring objects than those given by the original algorithms in terms of the suggested distributed Genetic-Voronoi algorithm outperforms the centralized one in terms of speed of computing.

KEYWORDS: Coverage, Distributed Deployment, Genetic Algorithm, IoT collection networks, Optimization, Voronoi Diagram

1. Introduction

In recent years, IoT has been applied in several areas such as cities, warehouses, buildings, hospitals, universities and companies [1, 2]. An IoT data collection network is generally composed of a large number of multi-functional connected objects called nodes which form the wireless sensor network. The latter can gather and send information. It also allows controlling or detecting objects directly via the used network technology used, establishing a closer connection between the real world and computer networks and improving network performance metrics [3, 4].

The basic elements of a data collection network are sensor nodes made up of detection unit, processing unit, storage unit and communication unit [5]. The network operates according to three phases: detection, processing and transmission of data to the receiver through a number of intermediate nodes [6]. The detection unit of a sensor node interfaces with its physical environment to accumulate the required information. In fact, the transmission of data and control packets through the network is performed by the communication unit of a node [7]. Sensor nodes are also equipped with a processing unit that can process data. Generally, this unit consists of a microprocessor or microcontroller. It is also linked to a memory unit used to store a set of instructions and detected data [8].

The main objectives of using IoT data collection networks are to monitor and control the target within the region of interest [9, 10], on the one hand, and determine any physical action (e.g. light, heat, sound, etc.), on the other hand The sensor node detects, processes, and convert these observations into a compatible format. IoT collection networks are implemented for many uses and

applications in various fields such as military applications [11], industrial applications [12], commercial applications [13], home applications [14], healthcare applications [15] and environmental applications [16].

Many issues, such as limited storage in a node, routing problem and how to develop a good routing algorithm that guarantees efficient data transfer between sensor nodes, are encountered in IoT data collection networks. In fact, the performance of the latter is affected by some parameters like the localization of a sensor node in a region of interest and the deployment of nodes. The authors [17] pointed out that the latter is an essential design aspect in setting up a network because it reflects the detection and control ability as well as the cost of an IoT network. It also affects almost all its performance metrics like coverage, network lifetime, and connectivity between nodes [18].

The methods of deployment in a network of connected objects can be classified into two categories: deterministic and random. In fact, random deployment is carried distributing sensor nodes randomly over the whole region of interest (RoI) [19, 20]. This type of deployment is usually used in applications where the area to be monitored is too large or where the region of interest is inaccessible due to adverse and hazardous environmental conditions In this case, objects can be dispersed from an aircraft or by using multi-robot systems [21]. To attain complete coverage, the random deployment technique requires more sensor nodes than the intended deployment [20].

An optimal deployment of sensor nodes has two main objectives. The first aim is to maximize the coverage of a given region of interest, while the second objective consists in minimizing the number of sensor nodes to be deployed [22, 23]. This type of problem is classified as an NP-hard optimization problem [24].

Many stochastic optimization algorithms have been designed to solve different optimization problems. Among these algorithms commonly used in the deployment of data collection networks, we can mention: the Genetic Algorithm (GA) [25, 26], the Particle Swarms Optimization (PSO) [27, 28], the Artificial Bee Colony (ABC) [29], Ant Colony Optimization (ACO) [30], Fruit Fly Optimization (FOA) [31], Bacterial Food Search Optimization algorithm (BFO) [32], Group Search Optimization (GSO) [33], Harmony Search Algorithm (HSA) [34], Charged Search System (CSS) [35], Rivers Formation Dynamics (RFA) [36]. In previous academic studies, these algorithms were combined and hybridized with other paradigms to enhance the performance of deployment in terms of convergence and precision rate.

In this paper, we propose a distributed approach based on the hybridization of a geometric deployment method, used in the Voronoi Diagram, and a genetic algorithm. This processing is performed in several nodes in parallel to reach the desired solution in a shorter time compared to the centralized approach. This hybridization aims at positioning the nodes in a network and, subsequently, to maximize the coverage of a RoI with the minimum number of nodes. The Voronoi Diagram (VD) presents the starting point of our work that generates an initial population with a random deployment of objects. This task is performed on a single M5StickC node. Then, the initial population will be distributed over all the other M5StickC nodes forming the data collection network. Thus, a genetic algorithm is executed in each of these nodes to optimize deployment.

The work presented in this article has three main contributions:

1. A hybridization between distributed VD and GA is introduced, with the aim of improving the coverage rate in data collection networks.

2. The introduced distributed VD-GA approach was evaluated in an experimental environment by prototyping on real testbeds using M5StickC nodes (This type of nodes is used for the first time for addressing the deployment issues).

3. Evaluate and compare the found result with a centralized VD-GA approach and other deployment paradigms.

This paper is divided into four sections: Section 2 overviews some research works related to deployment optimization. Section 3 presents our distributed approach based on the hybridization of the VD algorithm and the genetic algorithm (GA) proposed for the deployment of objects in IoT collection networks. Section 4 illustrates and discusses the obtained results and compares the performance of the suggested approach with that of our centralized approach [37] is performed on a single node.

2. Related works

2.1. Hybridization of DV and optimization algorithms

The heuristic method that is widely used for the deployment and optimization in IoT data collection networks is optimization by genetic algorithms (GA) applied to improve the positions of nodes in order to maximize the region of interest coverage and, subsequently, extend the life of the network. This technique is also utilized to reduce energy consumption. Other commonly-used heuristics include optimization by particle swarms (PSO), optimization by ant colonies (ACO), which is generally employed to optimize routing paths between nodes. Voronoi-based approaches used in many studies to maximize the coverage in an area of interest by detecting coverage holes in data collection network.

In this section, we present some studies that proposed hybridization of VD and optimization algorithms in different applications and contexts. Indeed, several works combined Voronoi-based approaches with other nature-inspired algorithms such as ant colonies optimization, particle swarms optimization and genetic algorithms to maximize the coverage of a region of interest, as shown in Table 1.

Table 1: Hybridization of Voronoi and other optimization algorithms (ACO), (PSO) and (GA)

	Hybridization methods	Functioning	Impact
Voronoi + ACO [30, 38,39]	Voronoi: determine all the possible paths in a network ACO: identify the shortest path among all the paths generated by Voronoi	Assign weight values to the Voronoi edges for the routing path search.	-Nodes distribution -Weight values - Evaluation function.
Voronoi + PSO [27, 40, 41]	Voronoi: detect coverage holes in a region of interest PSO: generate Voronoi vertices (virtual points) or random endpoints to reduce power consumption and maximize the network lifetime.	Generate virtual points from the detected holes. The detection range is sometimes changed.	-Virtual points -Nodes localization -Nodes speed -Best local or global solution.
Voronoi + GA [42, 43, 44]	Voronoi: detect coverage holes in a region of interest GA: generate new candidate solutions (i.e. new node locations) to maximize the coverage of a region of interest.	Detection of holes, then repositioning of the nodes to be developed with the modification of the level of nodes distribution	-Impact on the evaluation function. -Impact on the hole coverage rate -Adding sometimes other mobile nodes to the detected holes

Many works are based on the hybridization of Voronoi and ant colonies optimization (ACO) for node deployment in a network. Moreover, VD was primarily used to optimize path planning to ensure efficient communication between the different nodes of the network. The most important roles of ACO are to: i) find connection paths in a network and ii) to search and adapt to the shortest path [45].

Hybridizations of Voronoi and particle swarm optimization (PSO) to maximize coverage and extend the network lifetime were also proposed in several works. For instance, in [46, 47], the VD was used to detect coverage holes and to assess fitness function, while the PSO was utilized to determine the next position of the sensor nodes in a given region of interest. In these studies, a centralized node was employed to collect data about the positions of all nodes, knowing that each node had prior knowledge about its own location as well as those of all other nodes. Then, calculations were done to determine the new locations of each node in the network. The fitness function can be generally applied either to minimize coverage holes or to reduce power consumption.

The literature review demonstrates that few studies combined GA with VD to solve the problem of object collection network deployment and re-allocation. This combination was also successfully used to improve the network coverage and extend its lifetime. However, despite their importance, these approaches applied the fitness function developed by a GA to assess candidate solutions and, then, select the next node positions. Moreover, the VD was only utilized to detect the coverage holes. Another limitation of these methods is that the solutions generated by GA are initialized inside the cells of D V. Despite the importance of these approaches, they have some limitations. In fact, the solutions generated by GA were initialized, in these works, inside the cells of VD. Besides, the nodes constituting the object collection network were put far from or towards their neighbors to minimize the coverage of the holes [47, 42, 43]. Moreover, new nodes were sometimes added at the specified locations to cover the holes [48]. Overall, these approaches were performed using knowledge about the locations of the nodes.

2.2. Parallel and distributed architecture of GA

As shown in the literature, in GA genetic algorithms, many operators can be executed independently of each other. The efficiency of parallel GAs is to find the desired solution in the shortest time with better performance. Indeed, these algorithms are frequently used to solve large problems and ensure substantial performance gains [49, 50]. Most of these algorithms have been run on huge number of parallel machines and their efficiency depends on the parallel computing system. In most of these problems, the ratings of the fitness function can be calculated independently for each candidate solution. In other words, each candidate solution can be computed at the same time (in parallel).

The major objective of using this parallel architecture consists in reducing the execution time and minimizing the number of resources required by GAs. Genetic operations on individuals, such as crossbreeding as well as population mutation and evaluation, can be performed in parallel. The main idea of most parallel programs is to divide tasks into smaller sub-tasks and execute them simultaneously on different nodes. This approach can be applied to genetic algorithms in different ways.

The fundamental difference between these different implementations is to use a single population or to divide it into sub-populations. According to [51], the PGAs (Parallel Genetic Algorithms) can be classified into three main categories as shown in Fig.1:

-The Master-Slave model [52, 53]: In this model, there is a master node that manages all sub-populations and distributes the individuals among the slave nodes. Then, the fitness values of the individuals are calculated in the corresponding slave nodes.

-The Coarse-Grained model: It is a distributed model [53] where the population is first divided into many sub-populations located in several "islands". Then, the GA operates independently in each "island". Since each island contains only partial individuals of the population, these islands exchange periodically information by migrating certain individuals to give diversity to the population [54, 55]. The model can execute all GA operators in parallel and distributed computing, so that different "islands" can explore periodically various parts of the search space.

-The Fine-Grained model: It is also called “cellular model” or “grid model”. It is applied to structure a population into quarters and place some individuals in a node. In this model, the GA is performed in parallel calculation to evaluate the fitness value of each chromosome and apply locally the GA operators. That is to say, selection, crossbreeding and mutation are executed on adjacent neighbors. Based on the massively-parallel architecture, fine-grain model can significantly speed up the evaluation of all chromosomes. However, this cannot be done only by using a massive clustering system to manage this model [56].

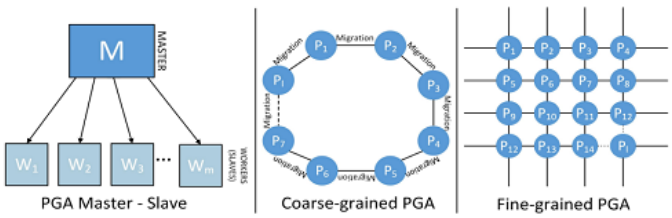

Figure 1: Different types of parallel Genetic Algorithms [57]

The objective of this study is to design a distributed approach where the hybridization of the Voronoi diagram and the GA is executed in parallel in several nodes. The VD is essentially used to divide the region of interest into cells and generate initial solutions that present the initial population of the GA. Then, this population will be divided into in sub-populations which will be, later, distributed to the different nodes constituting the employed data collection network. Afterwards, a genetic algorithm will be executed in parallel in each of these nodes. Each node will return its best solution having the maximum coverage in a RoI.

3. Research Design

3.1. Distributed strategy

In our proposed approach (Figure 2), two types of nodes are used: Voronoi nodes and Genetic nodes. The former (V.Node) generate solutions presenting the initial population which will be subdivided into sub-populations and send them to genetic nodes (G.Node). The hybridization of the two algorithms is done mainly at each G.Node. Subsequently, the fitness values of individuals are calculated in each G.Node to improve coverage. Finally, the found optimal solutions will be returned to the V.Node. As the suggested approach is based on two-way communication, it cannot be the Master-Slave model.

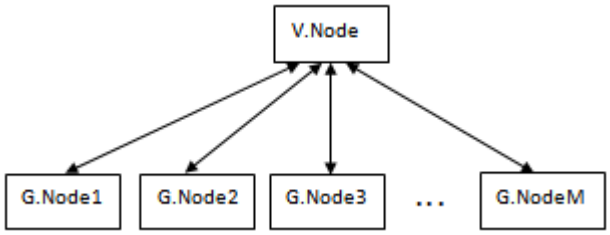

Figure 2: Proposed distributed architecture

Our major aim consists in developing a protocol that allows managing and carrying out communication between the different nodes in the approach presented in Fig. 2. This protocol is the core of the "ESP-NOW" protocol that presents a library under Arduino. According to [58], ESP-NOW, permits several electronic cards to communicate with each other based on direct links between nodes to form an ad-hoc network without using a Wi-Fi access point as an infrastructure. In fact, it is similar to high-speed wireless connectivity which allows the exchange of small 2.4GHz frequency bands data packets with low consumption in ESP-NOW.

To develop our protocol and design our distributed approach, we used the same type of nodes “M5StickC ESP32-PICO Mini IoT Development Kit” [59].

The introduced approach is based on dividing the initial population into smaller sub-populations and simultaneously performing the corresponding tasks on different nodes. For example, a population of 300 solutions generated by V.Node is distributed over 10 nodes (G.Nodes); each of which implements a population of 30 individuals. According to Fig. 3, the proposed protocol is

utilized in four types of frames; each frame has a payload of up to 250 bytes that can be transported:

- SPF: A Frame-Sub-Population contains M Voronoi solutions and it is sent from V.Node to all G.Nodes
- RF: Result-Frame includes the optimal solution of each node. After the execution of its algorithm, each G.Node returns a RF frame to the V.Node.
- FPF: Final-Position-Frame involves the final position of each node. The V.Node gathers all the RF frames returned by each G.Node and, subsequently, selects the best solution which presents the maximum obtained coverage.
- ACK: or Acknowledgment, transmitting in both directions (Figure 3), used to inform the application layer about the transmission success or failure of each type of frame.

The greatest amount of information is observed at the SPF frame. In this case, segmentation can be carried out at the TCP / IP layer; hence the SPF frame will be subdivided into sub-frames.

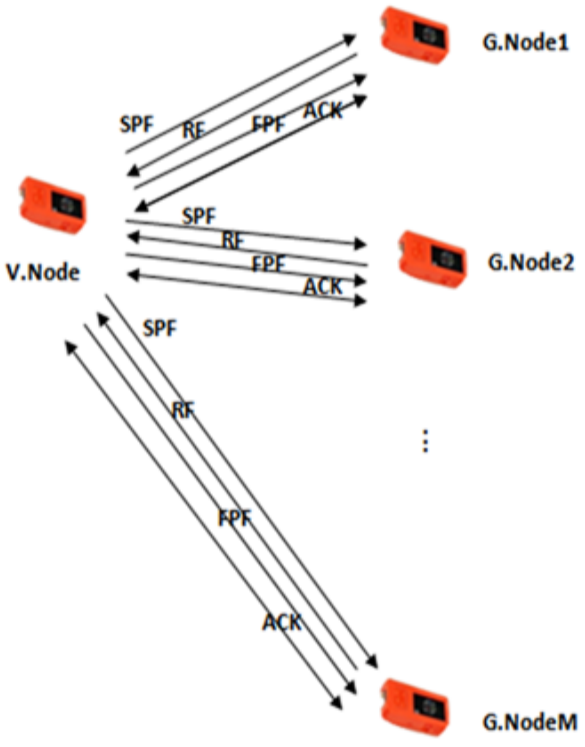

Figure 3: Proposed network architecture

Another criterion of the proposed protocol consists in automatically connecting one of the used devices to its counterpart to continue communication if it is suddenly reset or if there is a loss of power when it restarts.

Figure 4 shows a sequence diagram of our communication protocol applied on three nodes; each of which has a transmission role and a reception role (T / R) data frame. The V.Node in the middle and the two G. Nodes are on the left and right. At the instant t = 0, the V. Node generates first the

Voronoi solutions and, then, distributes them to the different G.Nodes. In this example, the generated Voronoi solutions are distributed over 6 SPF frames. The first three frames are those of G.Node n° 1, while the remaining frames are those of G.Node n ° 2. The sending delay of each frame is equal to 10ms. In fact, each G. Node receives its SPF frames that present the initial population to execute its VD-GA algorithm. After execution, each G.Node sends the found solution in an RF frame. The V.Node always "listening", gathers all the RF and applies the best found solution (the solution having the best coverage). This solution will be disseminated on G.Node by the FPF frame.

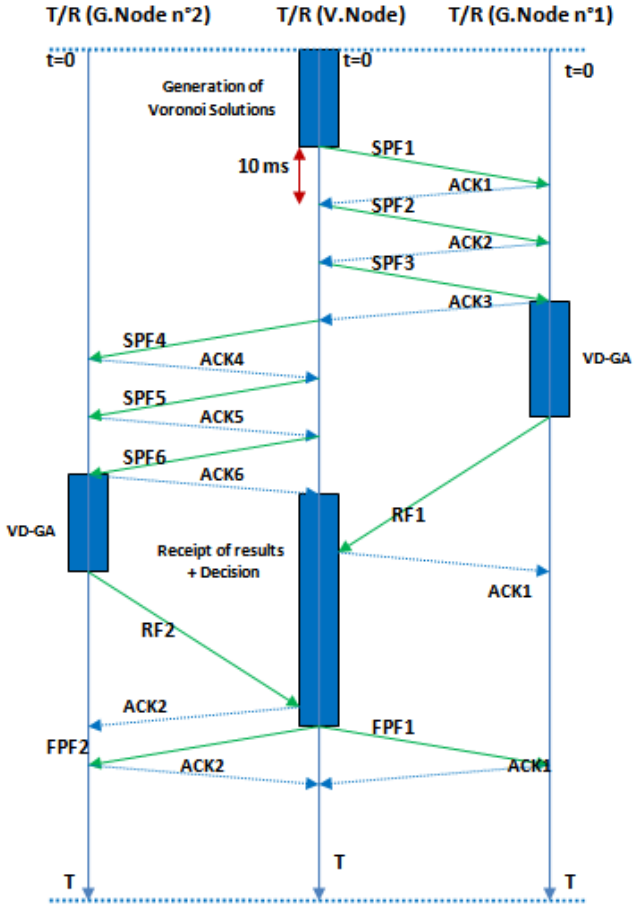

Figure 4: Sequence diagram of the proposed protocol of communication between three nodes

3.2. Design of the distributed positioning algorithm

3.2.1. Deployment Scenario

As shown in Fig.5 the introduced approach starts by generating the Voronoi solutions in V.Node that subdivides the latter into sub-populations; each of which will be assigned to a G.Node. The process independently develops its population until it decides to bring together its best individuals who will be candidates at the decision stage.

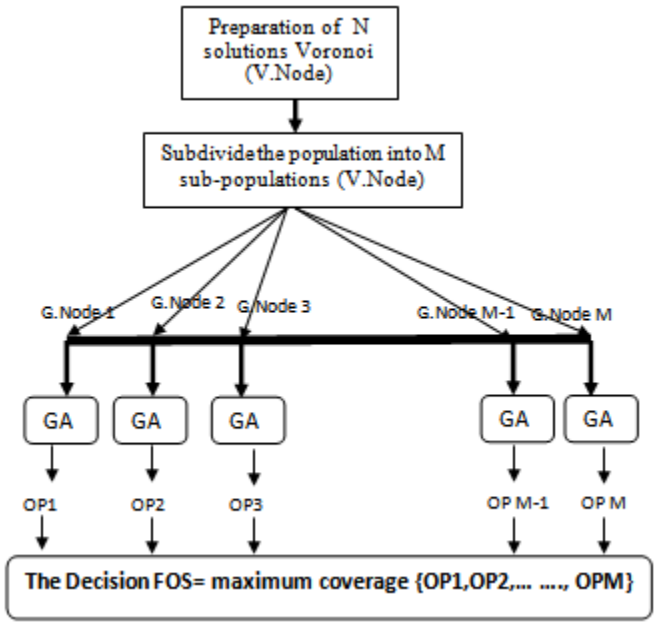

Figure 5: Functioning of the proposed approach

3.2.2. *Deployment scenario: A hybrid optimization algorithm*

This algorithm starts with implementing a Voronoi diagram to generate initial solutions (Pop initial) and, then, subdividing it into sub-populations (lines 2 and 3). Afterwards, the genetic algorithm is executed in parallel on all G.Nodes until a desired maximum coverage will be obtained (from line 3 to line 7 of the algorithm). The inputs of the algorithm are: M (the number of nodes to deploy), N-solutions (the number of solutions to generate by V.Node), dimension of region of interest, pop_size (the size of the population), the desired coverage (stop condition) or a given number of iterations.

Algorithm 1: VD-GA Voronoi-Genetic.

0) Define the evaluation function f (Maximum desired coverage);
1) Pop initial ← N solutions generated by the Voronoi diagram;
2) Subdivide the initial population initial (Pop)
3) Do it in parallel
4) Apply the AG on each G.Node Node (M Voronoi solutions for each node):
Repeat
a) Selection
b) Crossbreeding
c) Mutation
UNTIL the coverage will be converged
5) Find the best solution among all solutions generated by each node
6) Go to 3 or Stop,
7) **End** of parallelism,
8) Return the best Solution.
9) Assignment of the final position

Voronoi Diagram

Generally, VDs are used in networking to find collision-free paths. Therefore, they are employed to construct paths in cartes. To deploy node in data collection networks, we utilized the VD to generate initial solutions presenting the positions of the deployed IoT objects.

Let S be a finite set of n points on the map (as shown in Figure 6), a Voronoi region associated with an element p of S is the set of points of S which are closest to p.

$$Vors(p) = \{x \in \mathbb{R}^2 \ \forall q \in S \| x - p \| \leq \| x - q \| \} \quad (1)$$

Where $\| x - p \|$ is the distance between x and p.

Genetic algorithm

In this paper, we apply the standard GA with some adequate modifications explained in the following sections. The GA process begins with a set of individuals constituting a set of randomly-generated possible solutions called population. This genetic process is repeated until a stop condition is met.

- **Chromosomes coding**: This step aims at presenting an individual that presents a solution (the position of each node in a given region of interest). Fig. 6 illustrates a chromosome showing a feasible solution in the search space, an example of individual representation, with n = 6 objects and k = 1 (a single type of node).

Object1	Object2	Object 3	Object 4	Object5	Object 6
(x_1,y_1)	(x_2,y_2)	(x_3,y_3)	(x_4,y_4)	(x_5,y_5)	(x_6,y_6)

Figure 6: Representation of a chromosome in the GA

Initial Population: The GA process generally begins with an initial population which presents the set of all individuals used to find the global solution. In our approach, the initial population presents a subpopulation received and generated by the V.Node (the node which will generate the initial solutions).

Fitness Function: The objective of our approach is to determine the best positions that guarantee the maximum coverage of RoI. The fitness function is usually applied in GA to assess and identify the best-found solutions.

$$\text{Fitness} = S - \sum_{i=0}^{n} surfacesofallcircles \quad (2)$$

Where S denotes the region of interest (RoI) area and n is the number of deployed objects. The more the difference between S and the sum of all the areas of the objects decreases, the more the coverage increases. If there is no overlap between two objects, the distance separating them will be equal to or greater than 2r, as exposed in Figure 7 (b):

$$X = 2r - \text{distance}(p1, p2) \quad (3)$$

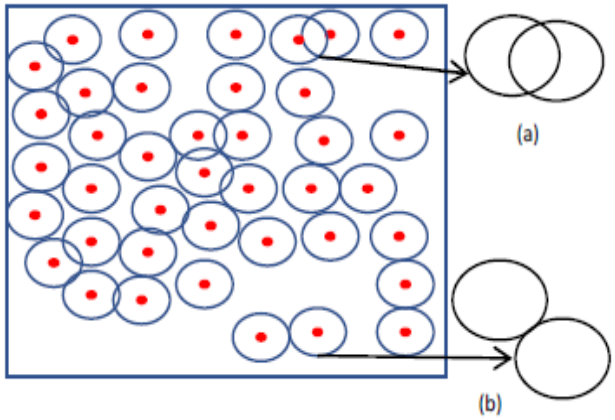

Figure 7: Objects overlap [37]

Selection of individuals: It consists in selecting two chromosomes as parents of the population to produce two new individuals.

Crossbreeding: A random point in the two selected individuals is chosen to exchange genes after this point.

Mutation: It consists in randomly choosing and mutating a gene in our approach, i.e. changing the position of a node within the individual. The mutation guarantees diversity and avoids premature convergence by sufficiently exploring the research space to bring innovation to the population.

Stopping condition: Two stopping criteria were used in our experiments: the coverage rate and the maximum number of generations.

4. Results and discussions

To evaluate the introduced distributed approach of node deployment by applying our VD-GA algorithm in a field of interest, a real prototyping is suggested. It was tested in a real environment with experiments carried out on a testbed containing of 6 to 10 nodes. Before this prototyping, we started with simulations.

4.1. Simulations

To evaluate our VD-GA algorithm with a distributed approach, we used OMNET ++ in the simulations. First, the DV was applied on a RoI of 80 * 80 meter. The DV divides this region into a set of Voronoi cells to generate a population of 100 solutions (individuals) that present the positions of each IoT object in a 2D plan. Then, this population was divided into sub-populations over 20 nodes; each of which has a detection range of 10 meters. The choice of the parameter values is based on empirical tests and on our previous studies presented in [37]. Table 2 shows the used simulation parameters.

Subsequently, the GA was executed on each node in parallel to optimize the solutions found by the VD by replacing the nodes in order to find the best positioning for them in the RoI and, subsequently, to obtain the maximum degree of coverage. Figures 8 and 9 show the difference, in terms of the degree of coverage, between the initial random coverage, generated only by the Voronoi diagram, and the degree of coverage provided by the proposed VD-GA.

Table 2: The simulations parameters

Parameters	
Population size: Number of individuals	100
Number of iterations	[100….1500]
Number of deployed objects	20
Crossover rate	0.9
Mutation rate	0.1
Size ROI	80*80
Stopping Condition	94%

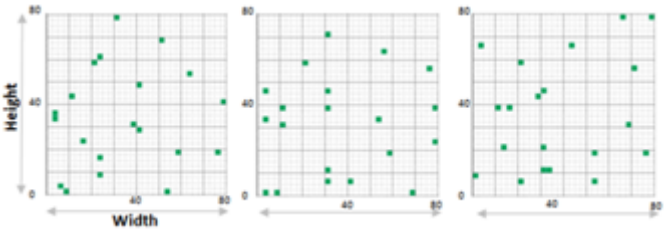

(a) Solution (b) Solution 2 (c) Solution 3

Figure 8: Deployment of 20 nodes by VD (example of 3 solutions)

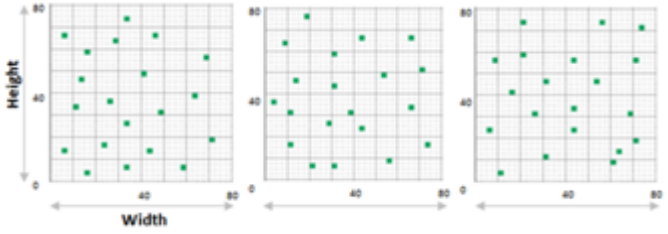

(a) Solution 1 (b) Solution 2 (c) Solution 3

Figure 9: Deployment of 20 nodes after executing VD-GA (example of 3 solutions)

Figure 10 clearly reveals the difference in terms of coverage between random deployment, deployment using only the VD, deployment utilizing only the GA and deployment of hybridization between VD and GA. It is obvious, in this figure, that the degree of coverage is improved as the number of GA iterations increases. It is also noticed that the GA outperforms the DV for a number of GA iterations inferior to 100. On the other hand, the GA gives a better degree of coverage during more than 100 iterations. The hybrid (VD-GA) is more efficient than VD and GA, if used separately during a number of GA iterations exceeding 56.

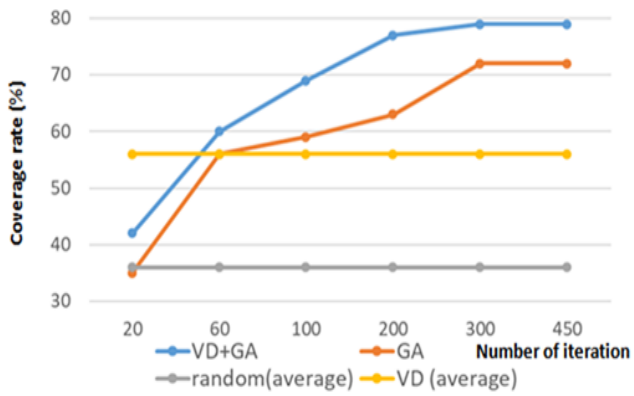

Figure 10: Comparison of the coverage degrees according to the Number of iterations for VD, GA and VD-GA

Figure 11 shows the increase of the coverage degree after each iteration in VD-GA.

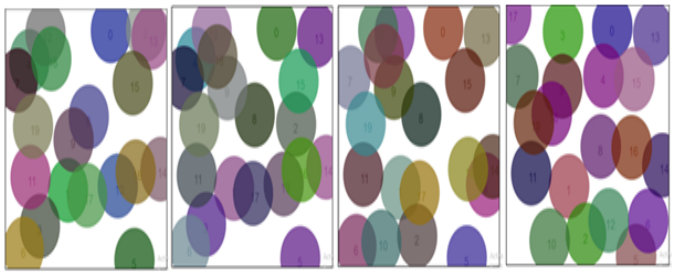

Iteration 1: 61% Iteration 20: 72% Iteration 100: 83% Iteration 197: 91%

Figure 11: Distribution of 20 nodes in a 80*80 region

Figure 12 shows the evolution of the GA execution over the first 15 iterations. This algorithm started with 58% coverage. After the operations of selection, crossbreeding (between Parent 1 and Parent 2) and mutation, the coverage could be calculated by applying the fitness function. In fact, if this degree of coverage increased, the new parents would be Fetus 1 and Fetus 2. Otherwise, a new selection will be executed.

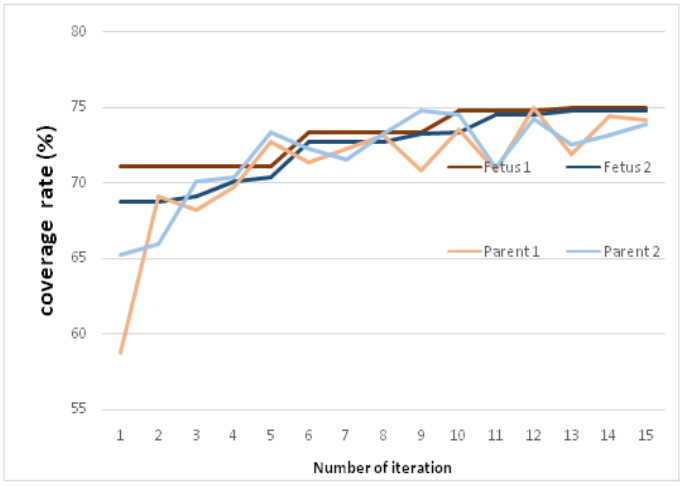

Figure 12: Functioning of GA in each node

4.2. Testbeds setting

A real testbed implementing several real nodes was designed and organized in a wireless network. Only one type of node was used in our experiments; it is the M5StickC node of the M5Stack family powered by ESP32, are electronic cards equipped with a 4 MB Flash memory, a 2.4G antenna, an IR transmitter, a microphone, buttons, LCD screen (0.96 inch), and built-in Lipo Battery as demonstrated in Figure13 M5StickC nodes can be developed on UIFlow, MicroPython and Arduino platforms.

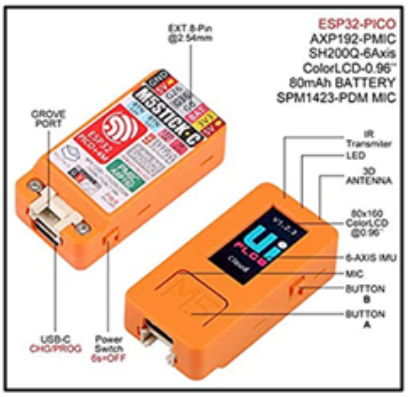

Figure 13: The used M5StickC ESP32 Mini IoT nodes [59]

Table 3: presents the used experimentation parameters

Parameters	
Population size: Number of individuals	100
Number of iterations	[400….1500]
Number of deployed objects	06
Crossover rate	0.9
Mutation rate	0.1
Size of RoI	25* 17 (2 floor)
Stopping conditions	94%
Threshold of the received result	80%

06 M5StickC nodes were deployed in an apartment composed of a ground floor and 2 other floors; each has a surface area of 25 * 17 meters. The ground floor and the first floor contain separately six bedrooms, a wall separation whose thickness ranges from 20 to 30 cm between 2 neighboring bedrooms (as shown in Figure 14) and a 30-cm concrete ceiling between the two floors. The second floor is a free space. The transmission range of the nodes was in an interval of 10 to 18 meters, depending on the obstacles encountered during transmission. The RSSI (Received Signal Strength Indicator) and FER (Frame Error Rates) were calculated. The transmission power of Wi-Fi was 100 mW. Due to the stochastic nature of optimization algorithms, the optimization process was performed 30 times and an average value was computed for all values presented in the next figures.

We noticed that most G.Nodes found their optimal solutions within the same timeframe, while there are other nodes which take longer time for data recovery and decision making to seek the best solution. Since our stop condition was defined by a desired coverage, a new parameter "Received result threshold" was added. For example, if 10 nodes were deployed and if the result threshold was set to 80%, the V.Node would force the process to stop and take the decision as soon as it received the results of 8 G.Node.

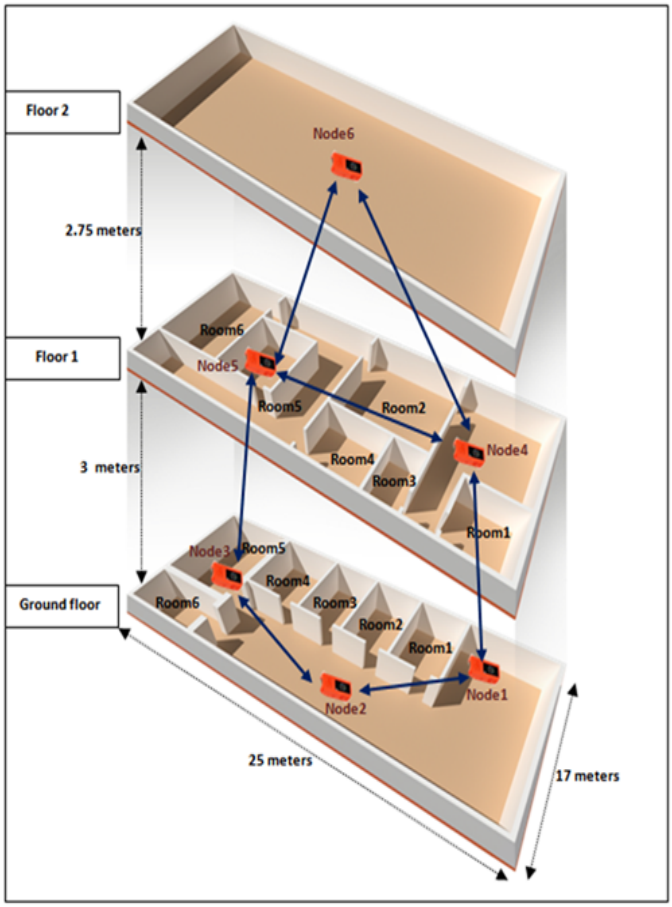

Figure 14: RoI of experimental tests

4.3. Results of evaluation of the proposed GA-VD algorithm

In this section, we compare the results obtained by the distributed approach proposed in the present work with those provided by a centralized approach in terms of percentage of found coverage and execution time. Moreover, the execution of GA, where we can use the mutation operation twice in each generation, is compared to use one mutation Third comparison on energy consumption in the two approaches. Fourth comparison with the average RSSI rates and the number of neighbors of the nodes. These results were provided with an execution average of 40 times.

4.3.1. Comparisons of the centralized approach and our distributed approach

We re-evaluated our previous study [37] on a single M5StickC node. That is to say, the all processing was performed on a single node; hence the use of a centralized approach based on a single population generated by the DV and combined with GA.

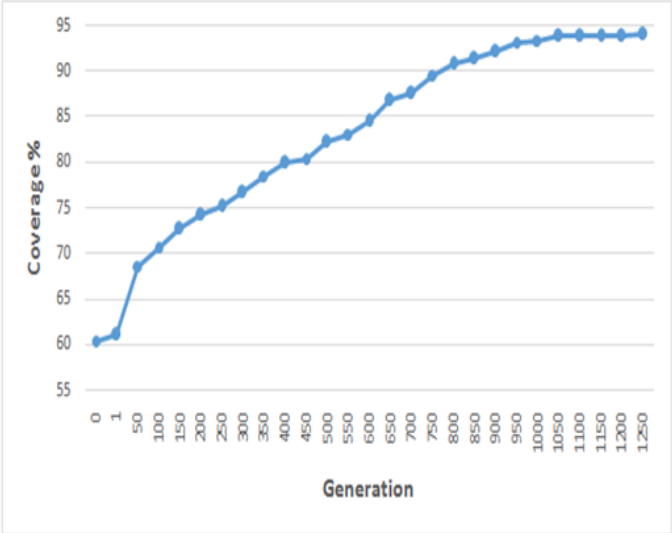

Figure 15: Coverage rate obtained by the centralized approach

As revealed in Figure 15, 94% coverage was provided by the centralized approach in the 1250th iteration.

Figure 16 shows the coverage rate of six nodes used in a distributed approach. Obviously, the nodes achieved their desired coverage (94%) at different numbers of iterations. For instance, node 4 attained its coverage in the 706th iteration, while node 5 found its cover in iteration number 952.

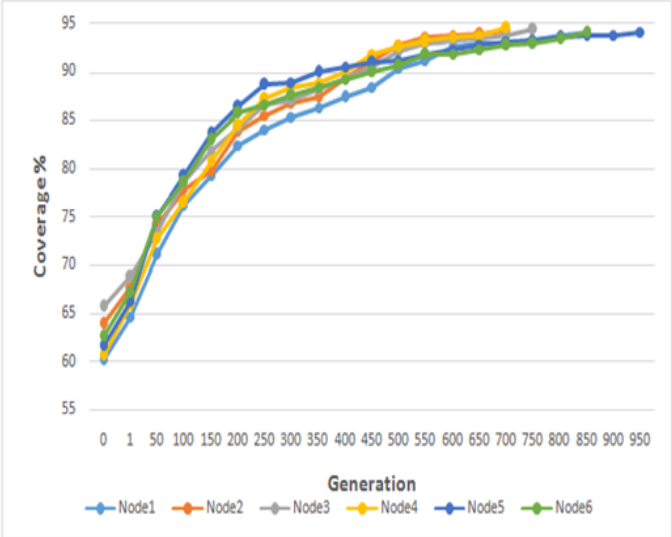

Figure 16: Coverage rate obtained by the distributed approach for the six nodes

The objective of these evaluations is to compare the coverage rate of the distributed approach with that of the centralized one.

We measured the percentage of surface coverage in the 2 approaches with a stop condition of 94%. In the distributed approach, we summed the averages of the results received from the different nodes that reached this coverage rate. We can clearly notice that a distributed

approach reached the goal in the 800thgeneration, while the centralized approach continued to run for 450 more iterations, as illustrated in Figure 17.

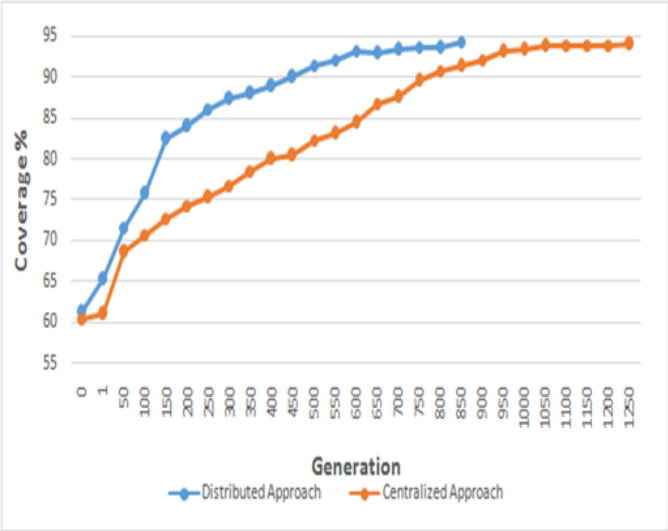

Figure 17: Comparison of the coverage rate obtained by the distributed approach with that provided by the centralized approach

Although in a distributed approach, there is a computational time cost (e.g. the time required to distribute the sub-populations to each node, the execution time and the time of returning the found solution), the graph presented in Figure 18 clearly shows that the distributed approach ended its operation in shorter time than that required by a centralized approach. This result can be explained by the cost of calculating the fitness function of each individual in a large population used in the centralized approach.

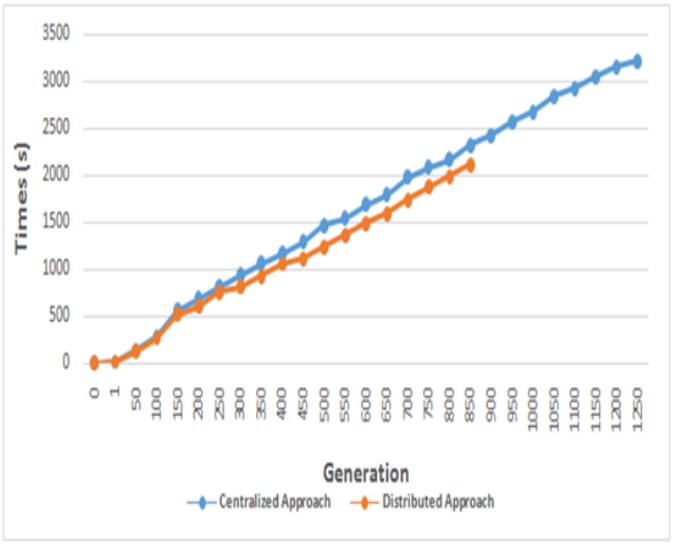

Figure 18: Average computing time required by the centralized approach and distributed one

4.3.2. *Evaluation of the proposed algorithm in terms of energy consumption*

Energy consumption is a parameter widely used to compare the two approaches. For this reason, in the conducted experiments, all nodes were fully charged (100%) at the same time. In the distributed approach, we calculated the average energy consumption of all nodes used in this approach. Tab.4 presents a comparison of the two approaches in terms of level of charge of battery. It also shows that an M5StickC node in the centralized approach consumed approximately 54% of the total energy until it stopped operating, versus 28% for the distributed approach.

Table 4: Battery charge level

Times (S)	0	500	1000	1500	2000	2500	3000
Centralized Approach	100 %	96 %	86%	71%	65%	57%	46%
Distributed Approach	100 %	96 %	83%	77%	72%	----	---

4.3.3. *Evaluation of the proposed algorithm with double mutation*

In a GA, after the selection and crossbreeding operations, each individual will participate in a mutation at a given time point. Usually, the location of the mutant gene that will be replaced with a different value is random. In this section, we compare the result provided by the proposed VD-GA hybridization in a distributed approach, which uses a single mutation, with those obtained by double mutation, i.e. instead of changing the position of a single node, we change the position of both nodes at the same time.

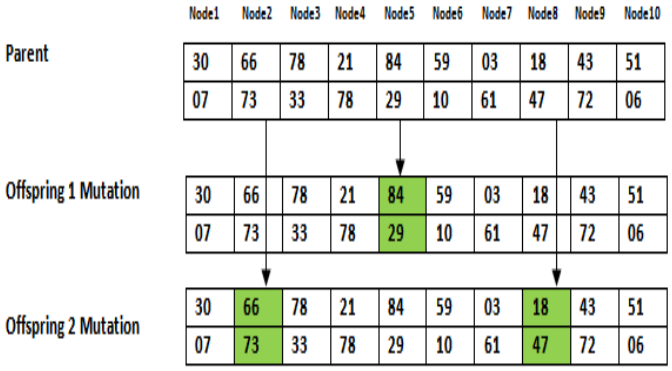

Figure 19: One-point and two-point mutation operator

Figure 19 illustrates an example of deploying 10 nodes in a 2D plane. For example, after the executing a single mutation, node 5, which is at position (84, 29), will be at position (24, 53). For the double mutation, two objects will be repositioned, node 2 (66, 73) will be at position (29, 79) and, at the same time, node 8 (18, 47) will be at position (68, 32).

After applying the introduced VD-GA hybridization in a distributed approach, a GA was used with a single mutation ending after about 800 iterations. However, a GA with two mutations required more than 750 iterations

to achieve 90%of surface coverage, as revealed in Figure 20.

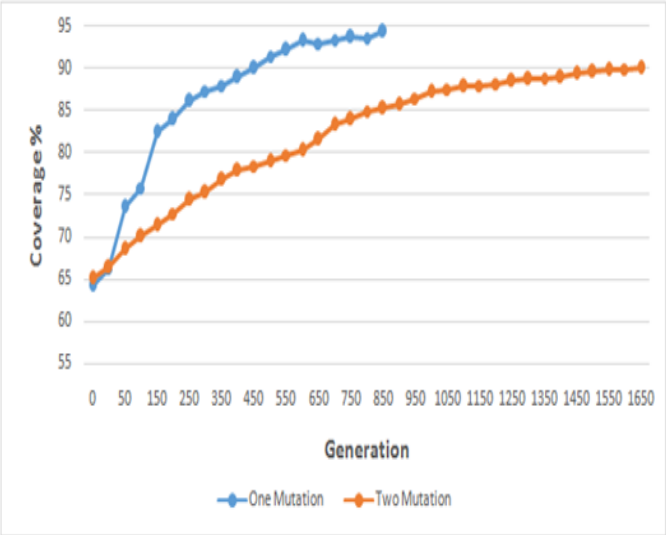

Figure 20: Comparison of one-point and two-point mutation operator

4.3.4. Evaluation of the genetic-Voronoi algorithm according to network metrics (RSSI, lifetime and number of neighbors)

RSSI or Received Signal Strength Indicator is a measure of a device's ability to receive a signal from an access point or router. This value helps determine if there is enough signal to establish a good wireless connection. The RSSI value is retrieved from the client device's Wi-Fi card, it is not the same as the transmit power from the router or AP.

Tables 5, 6 and 7 represent the average values of RSSI, lifetime and number of neighbors of the used nodes.

Table 5: Average values of number neighbors for 6 nodes

Node	VD	GA	VD+GA
1	132.39	131.83	137.28
2	135.28	128.92	136.64
3	131.23	125.17	131.55
4	114.72	116.28	115.21
5	89.29	92.88	91.53
6	129.82	127.76	129.16

Table 5 shows high values of RSSI issued from the nodes positioned according to the proposed hybrid genetic-Voronoi algorithm (VD+GA). The superiority of these RSSI values indicated a better ability of localization of nodes using the genetic-Voronoi algorithm.

Table 6: Average values of lifetime (in seconds) for 6 nodes

Node	VD	GA	VD+GA
1	1298	1367	1693
2	987	927	996
3	1029	1035	1083
4	703	749	753
5	870	883	892
6	943	932	921

Table 6 illustrates high lifetimes of nodes positioned according to the proposed hybrid genetic-Voronoi algorithm (VD+GA). This indicated a better ability of coverage (deployment) of nodes using the genetic-Voronoi algorithm.

Table 7: Average values of number neighbors for 6 nodes

Node	VD	GA	VD+GA
1	4.23	4.65	4.98
2	3.22	3.41	3.56
3	2.68	2.91	3.02
4	3.56	3.86	3.94
5	4.29	4.44	4.62
6	3.12	3.42	3.68

Table 7 indicates high numbers of neighbors of the nodes deployed according to the suggested VD+GA. The superiority of this number of neighbors reflects the better quality of connectivity of nodes using the genetic-Voronoi algorithm.

It can be deduced from tables 5, 6 and 7 that the proposed VG+GA algorithm achieved better results regarding highest RSSI average values, highest lifetime average values and highest number of neighbors average values. This can be explained by the advantage of the hybridization and the distribution. Indeed, the hybrid model takes advantages of the both genetic and Voronoi process in finding the most appropriate solutions for the repartition of the nodes. Moreover, the distribution allows a better managements of the computation tasks when calculating the costs of possible solutions and its corresponding evaluation network metrics (RSSI,...) which, in turn, ameliorate the quality of solutions.

4.4. Discussion and interpretations

Our VD-GA hybridization with a distributed approach shows better coverage, compared to the centralized approach. Our proposal used fewer nodes with better coverage, compared to other results [41, 42]. Moreover, a distributed approach with a GA that uses a single mutation is more efficient in terms of time calculation cost than a GA that uses two mutations.

By comparing the simulations, presented Fig.12 Fig.13 and Fig14, and the real experiments, shown in Fig.18, we notice that the distances separating some nodes are not the same. This difference can be explained by the existence of obstacles between two neighboring nodes in a real prototyping environment. The localization error obtained in the conducted indoor experiments was of the order of 20 cm, which is generally acceptable for indoor control systems and does not affect the results.

5. Conclusions and perspectives

In this study, the problem of deploying objects in an indoor data collection network was studied. The proposed

approach was used in two contributions: The first was to combine between a Voronoi diagram and the genetic algorithm, while the second is to design a distributed approach. VD was also applied to randomly generate the locations of IoT objects. These locations present the initial population that would be subdivided into sub-populations; each of which was assigned to a G.Node. The GA was applied to determine the best locations of objects. Compared to other approaches, that proposed in this manuscript allowed enhancing the deployment solution. The only encountered obstacle is that the memory size of an M5StickC node did not allow our approach to be executed when the number of nodes to be deployed exceeded 58 nodes. As a future study, the aim is to propose other models of hybridizations of the geometric deployment methods (other than VD) and optimization algorithms (other than GA).In addition, another future research direction is to evaluate the behavior of the proposed VD-GA on large-scale experimental environments in which the number of nodes exceeds 100.Since hybrid models generally have high complexities [60], we propose to establish an analysis of the temporal and algorithmic complexity and a statistical study in order to prove the scalability of the proposed model.

References

[1] P. Asghari, A. M. Rahmani, H. H. S. Javadi, "Internet of Things applications: A systematic review," *Computer Networks*, vol. 148, pp. 241–261, 2019, doi:10.1016/j.comnet.2018.12.008.

[2] D. C. Nguyen et al., "Federated Learning for Internet of Things: A Comprehensive Survey," *IEEE Communications Surveys and Tutorials*, vol. 23, no. 3, pp. 1622–1658, 2021, doi:10.1109/COMST.2021.3075439.

[3] A. A. Laghari et al., "A Review and State of Art of Internet of Things (IoT)," *Archives of Computational Methods in Engineering*, no. July, 2021, doi:10.1007/s11831-021-09622-6.

[4] V. H. Puar et al., Communication in internet of things, vol. 672, (Springer Singapore, 2018).

[5] J. Yick, B. Mukherjee, D. Ghosal, "Wireless sensor network survey," *Computer Networks*, vol. 52, no. 12, pp. 2292–2330, 2008, doi:10.1016/j.comnet.2008.04.002.

[6] P. Rawat et al., "Wireless sensor networks: A survey on recent developments and potential synergies," *Journal of Supercomputing*, vol. 68, no. 1, pp. 1–48, 2014, doi:10.1007/s11227-013-1021-9.

[7] J. Zheng, A. Jamalipour, Wireless Sensor Networks: A Networking Perspective (2008).

[8] Dulman, Stefan, and Paul JnM Havinga, "Introduction to wireless sensor networks." Networked Embedded Systems. CRC Press, 2017. 3-1.

[9] B. Rashid, M. H. Rehmani, "Applications of wireless sensor networks for urban areas: A survey," *Journal of Network and Computer Applications*, vol. 60, pp. 192–219, 2016, doi:10.1016/j.jnca.2015.09.008.

[10] M. Pule, A. Yahya, J. Chuma, "Wireless sensor networks: A survey on monitoring water quality," *Journal of Applied Research and Technology*, vol. 15, no. 6, pp. 562–570, 2017, doi:10.1016/j.jart.2017.07.004.

[11] M. S. Pragadeswaran, M. S. Madhumitha, D. S. Gopinath, "Certain Investigations on Military Applications of Wireless Sensor Networks," *International Journal of Advanced Research in Science*, Communication and Technology, vol. 3, no. 1, pp. 14–19, 2021, doi:10.48175/ijarsct-819.

[12] J. Yang et al., "Integration of wireless sensor networks in environmental monitoring cyber infrastructure," *Wireless Networks*, vol. 16, no. 4, pp. 1091–1108, 2010, doi:10.1007/s11276-009-0190-1.

[13] H. Wang, J. Wang, M. Huang, "Building a smart home system with WSN and service robot," *Proceedings - 2013 5th Conference on Measuring Technology and Mechatronics Automation*, ICMTMA 2013, pp. 353–356, 2013, doi:10.1109/ICMTMA.2013.90.

[14] H. Durani et al., "Smart Automated Home Application using IoT with Blynk App," *Proceedings of the International Conference on Inventive Communication and Computational Technologies*, ICICCT 2018, pp. 393–397, 2018, doi:10.1109/ICICCT.2018.8473224.

[15] Y. J. Chang et al., "Wireless sensor networks for vital signs monitoring: Application in a nursing home," *International Journal of Distributed Sensor Networks*, vol. 2012, 2012, doi:10.1155/2012/685107.

[16] D. Chen et al., "Natural disaster monitoring with wireless sensor networks: A case study of data-intensive applications upon low-cost scalable systems," *Mobile Networks and Applications*, vol. 18, no. 5, pp. 651–663, 2013, doi:10.1007/s11036-013-0456-9.

[17] N. Assad et al., "Efficient deployment quality analysis for intrusion detection in wireless sensor networks," *Wireless Networks*, vol. 22, no. 3, pp. 991–1006, 2016, doi:10.1007/s11276-015-1015-z.

[18] A. Patzer, "Deployment Techniques," JSP Examples and Best Practices, pp. 215–230, 2002, doi:10.1007/978-1-4302-0831-0_10.

[19] M. Cardei, D. Z. Du, "Improving wireless sensor network lifetime through power aware organization," *Wireless Networks*, vol. 11, no. 3, pp. 333–340, 2005, doi:10.1007/s11276-005-6615-6.

[20] T. S. Panag, J. S. Dhillon, "Two Stage Grid Classification Based Algorithm for the Identification of Fields Under a Wireless Sensor Network Monitored Area," *Wireless Personal Communications*, vol. 95, no. 2, pp. 1055–1074, 2017, doi:10.1007/s11277-016-3813-8.

[21] F. Nematy et al., "Ant colony based node deployment and search in wireless sensor networks," Proceedings - 2010 *International Conference on Computational Intelligence and Communication Networks*, CICN 2010, pp. 363–366, 2010, doi:10.1109/cicn.2010.138.

[22] R. Priyadarshi, B. Gupta, A. Anurag, "Deployment techniques in wireless sensor networks: a survey, classification, challenges, and future research issues", *The Journal of Supercomputing, 1-41* vol. 76, no. 9, (Springer US, 2020).

[23] P. Rajpoot, P. Dwivedi, "MADM based optimal nodes deployment for WSN with optimal coverage and connectivity," *IOP Conference Series: Materials Science and Engineering*, vol. 1020, no. 1, 2021, doi:10.1088/1757-899X/1020/1/012003.

[24] S. Mnasri et al., "Improved Many-Objective Optimization Algorithms for the 3D Indoor Deployment Problem," *Arabian Journal for Science and Engineering*, vol. 44, no. 4, pp. 3883–3904, 2019, doi:10.1007/s13369-018-03712-7.

[25] Holland, J. Adaptation in natural and artificial system. Cambridge, MA: MIT Press,1992.

[26] S. Mnasri et al., "3D indoor redeployment in IoT collection networks: A real prototyping using a hybrid PI-NSGA-III-VF," *2018 14th International Wireless Communications and Mobile Computing Conference*, IWCMC 2018, no. July 2019, pp. 780–785, 2018, doi:10.1109/IWCMC.2018.8450372.

[27] J. Kennedy, R. Eberhart, "Particle swarm optimization PAPER - IGNORE FROM REFS," *ICNN'95-international conference on neural networks*, pp. 1942–1948, 1995.

[28] Y. Li, J. Cao, "WSN Node Optimal Deployment Algorithm Based on Adaptive Binary Particle Swarm Optimization," *ASP Transactions on Internet of Things*, vol. 1, no. 1, pp. 1–8, 2021, doi:10.52810/tiot.2021.100026.

[29] Karaboga, D. (2005). An idea based on honey bee swarm for numerical optimization. Technical Report-TR06, ErciyesUniversity.

[30] M. Dorigo, V. Maniezzo, A. Colorni, "Dorigo-Maniezzo-Colomi_the-Ant-System-Optimization-By-a-Colony-of-Cooperating-Agents," *IEEE Transactions on Systems*, Man, and Cybernetics-Part B, vol. 26, no. 1, pp. 1–26, 1999.

[31] W. T. Pan, "A new Fruit Fly Optimization Algorithm: Taking the financial distress model as an example," *Knowledge-Based Systems*, vol. 26, pp. 69–74, 2012, doi:10.1016/j.knosys.2011.07.001.

[32] K. M. Passino, "Biomimicry of Bacterial Foraging for Distributed Optimization and Control," *IEEE Control Systems*, vol. 22, no. 3, pp. 52–67, 2002, doi:10.1109/MCS.2002.1004010.
[33] S. He, Q. H. Wu, J. R. Saunders, "A novel group search optimizer inspired by animal behavioural ecology," *2006 IEEE Congress on Evolutionary Computation*, CEC 2006, no. March, pp. 1272–1278, 2006, doi:10.1109/cec.2006.1688455.
[34] M. El-Abd, "An improved global-best harmony search algorithm," *Applied Mathematics and Computation*, vol. 222, pp. 94–106, 2013, doi:10.1016/j.amc.2013.07.020.
[35] A. Kaveh, S. Talatahari, "A novel heuristic optimization method: Charged system search," *Acta Mechanica*, vol. 213, no. 3–4, pp. 267–289, 2010, doi:10.1007/s00707-009-0270-4.
[36] Rabanal, P., Rodrı´guez, I., & Rubio, F. Using river formation dynamics to design heuristic algorithms. Lecture Notes in Computer Science, 4618, 163–177,2007.
[37] W. Abdallah, S. Mnasri, T. Val, "Genetic-Voronoi algorithm for coverage of IoT data collection networks," *30th International Conference on Computer Theory and Applications*, ICCTA 2020 - Proceedings, no. December, pp. 16–22, 2020, doi:10.1109/ICCTA52020.2020.9477675.
[38] A. Pietrabissa, F. Liberati, G. Oddi, "A distributed algorithm for Ad-hoc network partitioning based on Voronoi Tessellation," *Ad Hoc Networks*, vol. 46, pp. 37–47, 2016, doi:10.1016/j.adhoc.2016.03.008.
[39] O. Banimelhem, M. Mowafi, W. Aljoby, "Genetic Algorithm Based Node Deployment in Hybrid Wireless Sensor Networks," *Communications and Network*, vol. 05, no. 04, pp. 273–279, 2013, doi:10.4236/cn.2013.54034.
[40] K. Eledlebi et al., "Autonomous deployment of mobile sensors network in an unknown indoor environment with obstacles," *GECCO 2018 Companion - Proceedings of the 2018 Genetic and Evolutionary Computation Conference Companion*, no. July, pp. 280–281, 2018, doi:10.1145/3205651.3205725.
[41] K. Eledlebi et al., "Voronoi-based indoor deployment of mobile sensors network with obstacles," *Proceedings - 2018 IEEE 3rd International Workshops on Foundations and Applications of Self* Systems*, FAS*W 2018, pp. 20–21, 2019, doi:10.1109/FAS-W.2018.00019.
[42] Jianmin zou et al., "Bio-inspired and Voronoi-based Algorithms for Self-positioning of Autonomous Vehicles in Noisy Environments," 2015, doi:10.4108/icst.bict.2014.257917.
[43] K. Eledlebi et al., "A hybrid voronoi tessellation/genetic algorithm approach for the deployment of drone-based nodes of a self-organizing wireless sensor network (Wsn) in unknown and gps denied environments," *Drones*, vol. 4, no. 3, pp. 1–30, 2020, doi:10.3390/drones4030033.
[44] Tahir, N.H.M.; Atan, F. A Modified Genetic Algorithm Method for Maximum Coverage in Dynamic Mobile Wireless Sensor Networks. J. Basic Appl. Sci. Res. 2016, 6, 26–32.
[45] Li, Y.; Dong, T.; Bikdash, M.; Song, Y.D. Path Planning for Unmanned Vehicles Using Ant Colony Optimization on a Dynamic Voronoi Diagra. *In Proceedings of the 2005 International Conference on Artificial Intelligence, ICAI* 2005, Las Vegas, NV, USA, 27–30 June 2005; pp. 716–721.
[46] N. A. B. Ab Aziz, A. W. Mohemmed, M. Y. Alias, "A wireless sensor network coverage optimization algorithm based on particle swarm optimization and voronoi diagram," *Proceedings of the 2009 IEEE International Conference on Networking, Sensing and Control, ICNSC* 2009, pp. 602–607, 2009, doi:10.1109/ICNSC.2009.4919346.
[47] Y. Qu, S. V. Georgakopoulos, "A centralized algorithm for prolonging the lifetime of wireless sensor networks using Particle Swarm Optimization," *2012 IEEE 13th Annual Wireless and Microwave Technology Conference*, WAMICON 2012, 2012, doi:10.1109/WAMICON.2012.6208432. 3221–3232.
[48] N. Rahmani et al., "Node placement for maximum coverage based on voronoi diagram using genetic algorithm in wireless sensor networks," *Australian Journal of Basic and Applied Sciences*, vol. 5, no. 12, pp. 3221–3232, 2011.
[49] P. M. Pardalos et al., "Parallel search for combinatorial optimization: Genetic algorithms, simulated annealing, tabu search and GRASP," *Lecture Notes in Computer Science (including subseries Lecture Notes in Artificial Intelligence and Lecture Notes in Bioinformatics)*, vol. 980, pp. 318–331, 1995, doi:10.1007/3-540-60321-2_26.
[50] D. E. Goldberg, "Sizing populations for serial and parallel genetic algorithms," *in Proceedings of the Third International Conference on Genetic Algorithms*, pp. 70-79, San Mateo, CA, 1989.
[51] Erick Cantú-Paz. A survey of parallel genetic algorithms. CalculateursParalleles, reseaux et systems repartis, 10:30, 1998.
[52] S. Di Martino et al., "Towards migrating genetic algorithms for test data generation to the cloud," *Software Testing in the Cloud: Perspectives on an Emerging Discipline*, pp. 113–135, 2012, doi:10.4018/978-1-4666-2536-5.ch006.
[53] L. Di Geronimo et al., "A parallel genetic algorithm based on hadoop MapReduce for the automatic generation of junit test suites," *Proceedings - IEEE 5th International Conference on Software Testing, Verification and Validation, ICST 2012*, pp. 785–793, 2012, doi:10.1109/ICST.2012.177.
[54] F. Herrera, M. Lozano, "Gradual distributed real-coded genetic algorithms," *IEEE Transactions on Evolutionary Computation*, vol. 4, no. 1, pp. 43–62, 2000, doi:10.1109/4235.843494.
[55] W. Yu, W. Zhang, "Study on function optimization based on master-slave structure genetic algorithm," *International Conference on Signal Processing Proceedings, ICSP*, vol. 3, pp. 0–3, 2006, doi:10.1109/ICOSP.2006.345926.
[56] Y. J. Gong et al., "Distributed evolutionary algorithms and their models: A survey of the state-of-the-art," *Applied Soft Computing Journal*, vol. 34, pp. 286–300, 2015, doi:10.1016/j.asoc.2015.04.061.
[57] V. Muttillo et al., "An OpenMP Parallel Genetic Algorithm for Design Space Exploration of Heterogeneous Multi-processor Embedded Systems," *ACM International Conference Proceeding Series*, no. April, 2020, doi:10.1145/3381427.3381431.
[58] Available: https://www.espressif.com/en/products/ software/ esp-now/overview
[59] M5StickC. (2020). Accessed: July 28, 2020. Available: https://m5stack.com/products/stick-c
[60] S. Mnasri et al., "The 3D redeployment of nodes in Wireless Sensor Networks with real testbed prototyping", *In : International Conference on Ad-Hoc Networks and Wireless*, Cham, 2017. p. 18-24.. Springer, doi.org/10.1007/978-3-319-67910-5_2

Wajih Abdallah Received the M.Sc. degree (Hons.) in computer science from the University of Tunis, Tunisia, a doctoral student in computer science in the UT2J University of Toulouse . Currently, he is an associate-professor in the University of Gafsa, Tunisia. He conducted and published different high valued studies regarding the utility of using evolutionary optimization strategies on the resolution of real-world complex problems such as the deployment and connectivity in IoT networks. He also achieved several researches on Human-Machine Interface (HMI).

Sami Mnasri Received the bachelor's degree in computer science from the ENSIT engineering school, Tunisia, the M.Sc. degree (Hons.) in computer science from the University of Sfax, Tunisia and the Ph.D. degree in computer science from the UT2J University, Toulouse. Currently, he is an associate-professor in the University of Tabuk, KSA. He conducted and published different high valued studies regarding the utility of using evolutionary optimization strategies on the resolution of real-world complex problems such as the deployment, localization and routing in IoT networks. He also achieved several researches on multi-agent systems and artificial intelligence. He is the organizing co-chair, in different editions, of the IEEE International IINTEC conference and the WSDWSN international workshop. He was speaker in Saudiiot, ICCIT and HIS conferences.

Thierry Val His PhD was obtained in 1994 from the University of Blaise Pascal, Clermont-Ferrand, France. MCF and PU qualified in 61st and 27th sections. Currently, he is Professor of Universities 61st section at the IUT of Blagnac, UT2, Toulouse, France, since 2004.Qualified to Supervise Research (HDR) in Computer Engineering, University of Toulouse II Le Mirail, France, 2002. Director of RT1 studies, disability advisor and head of research department at the IUT Blagnac, Toulouse and are search manager at the laboratory IRIT-UT2J.His current research interests include IoT collection networks, Communications protocols, Localization of connected objects, Embedded computing and Computer architecture.

Received: 03 January 2022, Revised: 28 February 2022, Accepted: 05 March 2022, Online: 14 March 2022

DOI: https://dx.doi.org/10.55708/js0102003

Bridging the Urban-Rural Broadband Connectivity Gap using 5G Enabled HAPs Communication Exploiting TVWS Spectrum

Habib M. Hussien*[,1], Konstantinos Katzis[2], Luzango P. Mfupe[3], Ephrem T. Bekele[1]

[1] Addis Ababa Institute of Technology (AAiT), School of Electrical and Computer Engineering, Addis Ababa, Ethiopia

[2] European University of Cyprus, Department of Computer Science and Engineering, School of Sciences, Nicosia, Cyprus

[3] CSIR, NGEI, Pretoria, South Africa

*Corresponding author: Habib M. Hussien, E-mail: habib.mohammed@aait.edu.et

ABSTRACT: As with previous generations of mobile cellular networks, rural regions are projected to face financial and technological challenges in deploying 5G services. At the time, researchers all around the world are investigating the feasibility of utilizing TV White Spaces (TVWS). TVWS is an underutilized/unused section of television spectrum that might be used as a low-cost alternative to typical licensed wired/wireless broadband networks, as well as to bridge the broadband service availability gap between rural and urban regions. A feasible alternative is to deliver TVWS services via High Altitude Platforms (HAPs) for many developed and developing nations to deliver broadband services to a large proportion of their rural and low-income populations. This article examines the advantages of utilizing TVWS spectrum from HAPs as well as the challenges connected with this type of communication architecture. This article examines the advantages of leveraging TVWS spectrum from HAPs as well as the challenges that come with this type of communication architecture. They distribute messages across a large region while monitoring and optimizing radio resource allocation, owing to their position in the sky and the centralized design of the communication system. The article assesses the performance of such a system using the IEEE 802.22 standard and the ITU-R P.452 free space path-loss model. Moreover, this article pointed out the main challenge of using TVWS spectrum from HAP system.

KEYWORDS: Antenna Radiation Pattern, High Altitude Platforms, IEEE 802.22, ITU-T P.452, TVWS

1. Introduction

Internet connection has had a significant impact on contemporary society, transforming several areas of millions of people's lives by delivering far-reaching economic and social advantages. As a result, a slew of new wireless gadgets with novel capabilities are fast appearing, each needing a significant amount of radio spectrum to operate. Because wireless spectrum is a scarce resource, it must be managed carefully. In the years 2018 to 2020, CISCO virtual network index forecasts that by 2023, there will be 29.3 billion networked devices [1]. Mobile data consumption is predicted to increase by 46 percent (77 Exabytes per month) by 2022, according to VNI. Such expansion need extra capacity. This may be accomplished by providing more spectrum or by deploying tiny cells in densely populated locations. Despite this meteoric rise in internet use, an astounding 47% of the world's/global population remains unconnected [2]. Among this, 60–70% of this population lives in underdeveloped nations [3]. In Europe, rural regions cover 91 percent of the continent's land area and are home to 59 percent of the inhabitants. Rural regions fall behind metropolitan areas in terms of socioeconomic metrics. This is difficult since rural regions are sparsely inhabited and hence have a low business density, making it difficult to create private enterprises and public services in rural areas. According to the European Commission, rural regions are crucial in tackling a variety of key socioeconomic challenges, including climate change and sustainable food, biomass, and energy production [4]. Additionally, the World Bank [5] estimates that a 10% rise in broadband penetration will enhance the economy's growth rate by 1.38 percent. Ethiopia, for example, has an 80 percent rural population. Providing broadband access to rural regions would efficiently meet the majority of the nation's demands, while increasing the country's economic growth. However, rural broadband service

expansion has various hurdles, including [6] a lack of fiber infrastructure, a low average revenue per user, hilly terrain, and a lack of energy. It is not financially feasible for mobile service providers to establish traditional communication networks in sparsely inhabited regions. At the moment, academics and researchers from different organizations worldwide are looking into the possibility of exploiting TV White Space (TVWS), an underutilized/unused portion of the television spectrum, as a low-cost alternative to existing licensed wired/wireless broadband networks [6-14]. Due to its increased bandwidth, favorable propagation characteristics, building penetration, and wide coverage, the opening of TVWS for cognitive access is one of the first promising/tangible steps toward resolving rural connectivity and spectrum shortage issues. As a result, TVWS networks are well-suited for network access in underserved/unserved regions. Recently, Geolocation Spectrum Databases (GLSDs) technologies have been highlighted as a preferred enabler for White Space Devices (WSDs) in the construction of TVWS networks to provide broadband internet access across television bands [6-14]. While TVWS networks benefit from their propagation characteristics and use of unlicensed bands, implementation may be time consuming and challenging due to the fact that all TVWS base stations will need backhaul connection and electricity to function. High Altitude Platforms (HAPs) are airborne vehicles, such as airships or aircraft, capable of transporting many TVWS base stations. This paper demonstrates the potential benefits of TVWS derived from HAPs for underdeveloped nations such as Ethiopia. Ethiopia serves as our case study because to the high amount of its population that lives in rural regions. Literatures [6-14], demonstrated that the amount of underutilized TVWS spectrum in Ethiopia is abundant. Exploiting such spectrums from the HAP is expected to be a viable option so as to bridge the communication service between the rural and urban areas. The rest of the paper is organized as follows: Section 2 presents HAP s communication systems using TVWS. Section 3 provides the simulation analysis and discussions. Section 4 illustrates 5G services from HAP exploiting TVWS spectrum and Section 5 is discussing the technical challenges of designing / deploying such a system. Finally, the conclusions along with the future work are presented.

2. HAPs Communication System Using TVWS

HAPs are aircraft platforms that operate in the stratosphere, between 17 and 22 kilometers above the ground, and are capable of rapid deployment. They are self-sufficient in terms of energy (e.g., solar or kerosene) and have the ability to deliver broadband services to a high number of users across a vast region [15-17]. HAPs have the ability to carry a large number of wireless transceivers (base stations). According to [6], these transceivers are co-located on the platform and enable Line-of-Sight (LoS) communication to a geographic service radius of roughly 60 kilometers in diameter. By using specifically engineered antenna beam profiles, circular and equal-sized cells are produced on the ground [6]. Interference between cells in a HAP design is mostly determined by the gain profile and sidelobe levels of the antennas utilized. This may be advantageous in the case of HAPs, since the antenna gain profiles at the cell edges might result in usable overlap across cells [6],[15]and [16]. This approach is not commonly accessible in terrestrial systems since it requires the user's antenna to physically transition between cells, which is a very long procedure, and during which the user will be disconnected from any base station. Additionally, this will need a highly centralised system, since data regarding the channels accessible inside each cell must be sent at a rapid rate [6]. HAPs offer a centralized method in which all base stations are co-located on a single platform for synchronization. HAPs are designed to take use of their architecture and so utilize frequencies that terrestrial and satellite systems may be unable to exploit successfully [6]. According to previous studies, HAPs were used to transport frequency bands that needed Line of Sight (LoS) pathways and signals that are significantly reduced by rain [17], [18]. Nonetheless, HAPs may be utilized to access a broad spectrum of frequencies. More specifically, the ITU selected the following frequencies for HAP systems [6],[19-20]: 47.2-47.5GHz, 47.9-48.2GHz, 38-39.6GHz, 31-31.3GHz, 27.9-28.2GHz, 24.25-27.5GHz, 21.4-22GHz (Region 2), and finally 6440-6520 MHz, 6560-6640 MHz [6], [11], [13],[14] and [21] also studied the possibility of allowing HAP communication systems to deliver services that are already supplied by terrestrial communication systems. For TVWS networks, research on spectrum sharing including the coexistence of current terrestrial communications and HAP communications have been conducted [6]. The following are the advantages of providing TVWS messages over a HAP:

- Centralised control of TVWS base stations: Because all TVWS base stations are colocated on the platform, this enables greater resource coordination and less signaling.
- Although LoS communications are not required for TVWS to function, enabling LoS communications through HAPs may help further improve the link budget and decrease interference.
- There is no requirement for terrestrial infrastructure to enable the deployment of numerous TVWS base stations since TVWS base stations may be fueled by onboard power generation and/or renewable energy sources (photovoltaics).

- Rapid Deployment and easy relocation to a different area if necessary.

As per the study in [6] and [22], using HAPs to provide telecommunications services is a financially feasible option. Authors in [6] and [22] emphasizes that the common advantages of broadband penetration in rural nations include enhanced education and health service delivery, community development and expansion of small enterprises, and prevention of rural-urban migration and the interaction between communication infrastructure and the various services. HAPs are manned or unmanned aeronautical platforms that are typically situated between 17 and 22 kilometers in altitude and utilized for wireless applications [15] and [16]. Literature in [22] illustrated the benefits of HAPs over terrestrial wireless and satellite systems in solving certain wireless communication problems. The analyses adequately reflect the cost advantage of HAPs over terrestrial systems. According to [22], the cost of deploying, operating, and maintaining a macrocell with a radius of 1km is about 168 thousand euros (9.744 million birr). To offer continuous coverage across a 30km radius, at least 900 such macrocells are needed. As a result, the anticipated cost of the network is 151 million euros (8.758 billion birr), which is very substantial. On the other hand, as noted in [23], the projected cost of deploying, operating, and maintaining a HAP is about 5 million euros (290 million birr) for unmanned solar aircraft to cover the same service region. HAPs provide better coverage at a lower cost, easy to install, and allow for extended deployment [23]. These features encompass the requirements for a rural wireless communication system as stated in [16], indicating that HAPs are a viable option for rural wireless communication.

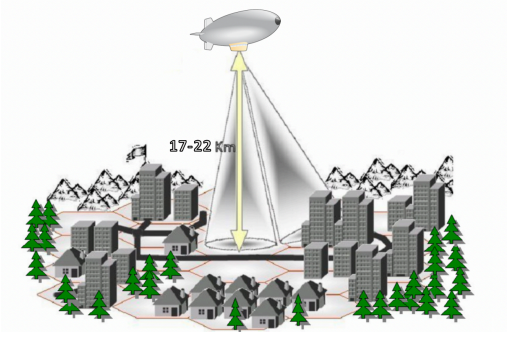

Figure 1: TVWS Cellular Architecture Delivered by HAP [6]

The HAP shown in Figure 1 is equipped with a number of TVWS base stations that provide coverage throughout a geographical region. To cover a radius of 100 kilometers and assuming that each cell is a normal hexagonal cell with a radius (R) of 10.5 kilometer, a payload of 121 TVWS base stations deployed in a hexagonal lattice is needed. The suggested platform's geometry is seen in Figure 2. Each cell has the ability to provide constant quality of service (64QAM) throughout its coverage area while supporting up to 512 Customer Premises Equipment (CPEs), but this number is heavily dependent on weather conditions due to the need to maintain a fixed-point to multi-point topology [6]. Users on the outside of the service region will encounter a 9.65° elevation angle.

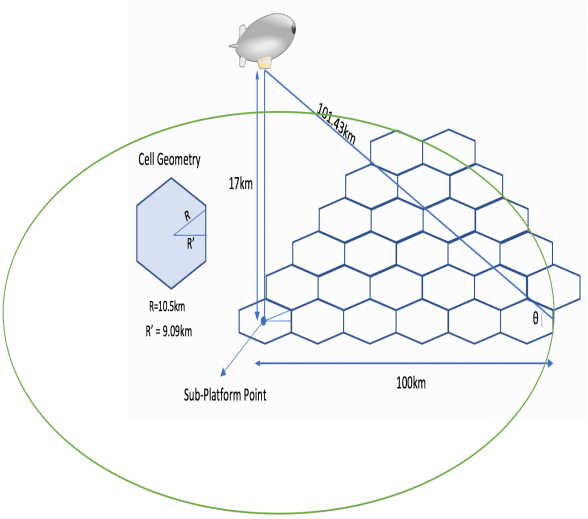

Figure 2: HAP Cellular Layout [6]

According to the country's total surface area of roughly 1,104,000km², Ethiopia would require at least 35 HAPs to offer comprehensive coverage throughout the country. This is dependent on cell / HAP design, population density, and, in some cases, a HAP's coverage area may be pushed farther to provide additional coverage [6].

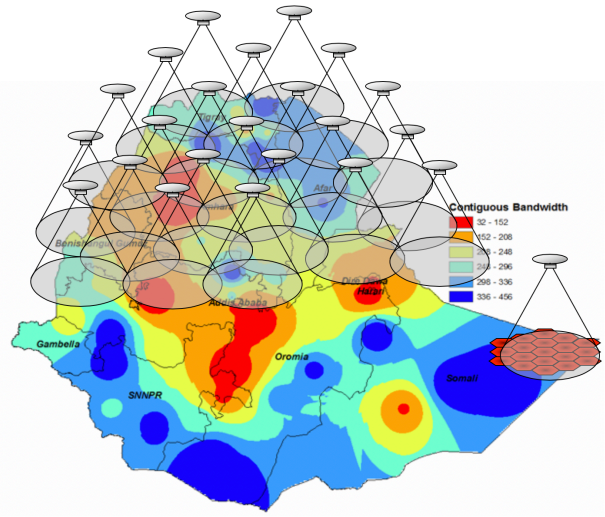

Figure 3: A fleet of HAPs providing coverage across Ethiopia

Figure 3 illustrates the fleet of HAPs providing coverage across Ethiopia. The color heat map depicts the amount of free available TVWS spectrums. The figure further illustrates the amount of contiguous TVWS bandwidth.

2.1. Receiver Sensitivity

The Bit Error Rate (BER) for an AWGN channel provides the required SNR values, according to the IEEE 802.22 standard [24] from which the receiver sensitivity may be determined in order to achieve the BER. The minimal

input level sensitivity of the receiver may be estimated as follows:

$$R_{ss}(dBm) = SNR_{(dB)} + kTB_{(dBm)} + NF_{(dB)} + IL_{(dB)} \quad (1)$$

Where k is Boltzmann's constant = 1.38x10-23 J/K, T is the receiver's input absolute temperature = 290 (K), B is the bandwidth (Hz), NF is the receiver's noise figure (dB), and IL is the implementation loss (dB). For our simulation, we picked a BER of 10^{-6}, which corresponds to the SNR values shown in Table 2.

Table 1: Assumptions for Receiver SNR [6] and [24].

Modulation and Code rate	SNR (dB)
QPSK½	9.4
QPSK¾	11.2
16-QAM½	16.4
16-QAM¾	18.2
64-QAM2/3	22.7
64-QAM¾	24.4

2.2. Antenna Radiation Pattern

The footprint, coverage, interference, and CIR values are all influenced by the antenna radiation pattern, all of which have a direct impact on the system's and network's quality of service and performance. The HAP payload consists of a collection of antennas aimed at various places around the coverage region. Gain is dependent on elevation (φ) and azimuth (θ) angles for each cell [6]. The HAP antenna gain can be obtained as:

$$A_{HAP}(\varphi) = \frac{32\ ln\ 2}{2\left(2arccos\left(\sqrt[nH]{\frac{1}{2}}\right)\right)^2}(cos\varphi)^{nH} \quad (2)$$

Where nH is the roll-off rate for the HAP antennas. On the other hand, the gain of the user antenna may be mathematically expressed as

$$\mathrm{A_{User}}(\theta) = \mathrm{G_{User\_boresight}}(\max[\cos(\theta)^{\mathrm{nU}}], \mathrm{S_f}) \quad (3)$$

Where nU is the roll-off rate for the user antennas. The user antenna was designed to be very directional in order to prevent interference from adjacent systems operating on the same frequency.

2.3. System Path Loss

Given that HAPs enable line-of-sight communications, the Free Space Path Loss (FSPL) model is often used to evaluate HAPs systems when the elevation angles are not too tiny. According to [6], FSPL can be determined as

$$\mathrm{FSPL_{HAP}} = \left(\frac{4\pi d}{\lambda}\right)^2 \quad (4)$$

Where d is defined as the distance between the HAP and user, and λ is the wavelength of the message conveying signal.

ITU-R P.452-16 [25] is a prediction model for determining if two stations are interfering. The model is suited to determining the level of interference between stations operating at frequencies ranging from 0.1 to 50 GHz. It is accurate for temporal fractions ranging from 50% to 0.001% using physical models for free space, diffraction, troposcatter, ducting, raised layers, and rain scatter. The advice classifies the route and evaluates the relevance of each propagation mechanism using a path profile. The total pathloss (in decibels) of PL452-16 may be computed as follows:

$$PL_{452-16} = \mathrm{FSPL_{HAP}} + CL + A_g \quad (6)$$

Here, Clutter Loss (CL) in dB, can be calculated as:

$$CL = 10.25F_c e^{-d_k}\left(1 - tanh\left(6\left(\frac{h}{ha} - 0.625\right)\right)\right) - 0.003 \quad (7)$$

where dk (in kilometers) denotes the distance from the notional clutter point to the received antenna, h (in meters) denotes the height of the received antenna above the ground, and ha (in meters) is the nominal clutter point's height above the ground. Fc may be computed as follows:

$$F_c = 0.25 + 0.375\left(1 + tanh\left(0.75(f_{GHz} - 0.5)\right)\right) \quad (8)$$

where f is the operating frequency in gigahertz (GHz). dk is 0.1 and 0.002 kilometers in rural and urban regions, respectively. The nominal clutter height is ha (in meters) and varies depending on the measuring setting. Its value varies between 4 and 20 meters in rural and urban settings. The total GA in dB is calculated according to ITU.R guideline P.676, which specifies the signal's attenuation owing to water vapor and dry air [26].

2.4. System Capacity

The availability of each modulation scheme for each cell is directly related to system operating characteristics such as the power of the aerial platform, the receiver's signal-to-noise ratio, and the available data rate of the channel. These criteria can be used to determine a percentage of availability based on the coverage area of a particular modulation type. Calculate the overall capacity of the aerial platform with N cells inside the coverage zone using the formula [6]:

$$\text{System TVWS HAP capacity} = \sum_{\mathrm{j=1}}^{\mathrm{N}} \text{Data rate of } \mathrm{j^{th}} \text{ modulation}\left(\frac{\text{Area of } \mathrm{j^{th}} \text{ modulation}}{\text{Area of the cell}}\right) \quad (9)$$

The maximum data rate can be obtained using [6]:

$$Data\ Rate\ =\ No.of\ used\ subcarriers\ *\ code\ rate\ \ no.of\ bits\ per\ modulation\ symbol/OFDM\ symbol\ time\ *$$

$$no.of\ channel\ bonded \quad (10)$$

3. Simulation Result Analysis and Discussion

Our simulation was conducted using the IEEE 802.22 standard [24] and the ITU-R P.452 free space path-loss model[6] and [25]. The HAP is placed at a height of 17 kilometers and is equipped with 121 beams that span a radius of 100 kilometers. Table 1 lists the parameters used in the simulation.

Table 2: Parameters for simulation [6] and [25]

HAP transmitter height (km)	17
Coverage Radius (km)	100
Number of Cells	121
Cell Radius (km)	10.5
Antenna efficiency (%)	80
Boresight gain (dBi)	*20*
HAP roll-off rate	3.3
User roll-off rate	58
Bandwidth (MHz)	8
Frequency (MHz)	617
NF (dB)	7
IL (dB)	5
Frequency range	54-862MHz
Data access technique	DAMA/OFDMA
Multiplexing method	TDD
Sampling factor(n)	8/7
Sampling frequency, Fs(MHz) $F_S=B*n$	9.14
FFT size (N_{FFT})	2048

Using the simulation parameter in Table I, it is possible to determine that the elevation angle, antenna gain, the pathloss, maximum data rate, SNR, and maximum cell and system capacity with and without channel bonding. The data rates associated with various CP factors for the downlink are shown in Table 3 with a channel bandwidth of 8 MHz. According to Table 3, various modulation techniques with CR 1/2 to 5/6 and CP factors ranging from 1/16 to 3/8 produce a range of data speeds in Mbps. For example, QPSK supports data rates ranging from 4.67 to 10.07 Mbps, 16-QAM supports data rates ranging from 9.3415 to 20.15 Mbps, 64-QAM supports data rates ranging from 14.01 to 30.22 Mbps, and 256-QAM supports data rates ranging from 18.68 to 40.29 Mbps. Modulation methods achieved vary according to the location of the Customer Premises Equipment (CPE). When 256-QAM, 5/6 coding rate, and a CP factor of 1/16 are used, the highest data rate achievable is 40.29Mbps, and the maximum spectrum efficiency is 40.29/8=5.04 bits/sec/Hz.

Table 3: TVWS WRAN data rates for various modulation and coding schemes

Modulation	CR	Data rate (MBps) for different CP factor			
		1/16	1/8	1/4	3/8
QPSK	1/2	6.05	5.71	5.14	4.67
	2/3	8.06	7.61	6.85	6.23
	3/4	9.07	8.56	7.71	7.01
	5/6	10.07	9.51	8.56	7.78
16-QAM	1/2	12.09	11.41	10.28	9.34
	2/3	16.12	15.22	13.70	12.46
	3/4	18.13	17.12	15.41	14.01
	5/6	20.15	19.03	17.13	15.57
64-QAM	½	18.13	17.13	15.41	14.01
	2/3	24.16	22.83	20.55	18.68
	¾	27.20	25.69	23.12	21.02
	5/6	30.22	28.54	25.69	23.35
256-QAM	½	24.18	22.83	20.55	18.68
	2/3	32.24	30.45	27.40	24.91
	¾	36.23	34.25	30.83	28.02
	5/6	40.29	38.06	34.25	31.14

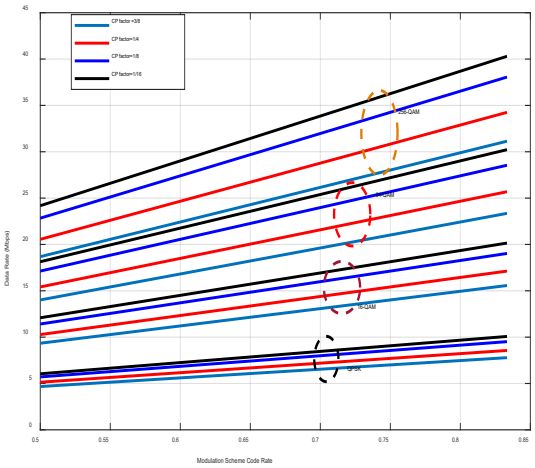

Figure 4: Data rate as a function code rate

Figure 4 depicts the relationship between data rate and code rate for QPSK, 16-QAM, 64-QAM and 256-QAM at different cyclic prefix factor. As can be seen from Figure 4, the maximum data rate achieved is 40.29 Mbps when 256-QAM, 5/6 code rate, and 1/16 cyclic prefix factor are employed. The minimum data rate is obtained at QPSK, 3/8 CP factor, ½ code rate. Thus, the highest data rate achievable is 30.22Mbps when using 64-QAM and 40.2989 Mbps while using 256-QAM. The elevation angle as a function of distance from the sub platform point is shown in Figure 5. As per the calculation performed the minimum elevation angle at the cell edge is 9.65° as depicted in Figure 5. As a consequence, the angle of departure from the boresight fluctuates, resulting in a reduced antenna gain. As can be seen from Figure 5, as the distance from SPP increases, the elevation angle decreases.

The user antenna should be extremely directional in order to prevent interference from adjacent systems operating on the same frequency as depicted in Figure 6. At 9.65° elevation angle, the user's antenna gain is 16 dB and the

HAP's gain is 19.34 dB. Figure 7 illustrated, the HAP antenna gain as a function of elevation angle. As can be seen from the figure as the beam width increases, range of the elevation angle increases, however the gain decreases. The decreasing beamwidth resulted in, the increase antenna gain, but the decrease the range of elevation angle.

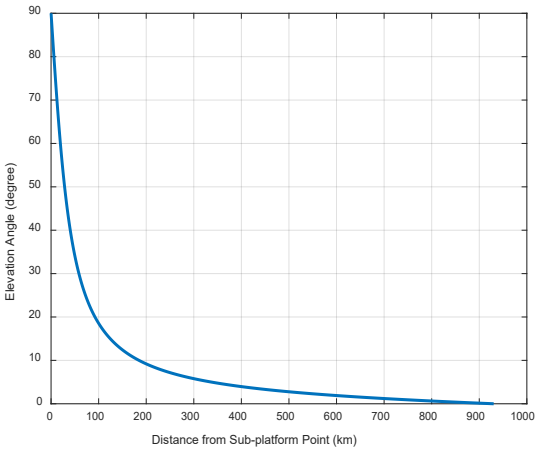

Figure 5: Distance from sub-platform point as a function of elevation angle

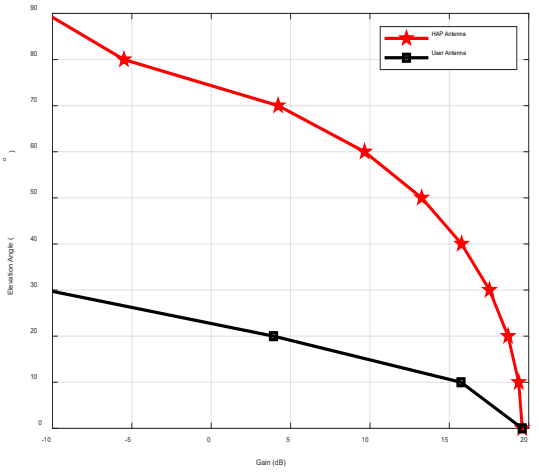

Figure 6: Antenna gain versus elevation angle for HAP and user Antennas

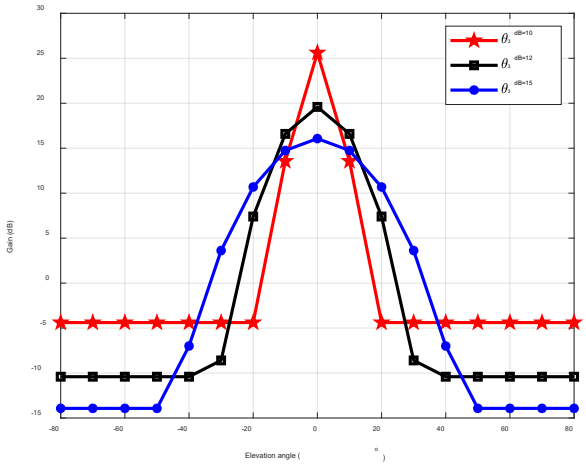

Figure 7: HAP Antenna gain as a function of elevation angle

The path loss as a function of the elevation angle is depicted in Figure 8. When the free space route loss is compared to the ITU-R P.452 path loss, the latter reveals a much larger loss, owing to the extra characteristics included, such as diffraction, scattering, and rain attenuation. As can be seen from Figure 8, at 9.65^{o}, ITU-R P.452-16 has a pathloss of 136.87dB and FSPL has a pathloss of 128.30dB.

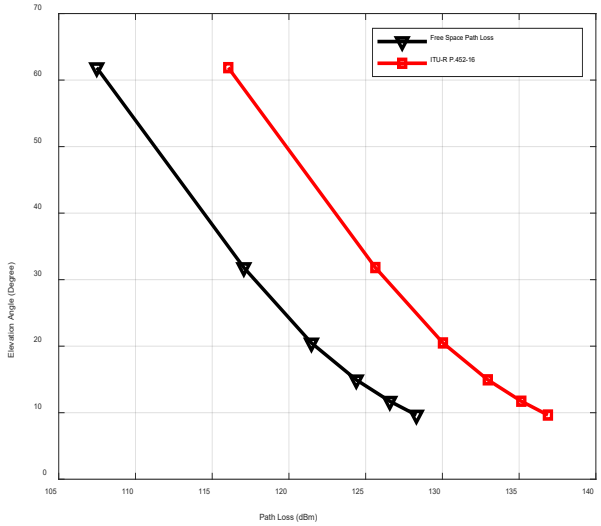

Figure 8: Path loss versus Elevation

The path loss as a function of the distance from SPP is depicted in Figure 9. When the free space route loss is compared to the ITU-R P.452 path loss, the latter reveals a much larger loss, owing to the extra characteristics included, such as diffraction, scattering, and rain attenuation. As can be seen from Figure 9, at 100km coverage radius, ITU-R P.452-16 has a pathloss of 136.87dB and FSPL has a pathloss of 128.30dB.

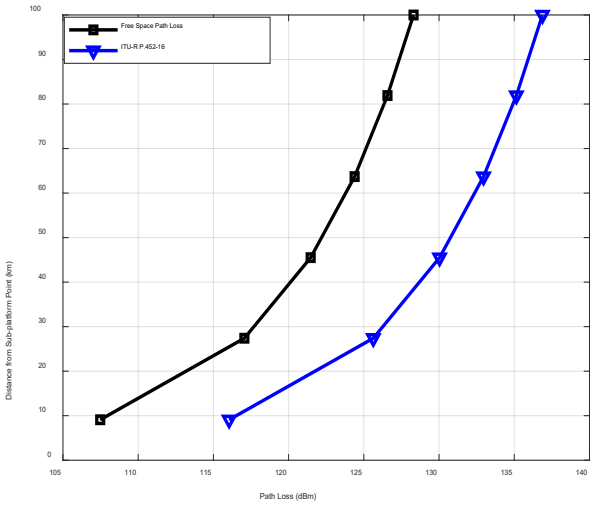

Figure 9: Path loss in relation to distance from the HAP SPP

Finally, using equation (9), we determined an overall system capacity of 2,734.7Mbps for our TVWS wireless services from HAP system model, which is a possible

technique for providing broadband services to a large number of people.

4. 5G Services from HAP exploiting TVWS

Numerous KPIs make it difficult to implement 5G services in rural and low-income communities. Several of these characteristics are discussed in [27]. High-priority applications must be separated from relevant quality of service (QoS) characteristics such as latency and reliability in a 5G network. Prioritization of traffic can be implemented by adjusting resource allocation or pre-empting lower priority traffic. The following KPIs from IMT2020 and 3GPP have been established for the Rural Macro scenario, according to the EU-funded project 5G-MiEdge:

- Downlink data rate: 50Mbps
- Uplink data rate: 25Mbps
- Downlink Area traffic capacity: 1 Gbps/km^2
- Uplink Area traffic capacity: 500 Mbps /km^2

While a single TVWS HAP system may deliver internet services to rural regions, it may fall short of meeting all of the 5G KPIs for rural areas outlined above. There are many potential solutions to this challenge, including reducing the coverage area, using channel bonding, or even introducing additional platforms [28]. Channel bonding seems to have been thoroughly addressed by a number of writers, for example in [29-32]. According to the IEEE 802.22 PHY/MAC definition [24], the data rate attained with channel bonding by applying equation (10), When three channels are bonded and 256QAM modulation with 5/6 CR, 1/32 CP factor is employed, the data rate computed using (10) is 145.45Mbps. When the same transmission parameters are utilized as in the single channel example, the maximum data rate has increased by 105.15Mbps. Uplink modulation techniques include BPSK, QPSK, 8PSK, 16QAM, and 64QAM. The use of QPSK modulation and a coding rate of 5/6 with a CP factor of 1/16 for uplink channel bonding (of three channels) resulted in a data throughput of 33.3Mbps, satisfying two of the rural 5G KPIs.

5. Conclusions, Challenges and Future Work

By combining the perfect propagation properties of TVWS spectrum with the LoS coverage offered by a HAP, a communication system capable of providing broadband services to rural regions may be created. 121 cells are needed to cover a radius of 100 kilometers. Each cell has a radius of 10.5 kilometers, giving coverage for an area of about 286 kilometers square. According to our findings, each cell is capable of providing 27-40MBps using 64QAM or 256QAM modulation techniques. This may be boosted further by incorporating channel bonding, which enables data transfer speeds of up to 145.45Mbps. To give rural consumers with a 5G experience, however, other strategies will need to be used, such as expanding the number of stations or reducing their coverage area. This, of course, will raise providers' costs and may dissuade them from constructing such a network in the first place. In this instance, it is more advantageous to establish this sort of network, even if it does not completely fulfill the 5G network's key performance indicators. This manner, people in rural / low-income regions would be able to access these services while still benefiting from the digital market. Providing TVWS services from HAPs presents a variety of issues. At the present, the most significant problem is platform availability. This may be handled by offering services through aircraft until a commercially accessible unmanned stratospheric platform becomes available (e.g. an airship). Additionally, new low-cost directional antennas are required to enable users to monitor the HAP. This will minimize interference, but they must account for the possibility of HAP migration. Additionally, at this level, the cohabitation of HAP TVWS networks and terrestrial incumbent users must be handled. Additionally, as part of the capacity assessment process, overlap between TVWS cells must be considered. TVWS frequency reuse methods must be used to optimize interference levels between cells and to prevent any detrimental interference to incumbent customers. While delivering wireless service from HAP exploiting TVWS spectrum, managing the interference from incumbent users can be mitigated using phased array antennas. However, HAP interference, induced by comparatively high transmitting power and antenna beam profile, has the ability to greatly impact the current incumbent system on the ground if HAP antenna beams situated are implemented without a proper strategy. Antenna beam pointing techniques utilizing phased array antennas on the HAPs is a challenge. Even though, the stratosphere is comparatively in a stable region, the HAP might face strong wind gusts. As a consequence, the HAP is capable of being oriented in any direction which will resulted in the patterns of received power and interference on the ground (footprints) will continue to move. To mitigate such difficulties, an energy and load aware scheme for maintaining uninterrupted system performance as well as minimizing power consumption is another challenge.

Conflict of Interest

The authors declare no conflict of interest.

References

[1] CISCO, Annual Internet Report (18-23) Whitepaper, https://www.cisco.com/c/en/us/solutions/collateral/executive-perspectives/annual-internet-report/white-paper-c11-741490.html

[2] I. T. U. ITU, "ITU releases 2018 global and regional ICT estimates," International Telecommunication Union, 2018.

[3] International Telecommunications Union, "*ICT facts and figures 2017*," 2017.

[4] European Commission, "9. Food security , sustainable agriculture and forestry, marine and maritime and inland water research and the bioeconomy," in Horizon 2020 - Work Programme 2016 - 2017, 2016.

[5] The World Bank: Ethiopia Digital Foundations Project (P171034), 2016,https://documents.worldbank.org

[6] K. Katzis, L. Mfupe and H. M. Hussien, "Opportunities and Challenges of Bridging the Digital Divide using 5G enabled High Altitude Platforms and TVWS spectrum," *2020 IEEE Eighth International Conference on Communications and Networking (ComNet)*, 2020, pp. 1-7, DOI: 10.1109/ComNet47917.2020.9306090

[7] H.M. Hussien, k. Katzis , L.P. Mfupe., E.T. Bekele, "Practical Implementation of Geo-location TVWS Database for Ethiopia," *Advances of Science and Technology (ICAST 2020),* vol 385. DOI: 10.1007/978-3-030-80618-7_34.

[8] H. M. Hussien, K. Katzis, L. P. Mfupe and E. T. Bekele, "Coexistence of TV White Space Devices and DTV Services in Ethiopian Geolocation White Space Spectrum Database," *2019 IEEE 24th International Workshop on Computer Aided Modeling and Design of Communication Links and Networks (CAMAD)*, 2019, pp. 1-5, DOI: 10.1109/CAMAD.2019.8858472.

[9] T. T. Terefe et al., "Reserved Distance and Significant Parameter Determination in Incumbent and TV White Space System Coexistence," *ICAST 2020 - 8th EAI Int. Conf. Adv. Sci. Technol.*,pp. 125-133, v. 384, 2021, DOI: 10.1007/978-3-030-80621-7_9

[10] H. Mohammed et al., "Coverage Determination of Incumbent System and Available TV White Space Channels for Secondary Use in Ethiopia," *in IntechOpen, Vision Sensors*, 2021, DOI: 10.5772/intechopen.98784.

[11] H. M. Hussien, K. Katzis, L. P. Mfupe and E. T., "A Novel Resource Allocation for HAP Wireless Networks Exploiting TVWS Spectrum," 2021 IEEE AFRICON, 2021, pp. 1-6, DOI: 10.1109/AFRICON51333.2021.9570928.

[12] H. M. Hussien, K. Katzis, L. P. Mfupe and E. T, "Calculation of TVWS Spectrum Availability Using Geo-location White Space Spectrum Database," *2021 IEEE AFRICON*, 2021, pp. 1-6, DOI: 10.1109/AFRICON51333.2021.9570915.

[13] H. M. Hussien, K. Katzis and L. P. Mfupe, "Dynamic Spectrum Allocation for TVWS Wireless Access from High Altitude Platform," *2021 International Conference on Electrical, Computer and Energy Technologies (ICECET)*, 2021, pp. 1-6, DOI: 10.1109/ICECET52533.2021.9698667.

[14] H. M. Hussien, K. Katzis and L. P. Mfupe, "Intelligent Power Allocation for Cognitive HAP Wireless Networks Using TVWS Spectrum," *2021 International Conference on Electrical, Computer and Energy Technologies (ICECET)*, 2021, pp. 1-6, DOI: 10.1109/ICECET52533.2021.9698778.

[15] J. Thornton, D. Grace, C. Spillard, T. Konefal, and T. C. Tozer, "Broadband communications from a high-altitude platform: The european helinet programme," *Electron. Commun. Eng. J.*, 2001, DOI: 10.1049/ecej:20010304.

[16] J. Thornton, D. Grace, M. H. Capstick, and T. C. Tozer, "Optimizing an array of antennas for cellular coverage from a high altitude platform," *IEEE Trans. Wirel. Commun.*, 2003, DOI: 10.1109/TWC.2003.811052.

[17] T. Konefal, C. Spillard, and D. Grace, "Site diversity for high-altitude platforms: A method for the prediction of joint site attenuation statistics," *IEE Proc. Microwaves, Antennas Propag.*, 2002, DOI:10.1019/ip-map:20020107.

[18] C. L. Spillard, D. Grace, J. Thornton, and T. C. Tozer, "Effect of ground station antenna beamwidth on rain scatter interference in high- altitude platform links," Electron. Lett., 2002, DOI: 10.1049/el:20020823.

[19] M. Oodo, R. Miura, T. Hori, T. Morisaki, K. Kashiki, and M. Suzuki, "Sharing and compatibility study between fixed service using high altitude platform stations (HAPS) and other services in the 31/28 GHz bands," *Wirel. Pers. Commun.*, 2002,DOI: 10.1023/A:1020945122344.

[20] ITU, "Minimum performance characteristics and operational conditions for High Altitude Platform stations providing IMT-2000 in the Bands 1885-1980MHz, 2010-2025MHz and 2110-2170 in the Regions 1 and 3 and 1885-1980MHz and 2110-2170 MHz in Region 2. - Reccomenda," 2000.

[21] J. Lun et al., "Solar Powered High Altitude Platform and Terrestrial Infrastructures," *University of York*, White Paper 2017.

[22] Arum et al.,"A review of wireless communication using high-altitude platforms for extended coverage and capacity," *Computer Communications*,Volume 157,2020, pp. 232-256, Doi:10.1016/j.comcom.2020.04.020.

[23] S. Karapantazis and F. Pavlidou, "Broadband communications via high-altitude platforms: a survey," *IEEE Communications Surveys & Tutorials*, vol. 7, no. 1, pp. 2–31, 2005, DOI:10.1109/COMST.2005.1423332

[24] "IEEE Standard for Information technology-- Local and metropolitan area networks-- Specific requirements-- Part 22: Cognitive Wireless RAN Medium Access Control (MAC) and Physical Layer (PHY) specifications: Policies and procedures for operation in the TV ," IEEE Std 802.22-2011. pp. 1–680, 2011.

[25] ITU-R, "ITU-R P.452-16," International Telecommunication Union. 2015.

[26] ITU-R, "Recommendation ITU-R, P.676-10: Attenuation by atmospheric gases," P Ser. Radiowave Propag., 2013.

[27] L. Chiaraviglio et al., "Bringing 5G into Rural and Low-Income Areas: Is It Feasible?," *IEEE Commun. Stand. Mag.*, 2017, DOI:10.1109/MCOMSTD.2017.1700023

[28] D. Grace, J. Thornton, G. Chen, G. P. White, and T. C. Tozer, "Improving the system capacity of broadband services using multiple high-altitude platforms," *IEEE Trans. Wirel. Commun.*, 2005, DOI: 10.1109/TWC.2004.842972

[29] J. Elias, F. Martignon, L. Chen, and M. Krunz, "Distributed spectrum management in TV white space networks," *IEEE Transactions on Vehicular Technology*, 2017, DOI: 10.1109/TVT.2016.2 597866

[30] R. Rajbanshi, Q. Chen, A. M. Wyglinski, G. J. Minden, and J. B. Evans, "Quantitative comparison of agile modulation techniques for cognitive radio transceivers," *in 2007 4th Annual IEEE Consumer Communications and Networking Conference*, CCNC 2007, DOI: 10.1109/CCNC.2007.230.

[31] H. Kim and K. G. Shin, "Efficient discovery of spectrum opportunities with MAC-layer sensing in cognitive radio networks," *IEEE Trans. Mob. Comput.*, 2008, DOI: 10.1109/TMC.2007.70751.

[32] H. Bogucka, P. Kryszkiewicz, and A. Kliks, "Dynamic spectrum aggregation for future 5G communications," *IEEE Commun. Mag.*,2015,DOI: 10.1109/MCOM.2015.7105639.

HABIB MOHAMMED HUSSEIN received his bachelor degree from Adama Science and Technology University, Ethiopia in 2008 and his MSc degree from Tianjin University, Tianjin, China in 2012 in Electrical and Electronic Engineering (Signal and Information Processing Technology). Now, he is a PhD Doctoral candidate at Addis Ababa University, Addis Ababa Institute of Technology (AAiT), Ethiopia. His current research interest includes high altitude platform, handoff schemes, TV white space technology (TVWS), radio resource allocation and optimization, call admission control, heterogenous network coexistence issues and 5G IoT.

DR KONSTANTINOS KATZIS received his BEng degree in Computer Systems Engineering and his MSc degree in Radio Systems Engineering from the University In 2006, Dr Katzis received his PhD degree in Electronics from University of York (UK). His current research interests include dynamic spectrum access and cognitive radio, architectures for 5G and beyond and wireless communications from aerial platforms. Konstantinos has also been working towards the development of highly efficient resource allocation techniques as well as handoff techniques optimised for the operation of High Altitude Platform communication systems. His work involved modelling of the platform movements and simulating the effects on the communications. He currently holds the position of the secretary in IEEE1900.6 standard and he is also MC member of COST action CA20120 (Intelligence-Enabling Radio Communications for Seamless Inclusive Interactions - INTERACT). Recently, he has been awarded with the Fulbright Visiting Scholar fund for his proposal "Requirement Analysis of 5G Networks Supporting IoT-Health Applications" in collaboration with the Information Technology Laboratory (ITL) of the National Institute of Standards & Technology (NIST) in Washington DC (USA). Dr Konstantinos Katzis is an Associate Professor at European University Cyprus.

DR LUZANGO PANGANI MFUPE earned his Bachelor's, Master's and PhD degrees in Electrical Engineering at Tshwane University of Technology in Pretoria, South Africa. He is an experienced principal research scientist, Innovator and Entrepreneur with demonstrated technical leadership in large & cutting-edge technology projects. Skilled in Dynamic Spectrum Management (DSM), Television White Spaces (TVWS), Defense & Civilian Spectrum Sharing Models, Formulation of Spectrum Regulations & Policies, Development of Geo-location Spectrum Databases, Advanced Wireless Networks Design and Modeling, Satellite Communications, Airborne Wireless Networks (AWNs), Artificial Intelligence/Machine Learning for Future Wireless Communications such as 5G, Computer Simulations,

DR EPHREM TESHALE BEKELE received the BSc degree in Electrical Engineering from Bahir Dar University, Bahir Dar, Ethiopia, in 2007, the MSc degree in Telecommunications Engineering in 2011, and the PhD in Information and Communications Technology in 2015 both from the University of Trento, Trento, Italy. He has worked as an Assistant Lecturer in Bahir Dar University, from 2007 to 2009. He is currently an Assistant Professor at the Addis Ababa Institute of Technology (AAiT) in Addis Ababa University, Ethiopia, and a Associate Faculty Member of the ELEDIA Research Center. He is also a visiting lecturer at Bahir Dar University, Bahir Dar, Ethiopia, and a member of the Applied Electromagnetic Research Group in AAiT. His main research interests are Electromagnetic Nondestructive Testing, Technology 'Domestication', and RF Regulation.

JENRS

Received: 15 December 2021, Revised: 25 January 2022, Accepted: 03 February 2022, Online: 14 March 2022

DOI: https://dx.doi.org/10.55708/js0102004

Prakriti: A Gamified Approach to Saving Water

Tathagata Bhattacharya*, Xiaopu Peng, Ishita Joshi, Ting Cao, Jianzhou Mao, Xiao Qin
Department of Computer Science and Software Engineering, Auburn University, Auburn, 36832, USA

*Corresponding author: Tathagata Bhattacharya, ph. - 334 498 0832, tzb0063@auburn.edu, Auburn University, Auburn, 36832, USA

ABSTRACT: Prakriti is a Sanskrit word which signifies Mother Nature. Our game Prakriti is designed to educate people about how they can save water resources and contribute to freshwater resources. This is a multiplayer game designed to set a thrilling, challenging and dramatic effect on the players. The game consists of its formal and dramatic elements. We design the game in Unity 2D and every move is created to provide information about water-saving to the players. We playtest the game with many players and updated the game in three iterations. This feedback gives us a direction to improve the quality of the game. The game was assessed with many strong qualities such as a good aesthetic quality, good user interaction and supportive of providing information about saving water resources, and players also stated that this medium of learning about water resources through gaming was very satisfactory.

KEYWORDS: Interactive Learning, UN sustainability Goals, Water Resource Management, Playtesting

1. Introduction

Earth comprises 71% water in which only 3% of freshwater. In that 3% of fresh water, only 1.5% of freshwater is accessible to the human being, rest is stored in the form of ice on the glaciers or mountain cap. More than half a billion people face water crisis every year throughout the world. Therefore, to bring a panacea to the globe, people should be aware of how to use and save water for their future. Today, hydrology and water management become a significant part of research as water depletion has taken a devastating form. The recent trend illustrates that we should incorporate interdisciplinary research to bring a panacea in today's water scarcity problem. We can approach this problem by:

- Making people aware of the interaction between man and nature
- Through technical skills, design entertainments that will engage people and teach them about how to minimize water consumption.

With the progress in science and technology, we believe it is possible to make people aware of the water depletion and iceberg melt in the poles. Since 1967, the link between social science and water resource education has been a prime highlight. The main motivations of this paper mentioned as follows:

- Motivation1: Build an interesting game that will attract and engage players.
- Motivation2: Bring awareness among the players on water consumption through the game.
- Motivation3: Introduce dramatic elements and formal elements of the game to increase the degree of competition and challenge.

If we discuss about preexisting environmental games like H2O Yeah or The River Basin, we will see that these games profoundly advocate for the need to conserve water. These games have successfully taught how to save or preserve the freshwater resource. Here lies the uniqueness of our game. Prakriti not only teaches the players about the need for water conservation through a joyful experience, but it also provides solutions that we can include in our day-to-day life to conserve freshwater resources. For example, it takes gallons of water to make toilet papers, but instead if we use jet spray in our washroom, we can conserve more water. Therefore, we can say that Prakriti is a unique game that not solicitously provide an opportunity to the players to learn why we need to conserve water and how we can preserve water to bring the panacea in the entire world. Also, in future we would like to update this game through series of evaluations in order to make it more sustainable,

interactive, engaging and fun. As an example, we may say that, in the third phase of rapid application development process, we have introduced the cards as the dramatic element that would determine the luck of the players. These cards will either make you save water, or it may make you lose water units. Therefore, we believe with each iteration of software development process we may end up having a better version of the game in future. Also, as a future direction, we may contribute or fusion the conservation of other natural resources like fossil fuel. Our future work would be focused on but not limited to resource conservation and ensuring sustainability.

- Affordable clean energy: water electricity initial water units to win the game [1].
- Sustainable cities and communities: Purifying water talks about Water Resource pollution Adoption (WRA) and the importance of promoting it
- Climate action: Affordable and scalable solution worldwide. It emphasizes cross-cultural education, • Life below water: Conscious management of water responsibility for managing the water resource, maintaining resource the public benefit and empathy and negotiating thinking.
- Life in the land: Encourages afforestation.
- Clean water and sanitation: Distribution of fresh waste.

As the consciousness started growing, interdisciplinary approach in understanding the relationship between water and society and in developing water policy led to the establishment of the concept of Integrated Water Resources Management (IWRM). The emergence of the concept of sustainable development in the same period reinforced the call for interdisciplinary approaches in teaching. In practice, interdisciplinary research slowed down due to the traditional form of teaching. Most of the countries put the concept of water management as a part of Geography or civil engineering. This results in the ignorance of people about water consumption [2]. Good health and well-being: This game teaches innovative ideas to remove water borne diseases and heir cure .Further we will do some literature survey to understand the concepts of pre-existing games and their types.

2. Literature Review

2.1. Electronic Games to reduce water consumption

In [3] author represents a derived study that represents how people compare their actual water consumption with that of forecasted water usage through a board game. Unlike Water-wise, this game derives from a game "Push your luck". The game comprises of one protagonist and one antagonist. The whole game revolves around drawing cards continuously until they meet the risk condition. This game uses scanning the QR code in the monster card with a smart mobile device. If the player answers the questions correctly, the negative points on the monster card turn into positive ones. This whole scene takes place on the cloud. Whereas, Water-wise is a Simple board game with a board with lots of concentric circles, four players, chores written on the tile and cards that boost the player's score. This game teaches water consumption in every move of the players. It creates a challenge as well as competition among the players to go to the end and select the correct card to gain more water units.

In [4], [5] and [6], the author discusses the game Drop which is created by SmartH2O research. The motto of the game is to save water. This technique compares the data collected by smartH2O and compares that data with the daily usage of the people in the town. This game determines ideal water usage and teaches people how they can reduce water consumption to save water. But the difference between our game and this game lies in the technique. Our game involves several ways to reduce water consumption by not negatively affecting our personal and social life. Along with that Prakriti is more user interactive and engaging. The players learn ways to save water while playing the game.

In [7], the author depicts the role two games; The River basin and The Globalization of Water role Play. Both these games represent different aspects of the water-saving approach. The first game experiences the user the risk of over utilization of water in the river basin and how that affects the person, society and the mutual interest among people. The second game makes the players familiar with the global dimension of water management. These two agriculture, industry, and public sector and playing the role of a water resource-related organization. Unlike to the previous games Prakriti provides a joyful experience among players by introducing ways to conserve water. It creates tension and thrill among the play testers to win and to save as much water as possible. This technique brings novelty and life in the game.

2.2. Traditional Board Games to reduce water consumption

In [8], the author Tells that board games are introduces in corporate settings since ten years but are not yet widely used. In general, the true value and impact of board games designed for learning are unrecognized by most people. This paper presents some of the myths,

specific solutions, and current research showing the power of certain types of board games to facilitate rapid learning and retention and the impact of "Pay for Performance." Board games are an important tool to provide hands-on and heads-on skill and knowledge development for people of all ages on all subjects. Not only do well-designed games create an engaging atmosphere, but they also provide a nonthreatening, playful, yet competitive environment in which to focus on content and reinforce and apply to learn. Mistakes are useful and point out what we need to learn. Game elements, discussions, and problem-solving with fellow team members about the content are vehicles for learning. Board games provide exceptional, cost-effective resources. Similarly, Prakriti is an aesthetically sound board game that helps players to chill and relax. With its super engaging techniques Prakriti is designed for families on a dining table. Playing the game with friends and family provides utter joy and feel of comfort and warmth among the players during their leisure.

2.3. Tabletop and Shared Display Games

In [9] and [10] the author Say tabletop displays allow people to sit around a shared display, facilitating group work. One advantage of tabletop displays is their support for face-to-face collaboration: with traditional computer monitors, people must sit shoulder to-shoulder to view the display. There are many aspects of tabletop displays to which board game designs can be applied. These can be grouped as follows: recognizability of graphical objects under various orientations; accessibility of display for interaction; demarcation of individual and shared space; and creation of public and private display areas. Prakriti is used as a shared display game. Because of its multiplayer approach it involves several players in the game and through shared display the game. Brings thrill, excitement and enjoyment among the players. Each move, each card is visibly shared among the play testers for a better clarity and honest vision.

2.4. Mobile Games

In [11] the author describes the purpose of this study is to implement a popular board game Turn Up the Heat incorporates a tablet computer app. The game playfully confronts power dynamics associated with the use of residential thermostats to control heating and cooling systems. The tablet computer app simulates a household heating and cooling system and gives all players (parents and children alike) the opportunity to adjust a thermostat on their turn. In [12]-[14], the authors tried to design a board game to encourage families to face largely energy usage problems playfully in their daily family practice and create opportunities for informal intergenerational learning around sustainability issues. Energy monsters go through a repetitive process in which many prototypes are developed and tested. They have listed two versions of the game for families to test at home. Both versions of the game contain traditional tangible elements, such as cards, tokens, and tiles that make up the game board. In the second design, however, they used the iPad app as an integral feature of play to the end-user. Considering that the users make decisions according to their concern and environmental awareness in conjunction with the belief that their actions shall be beneficial and effective making this aspect of utmost importance. The design strategy focuses on giving the users a tangible experience to make the players make changes for real. The game is a continuous parallel system that tracks the energy consumption of households. The players must choose between two groups, namely, Yellow or Blue. Competition is sparked in the game between the two factions through constant comparison. Researchers have particularly emphasized the importance of authentic and relevant real-world tasks in learning, social aspects of education, mediation skill through peer interactions. Researchers have stated that when their learning technique was based on real-world tasks and previous experiences, students were able to actively participate and retain knowledge. The major difference between pervasive games and traditional simulations is the extension of the gaming experience brought to the physical world. Hence, the developers don't need to build a game world. Instead, we can adapt to the real-world environment and objects into—the game (augmented reality). Usually, the games make use of technologies such as adhoc computing networks and satellite positioning to link the devices together and track them along with the users in a physical environment. Pervasive games are trying to incorporate the virtual game world into our everyday physical spaces. Pervasive learning games extend the game world into the real world. However, ours is a board game so it doesn't implement a game world but equally tries to implement changes into the day to-day life of the players [15]. In [16], the authors express that in recent years, to raise awareness especially in the younger population regarding environmental issues and to stimulate pro-environmental behavior, designers have come up with various games that incorporate our daily life choices and crisis. We sincerely hope that our game not only targets the younger crowd but a larger demographic since ours is a board game along with a software version. Examples of these include

energy management simulations, multiplayer pervasive games, etc. Some games require visualizations of data relating to energy consumption such as charts and gauges. Design choices for the game get dominated by game-specific requirements.

3. Design Document

The design document comprises of 3 subsections. We describe the subsections below:

3.1. Wireframe

We design the wireframe as follows: The wireframe suggests that initially each of the players are assigned with x unit of water. Each player is represented by pawns, and they have cards, die as their formal element. Once the die rolls out even, players start playing. Based on the room of the board, they either loose water unit by doing some chores or the cards save them by teaching how to save water or moving them into the inner circle. The goal is to reach to the end and having maximum unit of water.

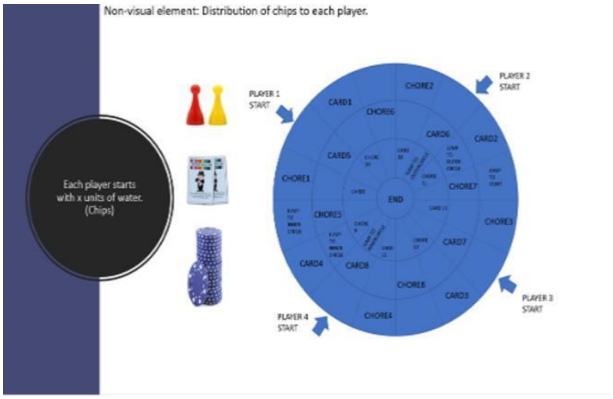

Figure 1: Wireframe of Prakriti

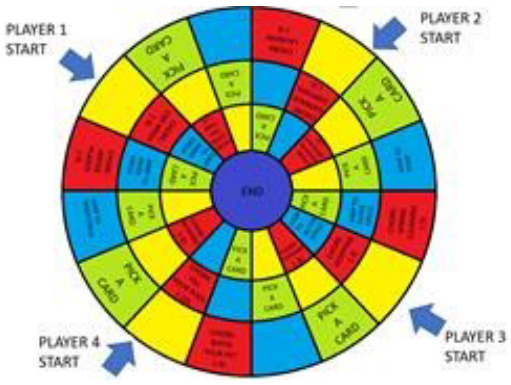

Figure 2: Conceptual Model of the game

3.2. Conceptual Model

The conceptual model (Fig 2) provides a detailed diagrammatic view of each move of a player in the game. Figure3 to Figure 7 illustrates the player movement in the game from beginning to the end. Two players will enter their field of play that is represented as a circular path circles). They begin on the outer circle, each player at a different location and travel in a clockwise direction, and once they have completed a circle, they enter the next outer most circle and so on until the reach the innermost circle. The player who has the maximum number of water units saved when they reach the center is the winner.

3.3. Software Requirements:

To execute this project, we incorporate the following software: Unity and C#. The software development process uses the Rapid Application Development (RAD) method. We rapidly develop each phase of the game and deliver the final product iteratively. Figure 9 depicts the software development flow of the game. We describe some moves of the players in the game in the following images:

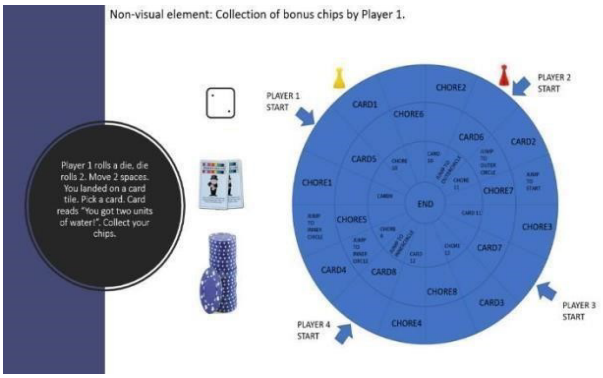

Figure 3: Player Move

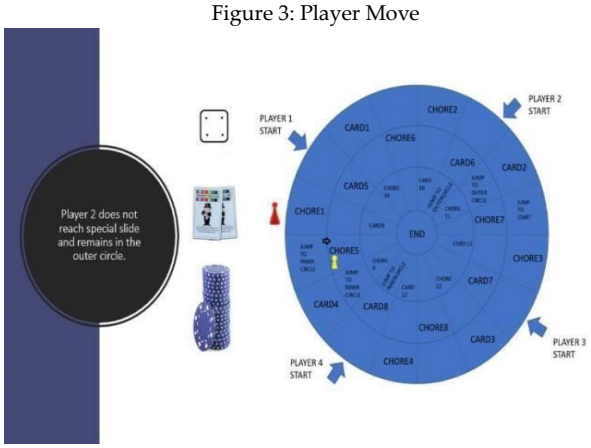

Figure 4: Player Move

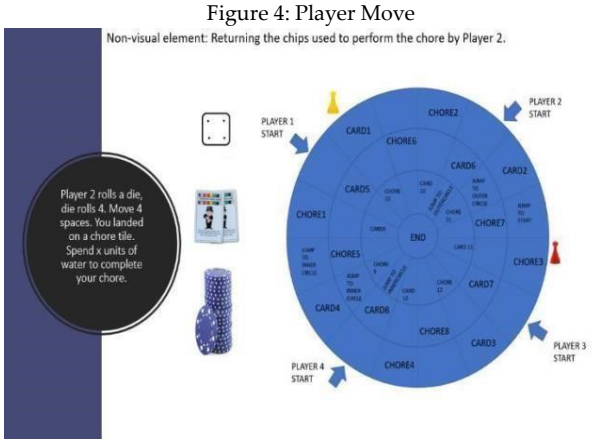

Figure 5: Player move

4. Evaluation

The aim of developing the game water-wise is to spread social awareness as well as make the game enigmatic, fun and engaging. Therefore, to playtest our game, we arrange a few playtesting sessions. After each of these playtesting sessions, we collected the playtesting data from each player. We prepared a series of questions in order to understand the demographic as well as the experiences of each player.

4.1. Evaluation methods

To evaluate the game, we used both co-discovery and remote testing methods. In a co-discovery method, 2 to 3 players playtest the game simultaneously. Each of them figures out the rules, procedures of the game together and share their experiences. Whereas in a remote testing method a player remotely playtests the game and submit their feedback. We adopt both methods to find out the following impressions.

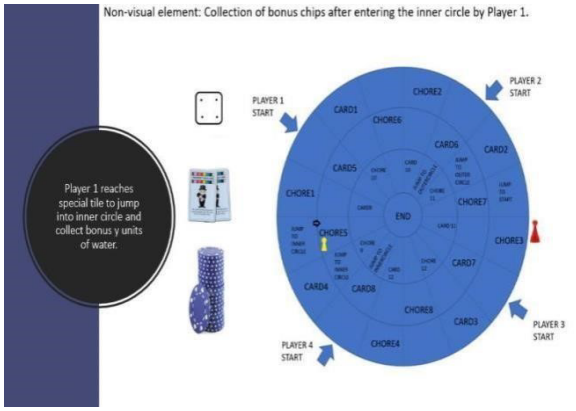

Figure 6: player Move

- The level of difficulty for the game
- The level of difficulty to understand the rules and procedures of the game.
- The magnetic power of the game.

Table 1: Results of pre-Questionnaire

Criteria	Value	Comments
Age	15-21	Most of the play testers are students
Sex	Male- 24	Most of the players
	Female-9	are men
Marital Status	Mostly unmarried	Only 3 to 4 play testers are married
Awareness	57%	They are mostly not aware about the global pollution and climate change
Education level	Undergraduate-10 Graduate-11	They are keen on game designing
Nature lover	98%	Only few play testers claimed they are not nature lover

4.2. Pre Questionnaire:

We incorporate pre-questionnaires to find the basic background of the players. These questions include age, sex, gender marital status, awareness, education level, etc. To broadcast the detailed view, we represent the data in Table1.

Once we collect the data for the background of the play testers, we move forward and prepare another set of pot questionnaire for the play testers.

Table 2: Post Questionnaires

Question	Feedback(Iteration 1)	Feedback(Iteration 2)
Complexity	3	5
Design	7	9
Rules	4	6
Previous Experience	6	8
Uniquenes s	9	10
X factor	6	9
Nature lover	5	7

4.3. Post Questionnaire:

Post questionnaires are designed to evaluate the player's experience once they finish their playtesting session. As we take the Rapid Application Development model approach to develop the software, we incorporate the post questionnaires after each iteration of the development procedure. These questions include interrogations about the complexity of the game, the game rules, the difficulty level of the game, the material of the game, the techniques of the player's move, the player interaction, etc. It becomes easier to modify the game based on the feedback after each iteration. We mention some of the feedbacks for 2 iterations in Tables 2.

Table2 evaluates each aspect of the game in different iterations. It can be seen that with each iteration the game design, board design, the x-factor and the other elements of the board game is taking a better shape. Sometimes, a few aspects were reviewed as poor than before, but in the next iteration we try to resolve the issue and make Table4: Feedback from iteration2 it better.

4.4. Feedbacks

We prudently review and work on each of the reviews we get from the play testers after each iteration of the playtesting session. We try different testing methods like the think-aloud method, co-discovery method, coach method to evaluate the game from every possible dynamic. Table 3, 4 depict the feedback after each iteration. The positive and negative feedbacks help us to consider software prototype repeatedly and the questions help us to build stronger Fig 8, 9 and 10 provide the screenshots of the final game. Directions, rules, and procedures for the game. We collected two-gallery walks as feedback. At least 30 people play tested the game. We describe the feedback below: We describe a few steps of the game in the above figures. The figures describe the die and the pawn movement, score update, card selection as well as the winner.

Table 3: Feedback 1

Positive	Negative	Interrogations
Concept was good	Incomplete board	Challenges
Unique concept	Card description absent	Card function
Local level of social awareness	Ending strategy not clear	How tiles can be named
Unique board design	Tiles need to be designed properly	Need more chores

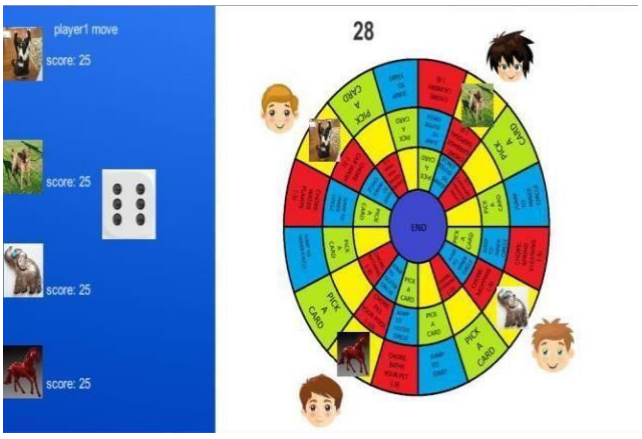

Figure 7: Score update

Table 4: Feedback 2

Positive	Negative	Interrogations
Positive	Negative	Interrogations
Teaches water conservation	Needs more interactions	Board design
Unique tile design	Reduce difficulty level	Introducing dramatic elements
Cards are fun	Difficult to reach end	Why some tiles are empty?

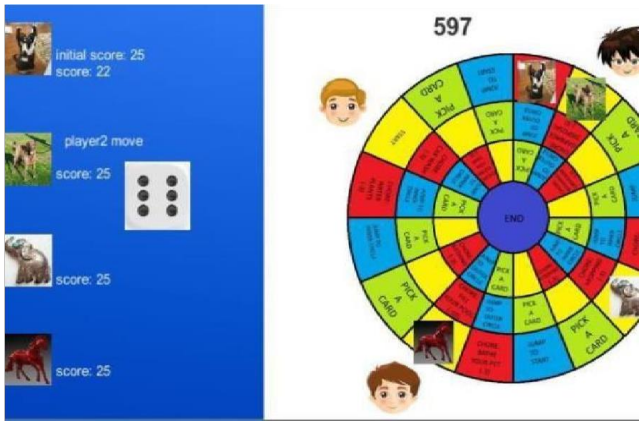

Figure 8: Player Move

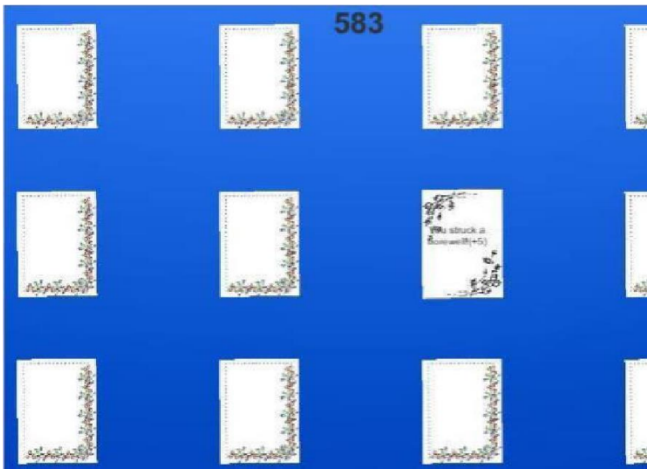

Figure 10: Cards as dramatic element

5. Conclusions

Prakriti is designed for educational purposes. It is a shared display, visually aesthetic, engaging and interactive software based board game. Prakriti supports UN sustainable goals by facilitating water conservation strategies and water conservation awareness. It is of utmost importance that we support this game and make it public aware so that people can get a thrilling, engaging and joyful experience of learning water conservation through a gamified approach during this Covid pandemic. Our game Prakriti makes the play testers time thrilling, fun and happy.

Conflict of Interest

The authors declare no conflict of interest.

References

[1] Arimoro, Augustine Edobor, and Habibah Musa. "Towards sustainable water resource management in rural Nigeria: The role

of communities." *Journal of Sustainable Development Law and Policy (The)* 11.1 (2020): 1-17.

[2] Xiang, Xiaojun, et al. "Urban water resource management for sustainable environment planning using artificial intelligence techniques." *Environmental Impact Assessment Review* 86 (2021): 106515.

[3] Fraternali, Piero, et al. "Integrating real and digital games with data analytics for water consumption behavioral change: a demo." *2015 IEEE/ACM 8th international conference on utility and cloud computing (UCC). IEEE, 2015.*

[4] Albertarelli, Spartaco, et al. "DROP and FUNERGY: Two gamified learning projects for water and energy conservation." *11th European Conference on Games Based Learning, ECGBL 2017. Academic Conferences and Publishing International Limited, 2017.*

[5] Besseling, Debbie. "Every Drop Counts-a water game to remember." *Civil Engineering= Siviele Ingenieurswese 2013.5 (2013): 62-64.*

[6] Hoekstra, Arjen Ysbert. "Computer supported games and role plays in teaching water management." *Hydrology and earth system sciences 16.8 (2012): 2985-2994.*

[7] Cheng, Ping-Han, et al. "Development of an issue-situation-based board game: A systemic learning environment for water resource adaptation education." *Sustainability 11.5 (2019): 1341.*

[8] Treher, Elizabeth N. "Learning with board games." *The Learning Key Inc (2011).*

[9] Whalen, Tara. "Playing well with others: Applying board game design to tabletop display interfaces." *ACM symposium on user interface software and technology. Vol. 5. New York: ACM Press, 2003.*

[10] Xu, Yan, et al. "Chores Are Fun: Understanding Social Play in Board Games for Digital Tabletop Game Design." *DiGRA Conference. 2011.*

[11] Horn, Michael S., et al. "Turn Up the Heat! Board games, environmental sustainability, and cultural forms." *Proceedings Games, Learning, and Society, GLS 14 (2014).*

[12] Banerjee, Amartya, Michael S. Horn, and Pryce Davis. "Invasion of the energy monsters: A family board game about energy consumption." *Proceedings of the 2016 CHI Conference Extended Abstracts on Human Factors in Computing Systems. ACM, 2016.*

[13] Grammenos, Dimitris, Anthony Savidis, and Constantine Stephanidis. "UA-Chess: A universally accessible board game." *Proceedings of the 3rd International Conference on Universal Access in Human-Computer Interaction, Las Vegas, Nevada (July 2005).* 2005. Harteveld, Casper, and Rafael Bidarra. "Learning with games in a professional environment: A case study of a serious game about levee inspection." *Proceedings of the 1st learning with games (2007): 555-562.*

[14] Rajabu, Kossa RM. "Use and impacts of the river basin game in implementing integrated water resources management in Mkoji sub- catchment in Tanzania." *Agricultural Water Management 94.1-3 (2007): 63-72.*

[15] Bang, Magnus, Anton Gustafsson, and Cecilia Katzeff. "Promoting new patterns in household energy consumption with pervasive learning games." *International Conference on Persuasive Technology. Springer, Berlin, Heidelberg, 2007.*

[16] De Luca, Vanessa, and Roberta Castri. "The social power game: A smart application for sharing energy-saving behaviours in the city." *FSEA 2014 27 (2014).*

Tathagata Bhattacharya

Tathagata Bhattacharya is currently pursuing his integrated masters PhD degree in computer science and software engineering from Auburn University, Auburn, AL, USA. He has received his bachelor's and master's degree from India. His domain of work in green computing, high performance computing, cluster computing etc.

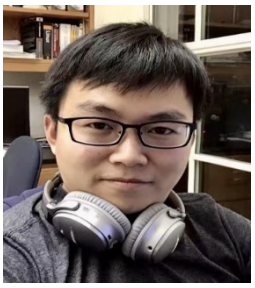

Xiaopu Peng

Xiaopu Peng received a B.S. degree in Mathematics from Jianghan University, Wuhan, China, in 2008; and a Master's degree in Economics from SUNY at Stony Brook. He is currently working toward the PhD's degree in the Department of Computer Science, Auburn University, under the supervision of Prof. Xiao Qin. His research interests include Data Science and Energy Efficiency of Data Center.

Ishita Naresh Joshi

Ishita Naresh Joshi received an M.S. degree in Computer Sc. And Software Engineering from Auburn University.

Ting Cao

Ting Cao received his Master of Science degree from Auburn University in 2017. He is currently pursuing the Ph.D. degree in Computer Science & Software Technology at Auburn University. His research focuses on distributed storage system and machine learning.

Jianzhou Mao

Jianzhou Mao received the B.S. degrees from Macau University of Science and Technology, Macau, China, in 2017. He is currently a PhD candidate in computer engineering supervised by Dr. Xiao Qin at the Auburn University, Alabama. His current research focuses on power-aware management strategy for datacenters.

Xiao Qin

Xiao Qin is a Professor in the Department of Computer Science and Software Engineering at Auburn University. He received the B.S. and M.S. degrees in Computer Science from Huazhong University of Science and Technology, China, in 1996 and 1999, respectively. He received the Ph.D. in Computer Science from the University of Nebraska-Lincoln in 2004. His research interests include parallel and distributed systems, real-time computing, storage systems, fault tolerance, and performance evaluation. His research is supported by the U.S. National Science Foundation, Auburn University, and Intel Corporation.

JENRS

Received: 30 December 2021, Revised: 19 February 2022, Accepted: 27 February 2022, Online: 14 March 2022

DOI: https://dx.doi.org/10.55708/js0102005

Geophysical and Geotechnical Investigations for Subsoil Competence at a Proposed Hostel Site at Oba Nla, Akure Southwestern Nigeria

Festus Olusola Eebo*, Abidakun Bayode Samuel, Gbenga Moses Olayanju

Department of Applied Geophysics, Federal University of Technology, Akure, Nigeria

*Corresponding author: Eebo Festus Olusola, +2348034380549 & festus.o.eebo@gmail.com

ABSTRACT: A foundation study was carried out at a proposed Hostel site for the student of Federal University of Technology Akure, Nigeria with the aim of evaluating the competence of the overburden as foundation materials. Geophysical survey involving Electromagnetic method and magnetic method were conducted in conjunction with geotechnical tests in the study area. Electromagnetics and Magnetics data were acquired along the five traverses established across the study area with 20 m inter-traverse spacing and 5 m inter-station spacing. The geophysical results were interpreted qualitatively and quantitatively, and the results were presented as profiles and geomagnetic sections. From the results of the Very Low Electromagnetic survey conducted, several conductive zones possibly characterized by clayey materials were found to make up the overburden materials in the area. Characteristic magnetic anomalies in the area also revealed series of features at shallow depths identified to be fractures / fault at shallow depths with depth to bedrock varying between 2 m and 7 m. The presence of geologic features such as fracture and conductive clayey materials are likely going to pose a serious threat to engineering structure in the area. Geotechnical tests were carried out on soil samples from the study area and different geotechnical parameters analyzed include the natural moisture content, Atterberg Limits, unconfined compressive strength and shear strength. The specific gravity of the soils is within the range of 2.722 – 2.73 g/cm^3, revealing materials of low water absorption capacity. However, the soils are highly plastic with the plastic limit ranging from 20.4 – 24.4% and a plasticity index range of 23.75 – 35.90%. In addition, the soils have shear strength within the range of 75 to 102 kPa and unconfined strength ranging from 150 to 203 kPa revealing stiff soils that are not suitable for shallow foundations. It was observed that the form of foundation suitable for infrastructural development in the study area is a properly designed deep foundation that can transfer load at grater depths.

KEYWORDS: Electromagnetic, Geotechnical tests, Magnetic anomaly, Competence, Engineering structure.

1. Introduction

Incessant failure of structures such as road, buildings, dam and bridges has become a common phenomenon in many parts of Nigeria. Hence, there is a need to identify the cause(s) of structure failure and find a means of tackling the problem to prevent loss of valuable lives and properties. Factors that can be responsible for structural failures include bad design, faulty construction, foundation failure and over loads.

A reliable foundation design depends on the characteristics of both the geological structures and the near subsurface soil or rock. Therefore, the nature (i.e. competence, strength and load bearing capacity) of the soil supporting the super structure becomes an extremely

important issue of safety, structural integrity and durability of the super structure. Hence, a detail investigation of the subsoil is required by non-destructive techniques such as geophysical methods which respond to the heterogeneous nature of soil particles through some physical parameters that govern the subsoil competency [1].

Foundation study usually provides subsurface information that normally assists civil engineers in the design of foundations. Standard engineering practice requires investigation of soil and the subsurface at the site chosen for engineering construction. This is routinely done to ascertain the sustainability of the earth material at such site for proposed structures i.e., in terms of bearing capacity and/or host fitness. Despite, some of the pre-construction investigation by site engineers, some impacts of infrastructural failures can manifest as ground subsidence, major cracks, failed road segment and fractional settlement of the structures [2] – [4]. These factors can be attributed to geologic nature of the environment where the structures are emplaced. Integrated geophysical and geotechnical investigations for foundation design have proved to be good veritable tools in effective foundation design and construction [5], and these methods are much more suitable in providing information about geologic and geophysical parameters that can aid foundation studies at low cost and time effective.

Environmental geophysics provides a wide range of geophysical methods that can effectively provide spatial information about the homogeneity of subsurface materials as well as structural disposition of the areas demarcated for civil engineering constructions in terms of suitability, integrity and load capacity of construction materials at low costs and man power size [6], [7].

On like sedimentary area where pronounced geological factor could be attributed to lithification and settlements of sedimentary overburden, geological factors in crystalline environment three major causes of potential failures of infrastructures are failure due to lateral inhomogeneity of the subsurface layers, failure precipitated by differential settlement and failure initiated by fractures and faults [8]-[10]. Therefore, since there is no substitute for pre-foundation investigation of proposed site for engineering structure in order to ensure effective construction programme.

In this paper, integrated geophysical and geotechnical evaluation of subsoil competence and suitability for erecting proposed hostel at site within the FUTA campus is presented. The investigation carried out focused on the suitability of the study area for civil engineering structures by mapping the subsurface conductive zones and geologic structures in order to identify subsurface structures or features that could be inimical to foundation in the area. The knowledge of spatial presentation of these structurally weak subsurface futures and zones are of great advantage for ensuring good foundation of infrastructures in the study area.

2. Study Area

The study area is located inside the Federal University of Technology, Akure (FUTA). It is accessible through FUTA North gate via the road to the undergraduate hostel directly opposite Jadesola and Adeniyi hostels and from South gate via the FUTA piggery section (Figure 1). The study area is bounded by Easting 736677E to 736669E and Northing 807650N to 807614N in Universal Traverse Mercator (UTM) coordinate system and Minna Zone 31 datum [11].

The study area is underlain by rocks of Precambrian Basement Complex of Southwestern Nigeria [12]. The crystalline rocks are porphyritic granite, biotite granite, quartzite and gneiss migmatite, while Charnokites rocks occur as discrete bodies in other parts of the area (Figure 1). The geology and boundaries of the lithological units were inferred in places where they are concealed by superficial residual soil.

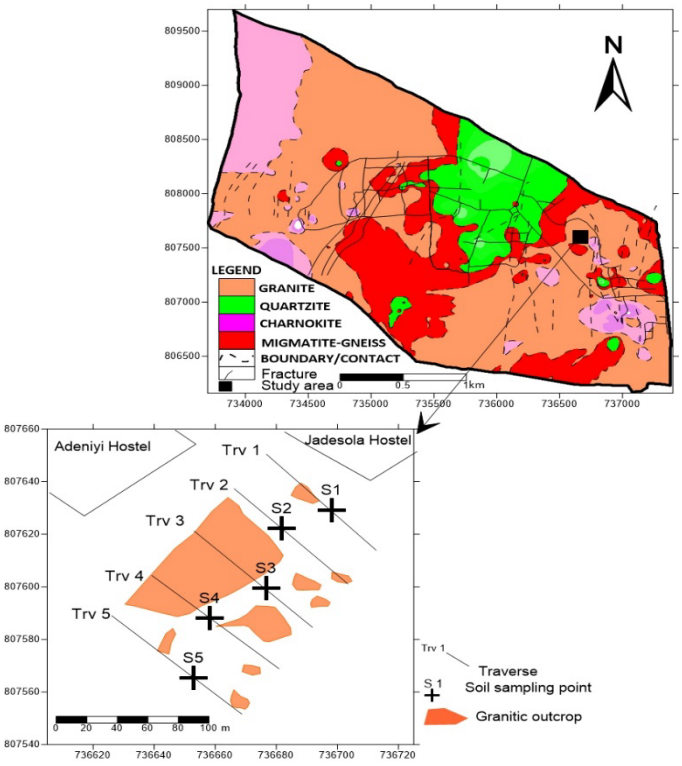

Figure 1: Geological map of FUTA Campus showing the Study Area [11].

3. Methodology

3.1. Geophysical Survey

3.1.1. VLF-EM Survey

Five traverses were established across the study area for both the VLF and magnetics surveys conducted. The VLF receiver used for the EM survey is a hand-held

receiver measuring the tilt-angle of the magnetic field polarization ellipse. The tilt-angle is obtained by rotating the instrument until a null is obtained (indicated audibly through a speaker, if the instrument is audio enabled) then, the angle is read from an inclinometer mounted on the instrument case. Field traverses were located perpendicular to strike direction so the anomalous zones can be compared to background levels. VLF data were collected along traverses, and anomalies are correlated from traverse to traverse. The sampling interval of 5m was used for the EM survey and the mode of measurement adopted was point-by-point data measurement with traverse-traverse spacing of 20 m. The VLF data was filtered using the Karous-Hjelt filter to enhance the data and convert the tilt-angle crossovers into peaks. The "real" and "imaginary" components of data collected from the field were plotted against distance along the traverse. The VLF data was interpreted qualitatively by the visual inspection of profiles generated from the data for anomaly signatures.

3.1.2. *Magnetic Survey*

The magnetic measurements were recorded using a proton precision magnetometer that involves the total magnetic intensities. Measurement of ground magnetic intensities were made along the five established traverses with station-to-station separation of 5m and traverse to traverse spacing of 20m. The ground magnetic survey conducted in the study area was processed to prepare the dataset for interpretations. The data processing steps includes, removal of International Geomagnetic Reference Field (IGRF) from the magnetic reading at each station, application of moving average filter to remove high frequency noise, removal of main magnetic field using polynomial fitting along the traverses. The residual is the obtained by removing the regional field calculated, where the expression for the residual anomaly becomes;

$$F_R = F_T - F_M \quad (1)$$

where F_M is the residual anomaly, F_T is the measured total field and F_R is the computed main field plus regional anomaly. The residual magnetic field is then presented as magnetic profiles and the depth estimation of the basement in the area was carried out using half-slope method and straight slope method [7].

3.2. *Geotechnical Tests*

3.2.1. *Sample Collection*

Five undisturbed soil samples were collected at different locations at a depth of 1m within the site.

These samples were preserved in a labelled polythene bags and transported to the laboratory.

The natural moisture content of the samples collected from the field was determined in the laboratory within a period of 24 hours after collection. This was followed by air drying of the samples by spreading them out on trays in a fairly warm room for four days. Large soil particles (clods) in the samples were broken with a wooden mallet. Care was taken not to crush the individual particles. The geotechnical tests conducted on the samples include the Natural Moisture Content determination, Atterberg Limits test, Compaction test, Shear Strength test and Unconfined Compressive Test. Methods of testing soils for engineering parameters were conducted in accordance with [13] for all the soil samples collected.

3.2.2. *Atterberg limits test*

Atterberg limits test was carried out on five soil samples taken randomly in the study area at a depth of 1 m. For the soil samples collected, a soil mass of at least 200 g which has been sieved through a 425 micron sieve was used. The geotechnical parameters derived from the Atterberg Limits Test include the Plastic limit, the Liquid limit and the linear shrinkage.

The liquid limit describes the moisture content at which the soil is on the verge of becoming a viscous fluid. The plastic limit is the water content where soil starts to exhibit plastic behaviour. It is a measure of the water content at which the soil begins to crumble when rolled into a thin thread of about 3 mm in diameter.

The linear shrinkage is described as the water content of a soil at which any further reduction in the water content does not result in a change of volume of that soil.

The linear shrinkage is given by the expression

$$LS = \frac{Li - Lf}{Li} \times 100 \quad (2)$$

where L_i = length of the specimen before drying;
L_f = length of specimen after drying.

3.2.3. *Compaction Test*

Compaction test was carried out for the various soil samples collected using the AST 698 standard proctor. 10 lbs of each samples analysed sieved through sieve No. 4 are placed in a mould of 944 cm^3 volume without the base and the collar. The compaction apparatus was assembled and the soil sample placed in the mould in 3 layers and compacted using 25 well distributed blows of the proctor hammer per layer with the collar and base in place. The collar was detached without disturbing the soil inside the mould. The base is removed the weight of the mould and compacted soil recorded. The compacted soil is the removed from the mould, the moisture content of 20-30 g of the sample determined. The remaining sample is then placed in the pan, broken down, and thoroughly remixed in 100 g of water and procedure repeated to obtain a set of 5 records of the average moisture content and dry density of the samples. Compaction curves are then drawn from the results in order to determine at which

point on the compaction the specific amount of water will produce the maximum dry density, which is known as the optimum moisture content.

3.2.4. Unconfined Compression (UC) Test

The Unconfined compressive strength of the soil in the area defines the compressive strength at which an unconfined cylindrical specimen of a soil will fail in a simple compression test. In this test, the unconfined compressive strength is taken as the maximum load attained per unit area, or the load per unit area at 15% axial strain. Soil samples were compacted into a hollow cylindrical cutter to achieve maximum density, from which trimmed sample in a cylindrical shape with height to diameter ratio of 2:1 was weighed using a balance. The soil mass was then tested for unconfined compressive strength in the UCS machine by applying load at a constant rate until the soil failed. The dial reading was recorded with load increase, while the load at which failure occurs represents the peak of compressive stress for the sample, which is the soil compressive strength. The trimmed cylindrical soil samples were thereafter tested for untrained shear strength in the triaxial test apparatus in accordance with [14]

4. Results and Discussions

4.1. Geophysical Survey

4.1.1. Very Low Frequency Electromagnetic (VLF) Survey.

On the filtered real component of the VLF-EM survey profile, positive peaks are indication of high conductive zones, which could be probable fault, fracture, or clay materials deposit. These conductive zones are detrimental to engineering foundation construction. Several positive peaks were observed on the filtered real profiles along the 5 traverses (Figures 2-6), which suggest conductive zones characteristic of clayey material, fractures, or some other linear features. From traverse 1, a conductive body was delineated within 10-15m and a highly conductive body was obtained within 30-35m along the same traverse (Figure 2).

In Figure 3, a low conductive body at 22-28 m and 36-40 m were delineated from the current density section. The highly and negative zone between 22 m and 28 m appears to be a boulder while the other conductive body have a characteristic of a clayey material at shallow depth. In Figure 4, an extensive conductive zone was observed to the west from the beginning of the traverse to a distance of 38 m, while a resistive body recognized to be a migmatite gneiss intrusion lies between 40m and 52 m. Similarly, from Figure 5, a high conductive body was delineated from 22-33 m along the traverse. The conductive body appears to be an extension across the traverse. The VLF-EM current density shown in Figure 6 indicates the presence of conductive bodies along the traverse. It was observed that the overburden material is generally conductive along this traverse.

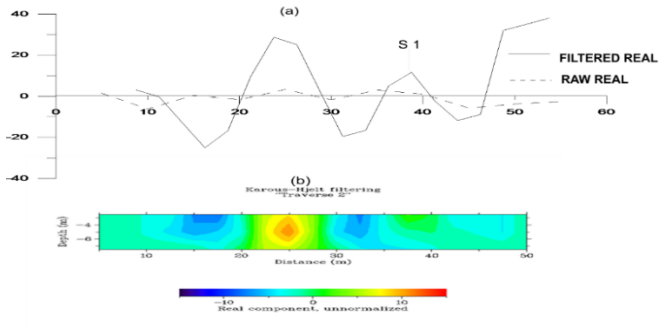

Figure 2: (a) Profiles of the EM raw real and filtered real component, (b) Pseudo-section along traverse 1.

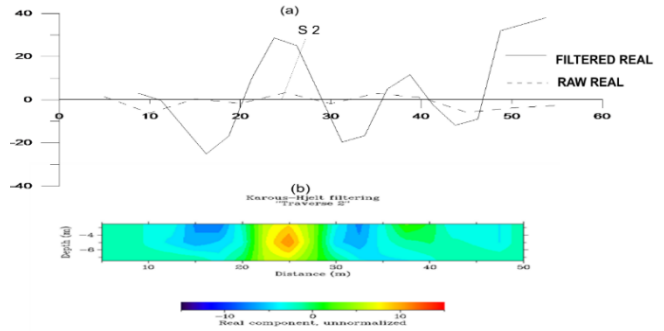

Figure 3: (a) Profiles of the EM raw real and filtered real component, (b) Pseudo-section along traverse 2

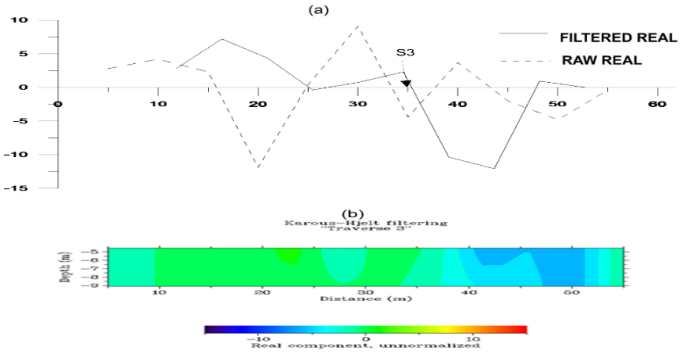

Figure 4: (a) Profiles of the EM raw real and filtered real component, (b) Pseudo-section along traverse 3

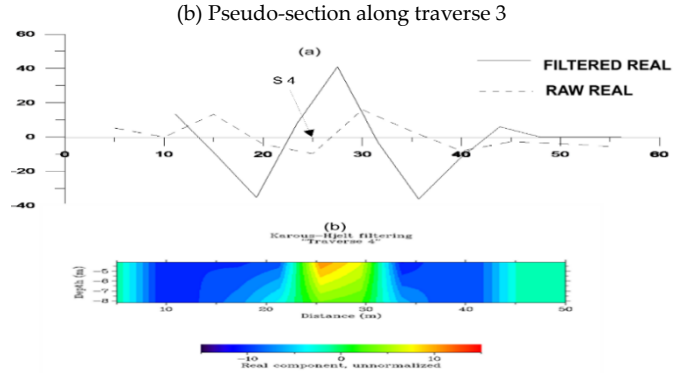

Figure 5: (a) Profiles of the EM raw real and filtered real component, (b) Pseudo-section along traverse 4

4.1.2. Magnetic Profiles

A total of five traverses were occupied and the results of the interpreted magnetic fields (residual anomalies)

displayed as residual anomaly profiles were used in the generation of geo-magnetic sections (Figure 7-11)

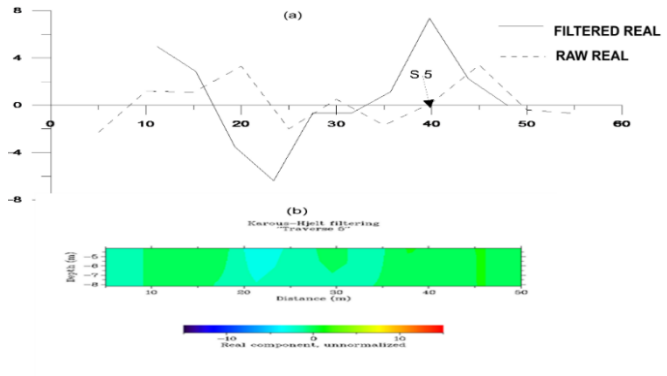

Figure 6: (a) Profiles of the EM raw real and filtered real component, (b) Pseudo-section along traverse 5.

The residual magnetic profile along traverse 1 is shown in Figure 7a with anomaly amplitude varying between -60 nT and 80 nT. The varying magnetic intensity suggests varying magnetic materials associated with the rock types in the area. The high amplitude at a distance between 20 m and 40 m suggest the presence of an intrusive body in the form of a dyke within the basement rock occurring at a shallow depth below the surface. The current density section shown in Figure 2b revealed an intruding resistive body at this point of anomaly, the depth to top of the anomaly was estimated to be 3 m and 6 m. The magnetic profile for traverse 2 is shown in Figure 8a. The profile shows amplitude variation between -191nT and 308 nT. A projecting anomaly observed between a distance of 18 m and 30 m appears to be characteristic of a dyke, which was observed to be a conductive body at shallow depth in the EM-VLF current density section in Figure 3b. The magnetic profile and geomagnetic section for traverse 3 are presented in Figure 9. The profile shows amplitude variation between -225 nT and 488 nT. The varying magnetic intensity suggests varying magnetic materials associated with the rock types in the area. The positive anomaly observed between the distances of 38-55 m suggests a change in rock types from granite to migmatite gneiss. The preluding anomaly between 12 m and 20 m is observed to be an extension of anomaly recognized along traverse 1 and 2 as an intruding dyke-like structure, which correspond to the conductive body observed in the current density sections in Figure 2b and 3b. The magnetic profile and geomagnetic section for traverse 4 are presented in Figure 10, where the profile shows amplitude variation between -1200 nT and 900 nT.

The varying magnetic intensity suggests varying magnetic materials associated with the rock types of different lithology and mineral content. The magnetic signature changing from high negative to positive anomaly at a distance from 40 - 55 m is characteristic of boundary between the granite and migmatite gneiss. The geomagnetic section reveals that the overburden thickness ranges from 3 m and 7 m along the traverse. The magnetic profile and geomagnetic section for traverse 5 are presented in Figure 11. The anomaly amplitude varies between -2100nT and 1400nT at a distance of 30 – 40 m suggesting varying magnetic intensity associated with varying magnetic materials in the underlying rock type in the area. The observed anomaly signature corresponds to contact between two rock types. Depth to bedrock ranges from 2m and 7m along the traverse.

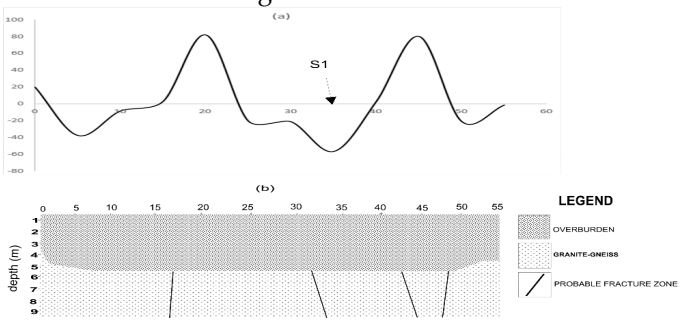

Figure 7: (a) Residual magnetic profile along traverse 1, (b) Geomagnetic section along traverse1.

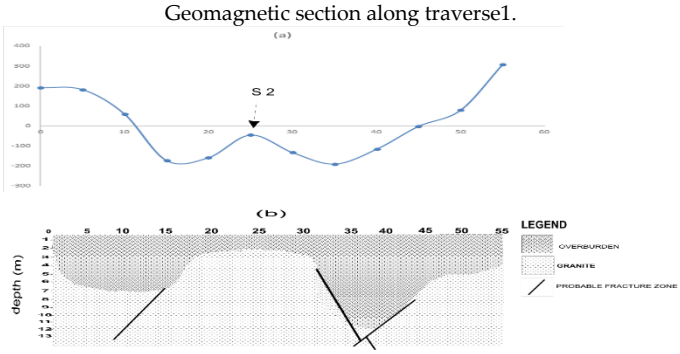

Figure 8: (a) Residual magnetic profile along traverse 2, (b) Geomagnetic section along traverse2

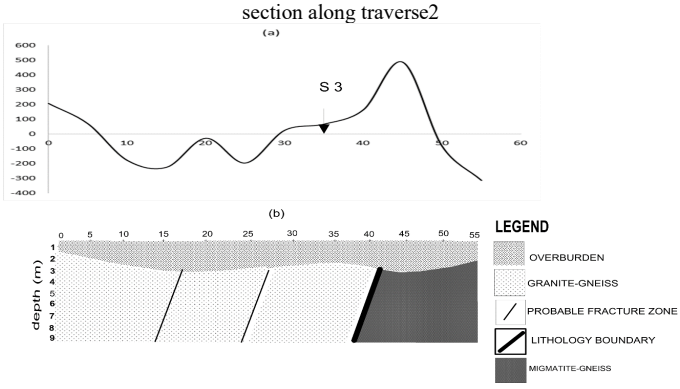

Figure 9: (a) Residual magnetic profile along traverse 3, (b) Geomagnetic section along traverse3

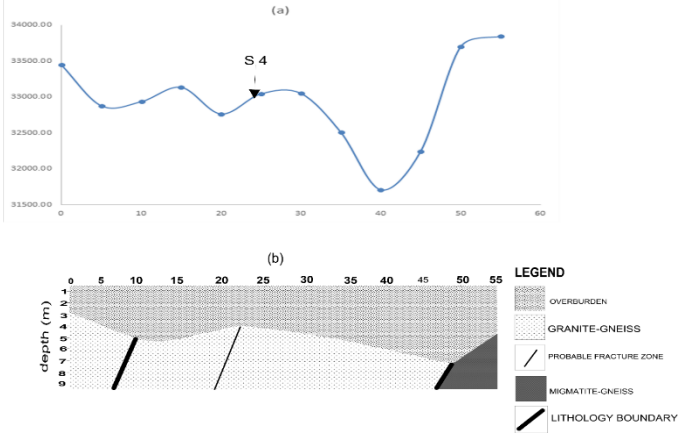

Figure 10: (a) Residual magnetic profile along traverse 4, (b) Geomagnetic section along traverse4

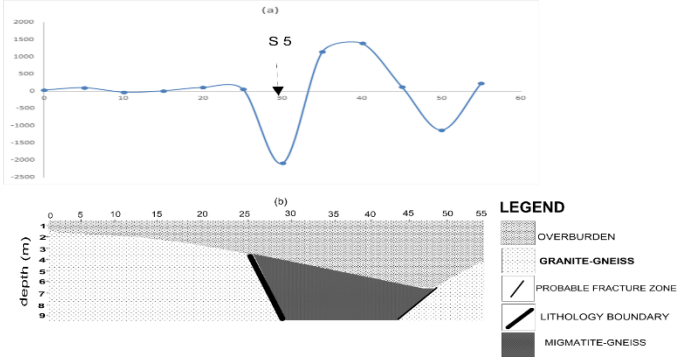

Figure 11: a) Residual magnetic profile along traverse 5, (b) Geomagnetic section along traverse

4.2. Geotechnical Analyses

The results from the various geotechnical analyses conducted on the soils samples from the study area are shown in Tables 1 and 2. From Table 1, the soil sample from the study area have a plastic limit range of 20.4 – 24.4% and a plasticity index range of 23.75 – 35.90% indicating a soil of high plasticity in according with [15]. Thus, the soils at the study location are not suitable for shallow foundations.

4.2.1. Particle Size Distribution and Specific Gravity

From Table 2, the percentage of silt and clay in the soil sample from the study area is within the range of 45.8 - 73.8% indicating that the soil samples are silty clay, which is not suitable for shallow foundation construction. The specific gravity values of the soil samples are within the range of 2.722 – 2.73 g/cm^3, which allows the rating of soil samples as good foundation material due to their low water absorption capacity. From Figure 12-16, the soil samples are above the A-line on the plasticity chart indicating that they are very plastic, thus making them unsuitable for foundation construction because they can crack when dry.

Table 1: Summary of Atterberg limits test, UC test, Compaction Test of Soil sample from the study area

Sample No	**1**	**2**	**3**	**4**	**5**
Liquid limit (%)	56.30	46.10	55.50	56.40	54.70
Plastic limit (%)	20.40	22.40	23.50	24.40	23.40
Shrinkage limit	7.70	8.70	7.70	7.70	7.70
Linear shrinkage	11.40	10.00	11.40	11.40	11.40
Field Moisture content (%)	16.20	14.60	17.10	17.20	16.80
Swell index	0.29	0.32	0.31	0.30	0.31
Plasticity index	35.90	23.75	32.05	32.00	31.30
Flow index	6.59	6.59	6.59	6.59	6.59
Consistency index	1.12	1.33 (Very stiff)	1.20 (Very stiff)	1.23 (very stiff)	1.21 (very stiff)
Liquidity index	-0.12	-0.33	-0.200	-0.23	-0.21
Average specific gravity	2.723	2.722	2.727	2.722	2.731
Unconfined compressive strength (kPa)	203.2	150.3	165.5	159.9	172.6
OMC (%)	27.6	25.7	27.8	27.9	27.1
Shear strength (kPa)	101.58	75.16	82.73	79.97	86.29
MDD (kg/m^3)	1528	1593	1521	1518	1545
BSCS Group Symbol	CH	CL	CH	CH	CH

Note: CH= High plasticity silty clay or clayey soil, CL= low plasticity silty clay.

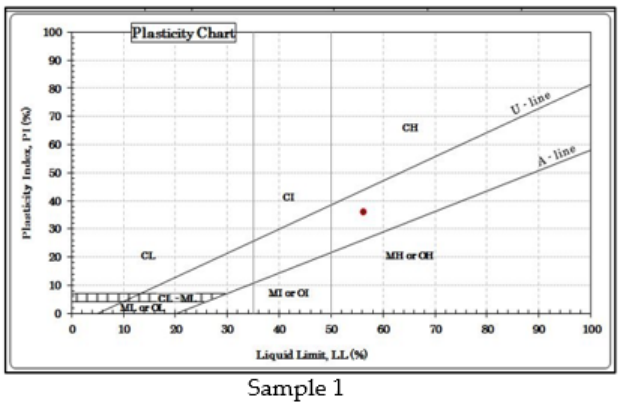

Figure 12: Plasticity Chart of soil sample 1 from the study area.

Table 2: Summary of Particle Size Distribution of Soil Samples from the Study Area

Sample number	1	2	3	4	5
Gravel (%)	1.4	0.0	0.0	0.0	0.0
Sand (%)	52.9	27.3	27.5	26.1	27.3
Silt (%)	13.5	34.6	34.7	36.4	33.5
Clay (%)	32.3	38.1	37.8	37.4	39.2

Moisture content (%)	16.2	14.6	17.1	17.2	16.8
Average specific gravity	2.723	2.722	2.727	2.722	2.731

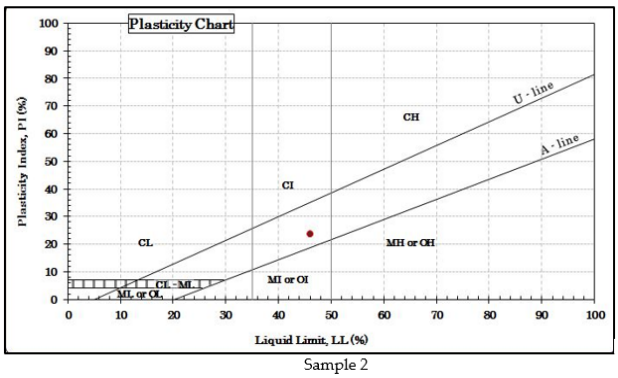

Figure 13: Plasticity Chart of soil sample 2 from the study area.

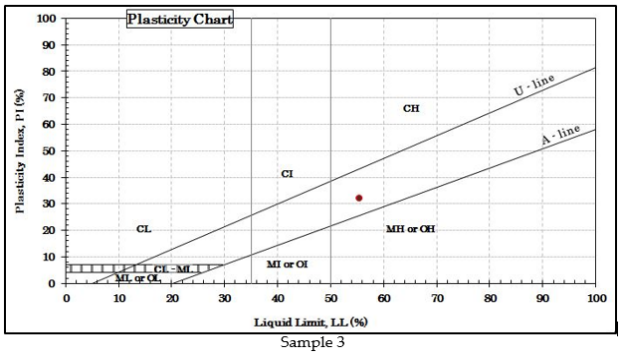

Figure 14: Plasticity Chart of soil sample 3 from the study area.

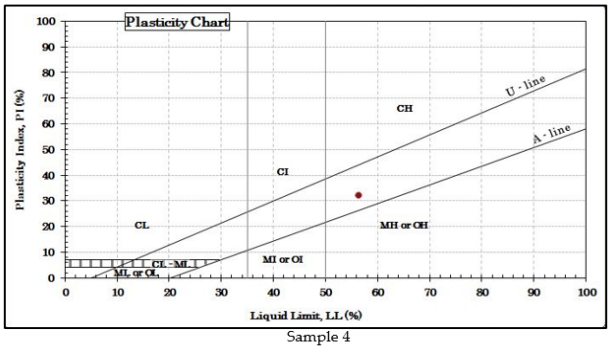

Figure 15: Plasticity Chart of soil sample 4 from the study area.

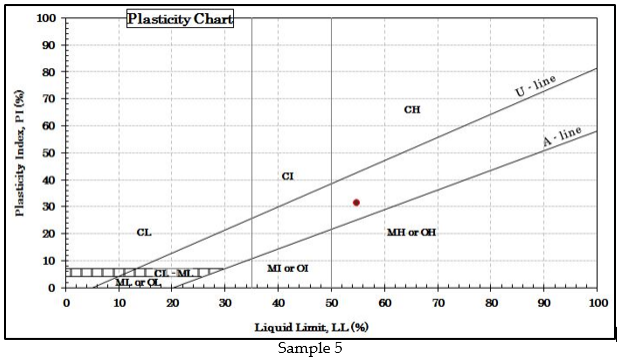

Figure 16: Plasticity Chart of soil sample 5 from the study area

4.2.2. Compaction Test

The compaction test was conducted to determine the maximum dry density (MDD) value of a soil sample with respect to its load capacity. The maximum dry density and optimum moisture content were determined from the results of the test using the [3] guidelines for compaction tests to determine their compaction parameters from the plot of the dry density against the moisture content. From Table 1, the OMC values are within the range of 25.7 – 27.9 % and the MDD values within the range of 1518 – 1593 kg/m^3.

4.2.3. Unconfined Compression Test

From Table1, the soil samples have shear strength value within the range of 75.16 – 101.58 **kPa** and unconfined compressive strength range of 150.3 – 203.2 **kPa** indicating that the soil samples are very stiff according to [16]. A very stiff soil is not suitable for foundation construction due to the fact that it can easily become plastic when wet.

5. Conclusions

The results of integrated geophysical and geotechnical evaluation of a site for development of proposed infrastructures for students' residential purpose have been presented to address suitability of soil material to sustain building and other civil constructions. From the geophysical surveys, several conductive zones identified to be characterized by clayey materials were observed to make up the overburden materials from the results of the EM-VLF survey conducted, while characteristic magnetic anomalies in the area also revealed series of features at shallow depths identified to be fractures / fault at shallow depths. Implications of these structural features suggest that, the overburden is generally prone to future instability from shear movement of erected structures, weakness of the overburden due to clayey nature of overburden in some areas and possible percolation of surface water into the foundations if proper stabilization and reinforcements are not made to enhance the load capacity of soil in the area as foundation material. However, places with shallow competent bedrock devoid of inimical features such as fractures or clayey overburden materials are appropriate for infrastructural development in the stud area.

From the geotechnical investigation, the soil samples were found to be characterized by high plasticity and poorly graded soil with high clay content. The result of compaction test revealed that the soils have shear strength within the range of 75 to 102 **kPa** and unconfined strength ranging from 150 to 203 **kPa** suggesting stiff soils which are not suitable for shallow foundations.

Thus, the combined application of geophysical and geotechnical methods in evaluating the soil stability and

capacity for carrying effective loads for the infrastructural development of the area has shown that a comprehensive design of suitable foundation programme must be embarked for the construction of the proposed students' hostel and other facilities in the area. Presence of fractures/ faults at shallow depth may results in development of cracks and lateral displacement of some parts of the structure if proper preventive measure were not taken at construction stage. It is therefore concluded that a deep foundation will be more appropriate to transfer load at grater depths due to the weakness of the overburden materials to accommodate and transfer loads.

6. Recommendations

In this paper the significance of geophysical and geotechnical investigations as part of pre-foundation evaluation has been demonstrated for the design foundations. In this particular case, it is recommended that for proper designing of the foundations of the proposed structures in the study area, the foundation pavements must be founded on competent underlying bedrock, which is close to the surface in the area since the near surface lithology revealed occurrence of highly plastic and clayey materials. In addition, preventive measures must be taken to avoid lateral movement that can result in the shearing of parts of the proposed structures.

Conflict of Interest

The authors declare no conflict of interest.

The research was self-funded by the authors.

Acknowledgement

The authors sincerely appreciate the assistance of the Mr. Mamukuyomi, A. who was involved in the geophysical data collection and the technical staff of Applied Geology Department, FUTA that also assisted in geotechnical tests conducted.

References

[1] S. Bayode, A. A. Egbebi, "Subsoil Characterization for Foundation Stability Using Geophysical and Geotechnical Methods," *Journal of Environment and Earth Science. Vol.10, No.6, 2020.Pp. 8,* 2020, https://doi.org/10.7176/jees/10-6-08

[2] L.O. Ademilua, M.O. Olorunfemi, "A geoelectric/ geologic estimation of groundwater potential of the basement complex area of Ekiti and Ondo state, Nigeria," Journal of Technoscience Vol. 4, Pp 4-18, 2000, https://ouci.dntb.gov.ua/en/works/legBpwg7/

[3] M.O. Olorunfemi, A.I. Idornigie, A.T. Coker, G.E. Babadiya, "On the application of the electrical resistivity method on foundation failure investigation- a case study," *Global Journal of Geological Sciences*, Vol 2(1), Pp139-151, 2004, https://doi.org/10.4314/gjgs.v2i1.18689

[4] O.J. Akintorinwa, F.A. Adelusi, "Integration of geophysical and geotechnical Investigations for a Proposed Lecture Room Complex at the Federal University, Akure, Nigeria," *Journal of Applied Sciencs* Vol 2(3): Pp 241, 2009, https://www.scirp.org/%28S%28vtj3fa45qm1ean45vvffcz55%29%29/reference/referencespapers.aspx?referenceid=2674470

[5] O. O. Falowo, M. B. Amodu, "Engineering Subsoil Characterization for Shallow Foundation Design in Ode Irele Area of Ondo State, Southwestern Nigeria," *European Journal of Environment and Earth Sciences. Vol 1 (2),* 2020, *http://dx.doi.org/10.24018/ejgeo.2020.1.2.6*.Pg.1

[6] W.M.Telford, L.P. Geldart, R.G.Sheriff, D.A. Keys, "Applied Geophysics Published by Cambridge University Press, Cambridge," pp7 – 215, 632 – 692, 1976, https://www.scirp.org/(S(i43dyn45teexjx455qlt3d2q))/reference/ReferencesPapers.aspx?ReferenceID=1748399

[7] J. M. Reynolds, (1997): "An introduction to Environmental *Geophysics*, John Willey & Sons London," U.K. 796pp, https://scirp.org/reference/ReferencesPapers.aspx?ReferenceID=1236461

[8] M.O. Olorunfemi, J.O. Fatoba, L.O. Ademilua, "Integrated VLF-Electromagnetic and Electrical resitivity survey for groundwater in a crystalline basement complex terrain of southwestern Nigeria," *Global Journal of Geological Sciences*, Vol.3, No. 1, Pp 71-80, 2005, DOI: 10.4314/gjgs.v3i1.18714

[9] M.O. Ofomola, K.A.N. Adiat, G.M. Olayanju, B.D. Ako, "Integrated geophysical methods for post foundation studies, Obanla staff Quarters of the Federal University of Technology Akure, Nigeria," *Pacific Journal of Science and Technology*, Vol 10(2), Pp 93-111, 2009, https://citeseerx.ist.psu.edu/viewdoc/download?doi=10.1.1.500.1327&rep=rep1&type=pdf

[10] A.O. Adelusi, A.A. Akinlalu, A.I. Nwachukwu, "Integrated geophysical investigation for post-construction studies of buildings around School of Science area, Federal University of Technology, Akure, Southwestern, Nigeria," *International Journal of Physical Science*, Vol 8(15), Pp 657-669, 2013, https://doi.org/10.5897/ijps2012.0204

[11] G.M. Olayanju and A.O.Ojo, "Magnetic Characterisation of Rocks Underlying FUTA Campus, South-Western Nigeria," *Journal of Environment and Earth Science*, Vol. 5, No. 14, pp 113 – 127, 2015, https://www.iiste.org/Journals/index.php/JEES/article/view/24260.

[12] M.A. Rahaman, "Review of the basement geology of southwestern Nigeria in Geology of Nigeria," *Elizabethan Publishing Company*, Nigeria. Pp. 44 – 58, 1976, http://www.sciepub.com/reference/51956

[13] American Society for Testing Materials, ASTM, 1557, "Test Method for Laboratory Compaction Characteristics of Soil Using Modified Effort," Annual Book of ASTM Standards, 1991, https://shop.iccsafe.org/astm-d-1557-07-test-method-for-laboratory-compaction-characteristics-of-soil-using-modified-effort-56-000-ft-lb-ft3-2-700-kn-m-m3-pdf-download.html

[14] British Standards Institution, BS 1377, "Methods of Test for Soils for Civil Engineering Purposes," British Standards Institute, Milton Keynes, 1990, http://worldcat.org/isbn/058018030

[15] American Society for Testing Materials, ASTM, "Standard test method for classification of soils for engineering purposes (Unified Soil Classification System)," ASTM standard D2487-90, 1992. Annual Books of ASTM Standards, Vol. 04.08, sec. 4, 1992, https://lauwtjunnji.weebly.com/uploads/1/0/1/7/10171621/astm_d-2487_classification_of_soils_for_engineering_purposes_unified_soil_classification_system.pdf

[16] R.B. Peck, W.E. Hanson, T.H. Thornburn, "Foundation Engineering, 2nd Edition," Willey, New York, Pp 113-115, 1974, https://www.worldcat.org/title/foundation-engineering-by-rb-peck-walter-e-hanson-thomas-h-thornburn/oclc/503644451

EEBO, FESTUS OLUSOLA obtained his bachelor's degree in Applied Geophysics from Federal University of Technology, Akure Nigeria, in 2014. He has participated in different research projects which includes, Geophysical Investigation of groundwater potential of an area, geophysical investigation of causes and characteristics of road failure in some part of Nigeria. He has published some research papers and his research interest includes, Hydrogeology; Groundwater and surface water Interaction, Contaminant transport and remediation, Application of geophysical methods in groundwater exploration, road failure investigation, Foundation Studies and pollution control and Seismic interpretation with reservoir modelling.

Abidakun Bayode Samuel has done his bachelor's degree in Applied Geophysics from Federal University of Technology, Akure Nigeria, in 2015.

OLAYANJU GBENGA MOSES is a Professor of Geophysics at the Department of Applied Geophysics from Federal University of Technology, Akure Nigeria. He obtained his bachelor's, Master and PhD degree from the same Institution in 1995, 2000 and 2010 respectively.